Characterization and genome-scale metabolic modeling of catechol-degrading *Pseudomonas fluorescens* isolated from a petroleum hydrocarbon-impacted site

A Thesis Submitted to the College of Graduate and Postdoctoral Studies

In Partial Fulfillment of the Requirements for the Degree of

Master of Science

Department of Chemical and Biological Engineering

University of Saskatchewan

By

Xiaoyan Huang

Permission to use

In presenting this thesis in partial fulfillment of the requirements for a Postgraduate degree from the University of Saskatchewan, I agree that the Libraries of this University may make it freely available for inspection. I further agree that permission for copying of this thesis in any manner, in whole or in part, for scholarly purposes may be granted by the professor or professors who supervised my thesis work or, in their absence, by the Head of the Department or the Dean of the College in which my thesis work was done. It is understood that any copying or publication or use of this thesis or parts thereof for financial gain shall not be allowed without my written permission. It is also understood that due recognition shall be given to me and to the University of Saskatchewan in any scholarly use which may be made of any material in my thesis.

Requests for permission to copy or to make other uses of materials in this thesis/dissertation in whole or part should be addressed to:

Head of the Department of Chemical and Biological Engineering

University of Saskatchewan

57 Campus Drive, Saskatoon, SK, S7N 5A9, Canada

or

Dean

College of Graduate and Postdoctoral Studies

University of Saskatchewan

116 Thorvaldson Building, 110 Science Place Saskatoon, SK, S7N 5C9, Canada

Abstract

Pseudomonas fluorescens is a candidate for efficient petroleum hydrocarbons (PHC) biodegradation. In this work, a *P. fluorescens* strain was isolated from a local PHC-impacted site. To investigate its PHC biodegradation performance, catechol, an important metabolic intermediate during monoaromatic hydrocarbon biodegradation, was chosen as the sole carbon source.

A set of experiments based on a 2^3 factorial design was undertaken to investigate how nitrate, sulfate, and phosphate ions affect catechol biodegradation by the isolated *P. fluorescens* strain. The experimental results were subjected to ANOVA. Maximum specific catechol degradation rates (the response) were estimated by a three-parameter logistic model to evaluate bioremediation performance. ANOVA results suggest introducing nitrate ions alone may lead to poorer bioremediation performance, introducing sulfate ions alone does not affect bioremediation performance, but supplementing with nitrate and sulfate ions together can enhance bioremediation performance. *P. fluorescens* was also shown to survive under sulfur-limited conditions. Injecting phosphate ions also led to better bioremediation performance.

To gain extensive and systematic knowledge of *P. fluorescens*, the first genome-scale metabolic model (GSMM) for *P. fluorescens* was reconstructed, termed lCW1057. The model was validated by *in vitro* growth data. The periplasmic compartment was constructed to better represent the proton gradient profile. The reconstructed proton transport chain has a P/O ratio of 11/8. Flux balance analysis (FBA) was performed to simulate the whole-cell metabolic flow. The simulation results suggested the β-ketoadipate pathway is involved in catechol metabolism by *P. fluorescens* while the uptake of oxygen is mandatory for cleavage of catechol's aromatic ring. The Entner-Doudoroff (ED) pathway was involved in glycolysis for *P. fluorescens*. Moreover, nitrates can be used as the terminal electron acceptor to support *P. fluorescens* growth under anaerobic condition.

Acknowledgment

First of all, I thank my parents for their love and support during my graduate studies. My sincere appreciation goes to my supervisor, Dr. Yen-Han Lin. His patient guidance helped me throughout my graduate studies. He also helped me to construct the basis for further research works. I thank my committee members, Dr Hui Wang, Dr. Jian Peng, and Dr. Wenhui Xiong, for their inspirational suggestions. I am grateful to my group members, Siyang Shen and Yishuang Zhang, for their contributions to the projects.

Table of contents

List of tables

List of figures

Nomenclature

c0, cytosolic compartment

e0, extracellular compartment

ED, Entner-Doudoroff

EMP, Embden-Meyerhof-Parnas

DW, biomass dry weight, g

ETC, electron transport chain

FBA, flux balance analysis

GSMM, genome-scale metabolic model

KDPG, 2-keto-3-deoxy-6-phosphogluconate

p0, periplasmic compartment

r_s, maximum specific catechol degradation rate, h^{-1}

S(t), catechol concentration at t hour, mg/L

$\hat{S}$, maximum catechol concentration, mg/L

$\overline{S}$, average catechol concentration, mg/L

t, time, h

t_s, time required till the catechol degradation rate research the maximum, h

Glossary

A

ATP A molecule carries energy.

C

Cytosolic compartment A compartment inside the living cell.

E

Extracellular compartment A compartment outside the living cell.

F

Flux balance analysis A mathematical method by which the flow of metabolites through the metabolic network can be estimated.

I

in silico An experiment performed by computer software.

in vitro An experiment performed outside of living cells.

P

Periplasmic compartment A compartment between the outside membrane and cytosolic membrane of the cell.

Phenotype analysis A method by which the composite of the organism's characteristics can be estimated.

P/O ratio A number that indicates the amount of ATP molecules produced by oxidative phosphorylation for each pair of electrons.

Chapter 1 Introduction and literature review

1.1 Literature review

1.1.1 Sources of petroleum hydrocarbon contamination

Petroleum hydrocarbons (PHC) are a predominant energy source around the world. PHC can become an important organic contaminant in many ways. One of the most widespread origins is leakage from underground storage tanks (e.g., at gas stations) and PHC transportation pipelines [1]. Accidents during the transport of PHC and improper disposal can also lead to pollution. Accidental spills at oil exploration sites can lead to serious contamination of local environments. For instance, PHC discharge from an oil spill in April 2010 from Deepwater Horizon, an oil prospect site of BP in the Gulf of Mexico, was estimated at 780,000 m^3 by the U.S. Federal Government [2]. The Deepwater Horizon spill caused serious environmental, economic, and societal impacts [3].

1.1.2 Characteristics of petroleum monoaromatic hydrocarbon

Petroleum aromatic hydrocarbons are recalcitrant to natural degradation due to the high resonance energy of the carbon bonds in the aromatic rings. Low molecular weight petroleum aromatic hydrocarbons are of concern due to their relatively high mobility [4]. When trapped in the soil, they can further leach into the groundwater and become a cause for human health concerns. For example, benzene, toluene, ethylbenzene, and xylene (collectively called BTEX) can result in such consequences. They are not only constituents of fossil fuels but also widely used as organic solvents in industrial processes [5]. In comparison to other petroleum aromatics, they have a higher solubility in water [6]. They are also highly toxic; according to the U.S. Agency for toxic substances and disease registry, benzene is ranked sixth in a list of toxic organic substances [7]. Benzene is associated with a risk of cancer [8]. Furthermore, it may cause childhood leukemia if fetal exposure occurs *in utero* in pregnant women [9].

Catechol is another important toxic aromatic hydrocarbon. Figure 1.1 shows catechol (1,2-dihydrooxybenzene) is a crucial metabolic intermediate during the biodegradation of benzene, toluene, and ethylbenzene [10]. It has been widely used as an antioxidant in the rubber, chemical, dye, photographic, pharmaceutical, cosmetics, and oil

industries [11]. However, it can lead to statistically significant changes in the function of erythrocytes, thereby [12]. Even though BTEX has a relatively higher solubility than other PHC, it is hard to evaluate BTEX biodegradation kinetics due to their high volatility. Catechol solution is more stable than BTEX solution, and therefore studying the metabolism behavior and kinetics of catechol degradation can provide insights to investigate BTEX biodegradation.

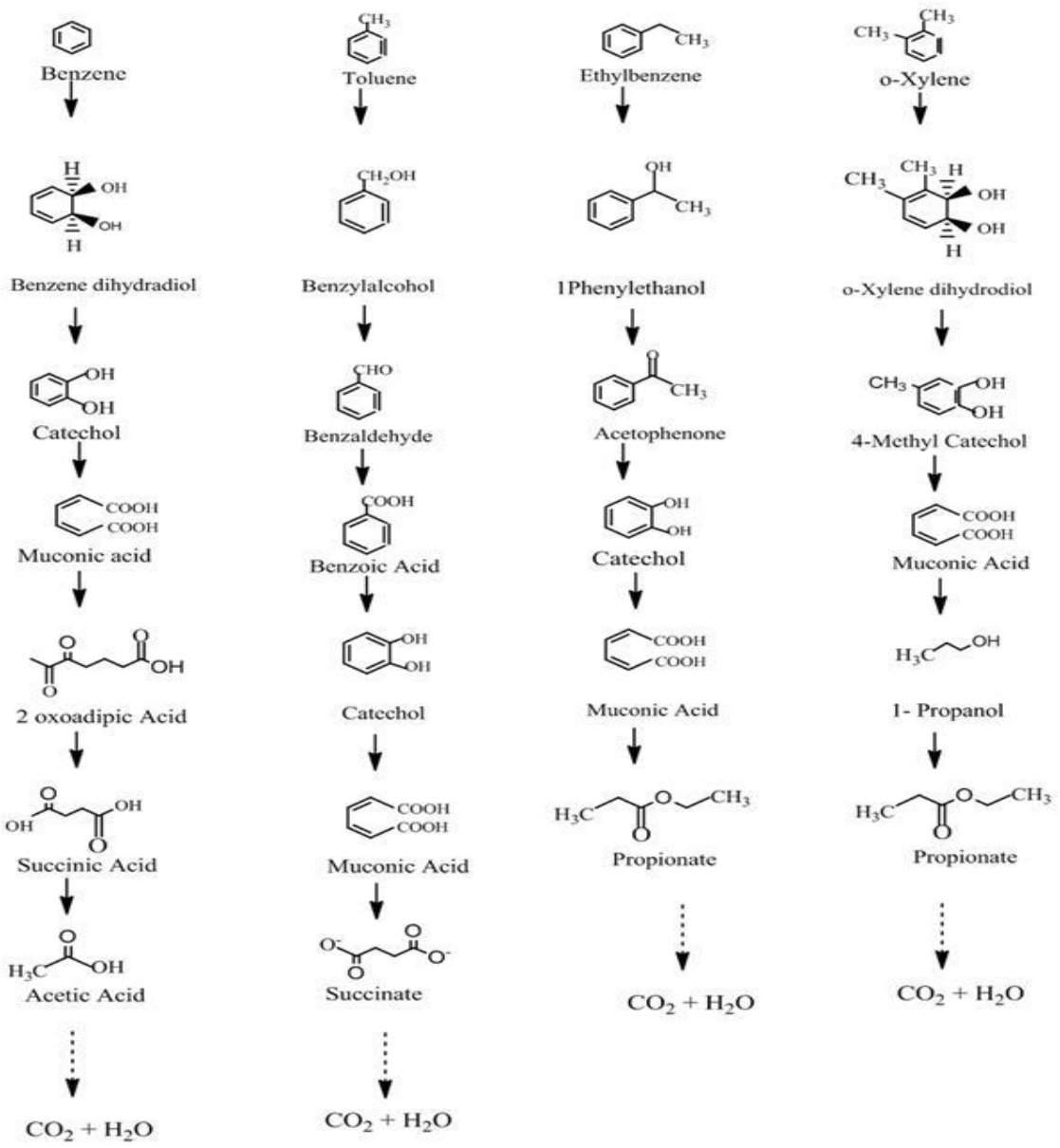

Figure 1.1 BTEX biodegradation pathway [13]

1.1.3 Bioremediation strategies

Various physico-chemical methods can be used to clean up PHC-impacted sites, including soil washing, oxidation of contaminants, and incineration [14]. However, these methods are often economically inefficient and have the potential to cause secondary contamination [14]. On the other hand, bio-based treatments, known as bioremediation, are more cost effective and can protect soil quality during the cleanup of PHC contamination [15].

In PHC-impacted sites, some indigenous living organisms that are adapted to the polluted environment may use PHC as a carbon and energy source to support biomass growth [16]. However, this is time-consuming under natural conditions and, therefore, bioremediation strategies have been developed to accelerate the process. Biostimulation, bioaugmentation, and phytoremediation are conventional bioremediation strategies. In the biostimulation process, the environment of the contaminated site is modified to stimulate the bioremediation ability of microorganisms [17]. In the bioaugmentation process, the impacted site is supplemented with microorganisms that are capable of degrading target contaminants. *Pseudomonas sp.* has been reported as the candidate in PHC bioremediation projects [18]. Phytoremediation is a technology that uses plants to clean up various pollutants, including petroleum hydrocarbons, pesticides, dyes, and heavy metals [14].

1.1.4 Factors affecting the bioremediation process

Many factors can affect the performance of bioremediation targeting PHC. The availability of nutrients, electron acceptors and the local temperature are crucial parameters that affect the bioremediation of PHC-impacted groundwater and soil [18]. Soil conditions and composition can also affect soil bioremediation [19].

1.1.4.1 Temperature

Temperature affects the bioremediation performance by influencing the bioavailability, enzyme activity, and solubility of hydrocarbon substances [20]. A higher temperature in the bioremediation environment can lead to better bioremediation performance because higher temperatures can result in higher enzyme activity. A lower viscosity of PHC in soil can enhance the availability of PHC to microorganisms, which can further result in better PHC bioremediation performance [4].

1.1.4.2 Nutrient availability

Oxidation-reduction reactions, as illustrated in Figure 1.2, play a crucial role as the energy source during microbial metabolism [18]. Therefore, the oxidized electron acceptor is important for PHC bioremediation. Due to the low solubility of oxygen, it is limited for impacted underground soil and water yet pumping in air or oxygen is not economically viable. Increasing the availability of electron acceptors has been employed as a popular bioremediation strategy [21]. Nitrate, sulfate, and ferric are alternative electronic acceptors for supporting the growth of some microorganisms [16]. Enhancing PHC biodegradation performance by adding nitrate and sulfate ions has been explored in many *in situ* projects [22]. Cunningham et al. report that introducing nitrates can enhance the performance of BTEX removal, while sulfates are observed to only stimulate the degradation of benzene, xylene, and toluene [16]. These authors suggest that, in comparison to sulfate ions, nitrate ions are preferentially utilized by microorganisms and more rapidly oxidize the hydrocarbons [16]. Using persulfate as the electron acceptor for BTEX biodegradation has been reported in both aqueous and soil slurry systems at ambient temperature (e.g., 20 °C) [23]. Furthermore, nitrate and sulfate salts can provide nitrogen and sulfur, which are essential elements for the production of biomass. Phosphorus is another essential element for the biomass growth. Dosing with phosphate to enhance PHC bioremediation performance has been reported [22]. However, introducing inorganic phosphate may lead to the precipitation of phosphate with cations and cause low phosphorus availability.

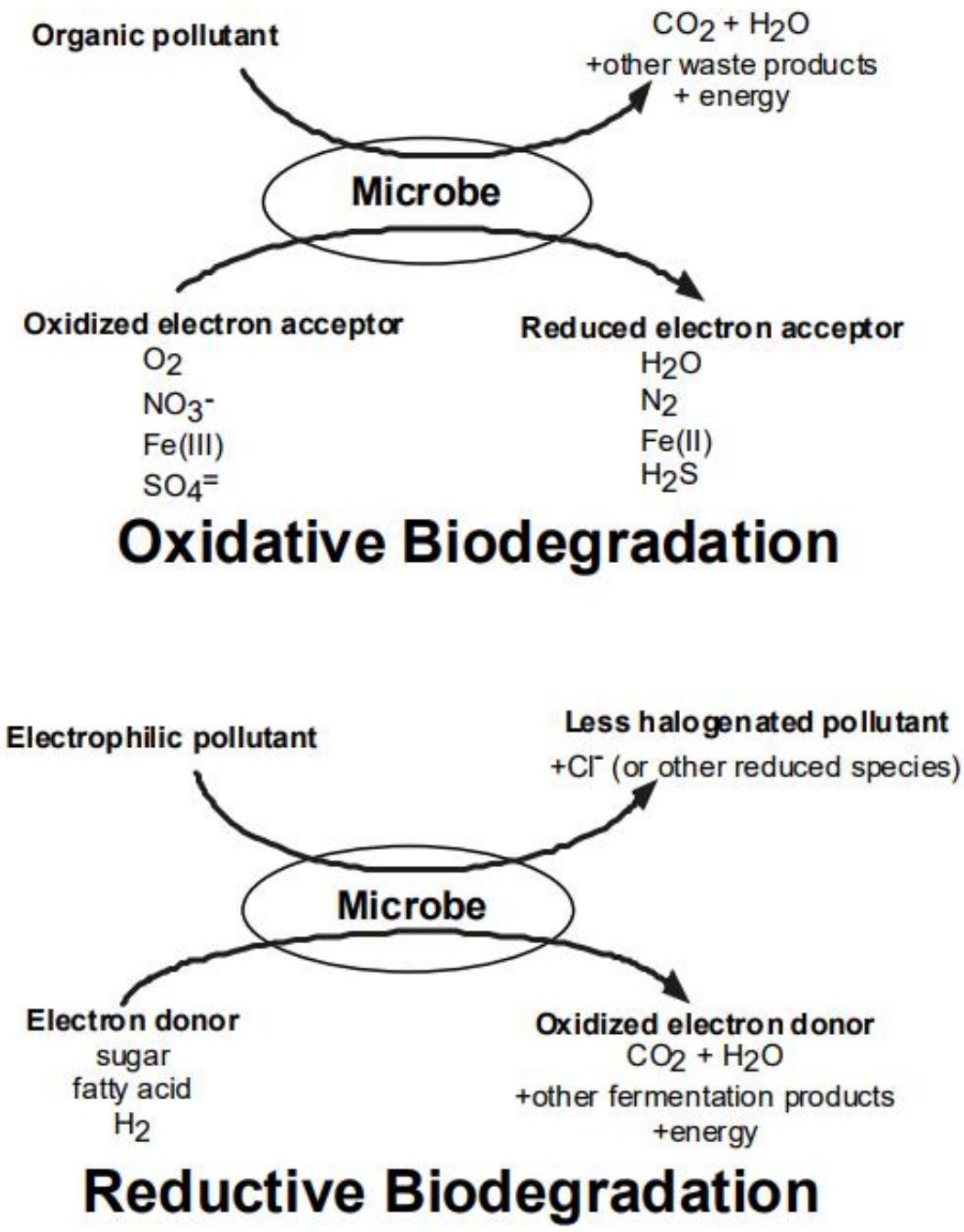

Figure 1.2 Microbial oxidation-reduction reaction [18]

1.1.4.3 Soil conditions

The surface area of soil particles and the soil's cation exchange capacity (CEC) are two important parameters affecting bioremediation performance in soils. Soil particles can break down into clay, silt, and sand according to their size (clay, 0-2 μm; silt, 2-50 μm; and sand, 0.05-2 mm) [24]. Smaller particle size provides a larger surface area. Soil particles mainly carry a negative charge, and represents the soil's CEC [25]. A larger surface area and higher CEC will lead to a larger adsorption capacity by the soil, and in turn lead to a low mass transfer rate for contaminants to microorganisms. Therefore, releasing contaminants from the soil is an important step for soil bioremediation [17]. Surfactants have the ability to increase the availability of contaminants to microorganisms by reducing the surface tension of soil particles. Therefore, they can be applied to enhance the contaminant mass transfer rate. In comparison to biosurfactants, chemical surfactants have a common disadvantage in that they may cause colloid mobilization and clog soil pores of microorganisms during the removal of aromatic hydrocarbons [26].

1.1.4.4 Soil composition

Some chemicals found in PHC-impacted soil can affect bioremediation performance in different ways. For example, due to the high toxicity of BTEX, the growth of microorganisms is inhibited in soils with a high initial BTEX concentration. Microorganisms that are grown using catechol or o-cresol as carbon sources may suffer a relatively lower inhibitory effect by BTEX [27].

The pH of the environment is also important for the bioremediation process. Alexander reports that hydrocarbon mineralization is optimized in a neutral pH environment [28]. However, microorganisms have better stress resistance in acidic environments because acidic environments can accelerate proton transfer and further lead to more efficient microbial ATP synthesis [29].

The water content of soil also influences biodegradation performance by affecting microorganism growth. The optimum water content for microorganism growth in soil is 50-75% [26].

1.1.5 Recent bioremediation strategies

Immobilizing microorganisms with polymeric materials can enhance bioremediation performance under various conditions, e.g., immobilization within chitosan beads. Chitosan can be obtained from chitin, which is one of the most abundant biopolymers. It can be extracted from the shells of lobster and crabs [30]. Chitosan has the advantages of lack of toxicity, availability in nature, and physiological inertness [30]. Furthermore, chitosan can be produced in many shapes, including beads, films, and membranes [31]. Chitosan powers can be dissolved in acidic conditions to form a chitosan gel, to which microbial biomass can be added. Immobilizing microorganisms with chitosan beads can stimulate the bioremediation process [32].

1.1.6 Genome-scale metabolic model

Traditional experimental technology, such as fermentation experiment, can provide useful information, for example raw material uptake and production excretion rates, to quantify the fermentation performance. However, experimental results can only provide limited knowledge about intercellular metabolism, like whole-cell flux distribution. A genome-scale metabolic model (GSMM) can be applied to estimate the microbial growth rate, predict gene essentiality, and explore the optimal metabolic pathway from specific substrates to given products [33]. Flux balance analysis (FBA) is a widely used method to calculate the flow of metabolites through the metabolic network [34]. The stoichiometry of reactions in the metabolic network imposes constraints on the flow of metabolites, which plays a fundamental role in FBA.

1.2 Knowledge gap

P. fluorescens is a candidate for PHC biodegradation. However, the effects of nutrients on PHC bioremediation performance, for example the availability of terminal electron acceptors, is unclear. Moreover, the information about intracellular metabolism behaviors of *P. fluorescens* is limited. Two summarized knowledge gaps are list below:

1. Few studies have considered the effects of nutrient availability on catechol biodegradation by *P. fluorescens.*
2. The GSMM for *P. fluorescens* has not been reconstructed.

1.3 Objectives

Based on the knowledge gap described in Section 1.2, the objectives of this work were to:

1. Isolate a PHC-degrading strain from a local PHC-impacted site in Saskatchewan.
2. Characterize the effect of various combinations of nutrients (nitrate, sulfate, and phosphate ions) on catechol bioremediation performance by the isolated strain.
3. Reconstruct a genome-scale metabolic model for *P. fluorescens*.

1.4 Thesis organization

This thesis is organized in manuscript format. The content of Chapter 2 is prepared according to the submission requirement by *Canadian Journal of Chemical Engineering*. In Chapter 3, the content is formatted according to the submission requirement by *Biotechnology and Applied Biochemistry*. The finding reported in Chapter 2 and 3 are summarized in Chapter 4 as concluding remarks. In Chapter 5, the recommendations for future works are presented.

In Chapter 2, a catechol-degrading *P. fluorescens* was isolated from petroleum hydrocarbon impacted site in Saskatchewan. Its fermentation knowledge about catechol biodegradation by *P. fluorescens* was introduced. To further explore its metabolic flux of catechol biodegradation, a three-compartment genome-scale metabolic model was reconstructed for *P. fluorescens* and debrided in Chapter 3. Hence a comprehensive knowledge regrading with catechol biodegradation by *P. fluorescens* was provided from both *in vitro* and *in silico* aspects.

Chapter 2 Biodegradation of catechol by *Pseudomonas fluorescens* isolated from petroleum hydrocarbon-impacted soil

The content in this chapter has been accepted by the *Canadian Journal of Chemical Engineering*.

Manuscript number: CJCE-19-0761

2.1 Abstract

Bioremediation strategies have been applied to clean up petroleum hydrocarbon (PHC)-impacted sites. Introducing PHC-degrading microorganisms (bioaugmentation) and enhancing the *in situ* nutrient availability (biostimulation) are widely used strategies. In this work, a wild-type *Pseudomonas fluorescens* strain was isolated from a PHC-impacted site in Saskatchewan. Through a 2^3 factorial design plan, the effect of various combinations of nitrate, sulfate, and phosphate ions on bioremediation performance by the isolated strain was investigated. Catechol, an essential metabolic intermediate of BTEX degradation, was used as the sole carbon source. The maximum specific catechol degradation rate was chosen as the response to evaluate catechol bioremediation performance. ANOVA results suggest the presence of nitrate ions alone lowers the maximum specific catechol degradation rate, which may be explained by the accumulation of nitrites and ammonia during the denitrification process by *P. fluorescens*. Dosing with sulfate ions alone did not affect the bioremediation performance. This observation indicates *P. fluorescens* can grow in a sulfur-limited environment. Moreover, the presence of sulfate and nitrate ions together can lead to a higher maximum specific catechol degradation rate. This may be due to the presence of sulfate suppressing the production of nitrites. The importance of phosphate ions on catechol bioremediation was also investigated. The absence of phosphate leads to incomplete bioremediation but the introduction of phosphate ions can accelerate catechol degradation, which may be explained by the secretion of organic acids.

2.2 Introduction

Many petroleum hydrocarbons (PHC) enter soil and groundwater bodies through spills, disposal, and leakage [20]. They are toxic to both fauna and flora [35]. Microorganisms, once adapted to the impacted site, can utilize petroleum hydrocarbons as a carbon and energy source to grow, thereby minimizing the impact of PHC on the environment [21]. Bioremediation strategies have been used to accelerate this process [36].

Monoaromatic hydrocarbons are an important part of PHC contamination due to their relatively high solubility, mobility, and toxicity [4]. Catechol is a crucial metabolic intermediate in the β-ketoadipate pathway, which is involved in the metabolism of monoaromatic hydrocarbons (e.g., BTEX and phenol) for *Pseudomonas* species [37, 38]. Furthermore, even though catechol may inhibit microorganism growth, those pre-grown on catechol have a higher survivability in the environment in the presence of BTEX [11, 27]. Our preliminary results suggested that catechol loss without biodegradation involved is neglectable. Therefore, elucidating the factors affecting catechol bioremediation can help to design biostimulation and bioaugmentation strategies, especially for treating monoaromatic hydrocarbon pollution.

Enhancing nutrient availability, for example the availability of electron acceptors, is one bioremediation strategy termed biostimulation [18]. Oxygen is the common electron acceptor in oxidation-reduction reactions and plays a crucial role as the energy source during microbial metabolism. However, oxygen is limited in impacted underground soil and water, and pumping in air or oxygen is not economically efficient [39]. Therefore, dosing with alternative electron acceptors, such as nitrates and sulfates, can be employed as a biostimulation strategy [40].

Introducing PHC-degrading microorganisms to impacted sites is another bioremediation strategy termed bioaugmentation. *Pseudomonas* species have drawn attention as candidates for bioaugmentation due to their versatile metabolic subsystems and high tolerance for environmental stress under various bioremediation conditions [41, 42]. *P. fluorescens*, *P. aeruginosa*, and *P. putida* are effective bioaugmentation agents to clean up PHC contamination [43, 44, 45].

Biostimulation and bioaugmentation strategies can be combined to enhance bioremediation performance [46]. Even though *Pseudomonas* species have been widely

involved in bioaugmentation projects, nutrients affecting PHC bioremediation performance by *Pseudomonas sp*. have received little attention. Hence, investigating nutrients affecting the bioremediation performance by *P. fluorescens* may provide opportunity to combine biostimulation strategy and bioaugmentation with *P. fluorescens*.

The purpose of this work was to elucidate the effects of three commonly used nutrients (i.e., nitrate, sulfate, and phosphate ions) to stimulate PHC bioremediation by *Pseudomonas* species. A wild-type strain of *P. fluorescens* was isolated from a local PHC-impacted site, then a 2^3 factorial design applied to predict the effects of various combinations of nitrate, sulfate, and phosphate ions on catechol degradation by the isolated *P. fluorescens* strain.

2.3 Materials and methods

2.3.1 Microbial isolation

PHC-impacted soil was collected from a local polluted site in Saskatchewan, Canada. The sample was stored at 4 °C before using. First, the microbial population in the soil was enriched in a growth medium consisting of 10 g/L yeast extract, 5 g/L urea, and 200 mg/L catechol. One kg of PHC-impacted soil was placed into a 10-L fermenter with 5 L of growth medium and then cultured for 72 h. Next, 100 mL of culture was transferred into a 2-L batch fermenter with 1-L M9 minimal medium consisting of 6 g/L Na_2HPO_4, 3 g/L KH_2PO_4, 1.4 g/L $(NH_4)_2SO_4$, 0.5 g/L NaCl, 0.2 g/L $MgSO_4 \cdot 7H_2O$, and 200 mg/L catechol as the carbon source. After the optical density reached 0.8 at a wavelength of 600 nm (described in Section 2.3.3), the bacterial population was isolated by serial dilution on minimal salt-catechol agar plates until the dominated strain appeared.

2.3.2 Measurement of catechol concentration

Samples collected during the bacterial culture period were centrifuged at 4 °C and 5000 rpm for 25 min. The supernatant was collected and filtered through a 0.2-μm nylon membrane. High performance liquid chromatography (HPLC) equipped with a UV detector was used to analyze these samples at a wavelength of 254 nm. The HPLC used a C_{18} column (Agilent Eclipse XD8-C_{18} 4.6×150 mm) at 35 °C. The chromatography was isocratic with a mobile phase consisting of water/acetonitrile (50%/50%, v/v). The flow rate was set at 1.2 mL/min.

2.3.3 Biomass concentration estimation

The accumulation of biomass is proportional to the optical density (OD) of a sample. UV-VIS spectrophotometry (UVmini-1240, SHIMADZU) was used for OD measurement. To determine the biomass dry weight, the samples were centrifuged at 8000 rpm for 15 min and dried in an oven at 80 ^{o}C for 12 h. The correlation between biomass dry weight and OD was established.

2.3.4 Data smoothing

A logistic growth model can be used to simulate the population dynamics that correlate with seasonal variations [19]. A three-parameter logistic growth model was chosen to predict the substrate uptake pattern. The detailed data fitting process has been

previously reported [14]. Briefly, the experimental data collected were fitted using Equation (2.1). The Matlab optimization toolbox was used to estimate the maximum specific biomass growth rate and maximum specific substrate degradation rate. A simple r^2 criterion was used to evaluate the goodness of fit (Equation 2.2).

$$S(t) = \frac{\hat{S}}{1+\exp\left[-r_s(t-t_s)\right]} \tag{2.1}$$

$$r^2 = 1 - \frac{\sum(S(t)-\hat{S})^2}{\sum(S(t)-\bar{S})^2} \tag{2.2}$$

2.3.5 Experiments

To investigate the individual and interactive effects of nitrate, sulfate, and phosphate ions, a 2^3 factorial design was employed (Table 2.1). The microorganism was firstly incubated in the seed medium consisting M9 minimal salts medium and 200 mg/L catechol. After OD in the seed medium reached 0.8, the seed medium was transferred into growth medium with incubation rate at 10%. In addition to nitrate, sulfate, and phosphate ions, the growth medium contained 170 mg/L catechol as the sole carbon source, 500 mg/L sodium chloride, and 200 mg/L magnesium chloride heptahydrate. A lower catechol concentration in growth medium was chosen to minimize the inhibition effect of catechol to *P. fluorescens*. Cunningham et al. suggest nitrate concentrations above 100 mg/L may lead to *in situ* N_2 gas bubbles and exceed EPA regulatory limits for NO_3^- [20]. Therefore, in this study, the maximum nitrate ions concentration was set at 100 mg/L (1.61 mmol/L). Furthermore, according to Norris, degrading the same amount of toluene using nitrate and sulfate ions as terminal electron acceptors results in a mole ratio of nitrate to sulfate ions of 1.6:1 [21]. Therefore, in this work, a sulfate concentration of 1.01 mmol/L (96 mg/L) was chosen. The mole ratio of phosphate to nitrate ions was set at 1:1. Ammonium nitrate, ammonium sulfate, and ammonium phosphate dibasic were used as the nitrate, sulfate, and phosphate sources, respectively.

Table 2.1 2^3 factorial design*

Run**	Factors (mM)			Responses (h^{-1}) Set 1	Responses (h^{-1}) Set 2
	Nitrate	Sulfate	Phosphate	r_s	r_s
1	+	+	-	0.114	0.134
2	+	-	+	0.148	0.123
3	+	+	+	0.145	0.145
4	+	-	-	0.091	0.092
5	-	+	-	0.137	0.108
6	-	-	+	0.198	0.186
7	-	+	+	0.191	0.174
8	-	-	-	0.170	0.140

*__Nitrate__: +, **1.61 mM** and -, **0 mM; Sulfate**: +, **1.01 mM** and -, **0 mM; Phosphate**: +, **1.61 mM** and -, **0 mM**

**__For example: Run 1 (Nitrate +; Sulfate +; Phosphate -) contains 1.61 mM nitrate, 1.01 mM sulfate, and 0 mM phosphate__

***__The experiment was duplicated to predict the p-value.__

2.4 Results and discussion

2.4.1 Identification of isolated *P. fluorescens*

The isolated microorganism strain was identified as *P. fluorescens* using a BIOLOG kit (Biolog Inc., Hayward, CA, USA), which is based on the sequencing of its DNA [47]. This identification was contracted to Bio-Chem Consulting Services Ltd., Calgary, AB, Canada.

2.4.2 Establishment of logistic growth model for data smoothing

Figure 2.1 illustrates the application of the modified three-parameter logistic model to simulate the catechol degradation profiles in the media described in Table 2.1. The r^2, which was calculated as described in Equation 2.2, was used to evaluate the goodness of fit for the model. The results show r^2 values for all 16 runs are greater than 0.99, indicating the modified model can be applied to predict the catechol degradation profile by *P. fluorescens* with high accuracy. However, it should be noted that the catechol degradation ceased at around 28^{th} hour and before the depletion of catechol for runs without the presence of phosphate ions (Runs 1, 4, 5, and 8). Hence, experimental data points after hour 28 for these runs were not used in the simulation.

2.4.3 Maximum specific catechol degradation rate

According to the model predicted by the logistic model described in Section 2.4.2, the maximum specific catechol degradation rate was estimated to evaluate the catechol bioremediation performance. These data were regarded as 'responses' to carry out the ANOVA. The effect of nitrate ions, the effect of phosphate ions, and the interactive effect of nitrate and sulfate ions are significant with respect to maximum specific catechol degradation rate (p-value < 0.05). An estimated correlation between the combined effect of the nutrients (nitrate, sulfate, and phosphate ions) and the response is as follows:

$$r_s = - 0.02 \times \text{Nitrate} + 0.02 \times \text{Phosphate} + 0.011 \times \text{Nitrate} \times \text{Sulfate} + 0.144 \quad (2.3)$$

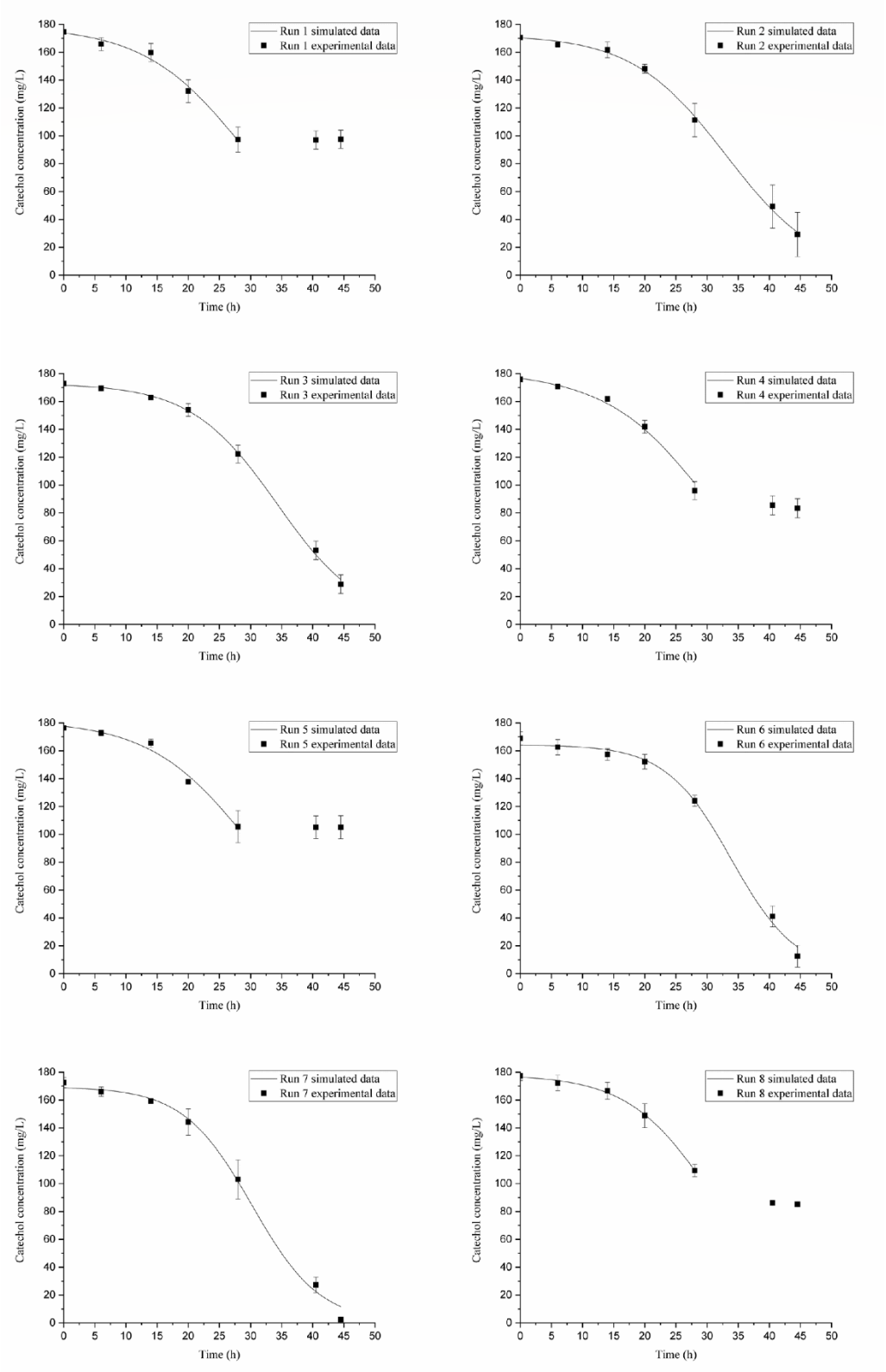

Figure 2.1 Application of three-parameter logistic model to the experimental data

2.4.3.1 Effect of nitrate ions

Equation 2.3 indicates that dosing with nitrate ions alone lowers the maximum specific catechol degradation rate. Note, however, that even though Figure 2.1 shows complete catechol degradation was obtained for runs without nitrate ions added (Runs 6 and 7), this does not imply a nitrogen source is not crucial during catechol biodegradation as a nitrogen source (ammonia phosphate dibasic) was present for Runs 6 and 7.

Better PHC bioremediation performance following the introduction of nitrates has been reported in many *in situ* studies [22, 48, 49]. However, the effect of injecting nitrate to enhance PHC bioremediation is not guaranteed. Chaillan et al. report that urea has a detrimental effect on hydrocarbon-degrading fungi due to the production of toxic ammonia [19]. Dosing with nitrate alone also did not noticeably improve underground benzene removal in Mississippi, USA [50].

Pseudomonas sp. can utilize nitrate as a terminal electron acceptor through respiratory denitrification, as illustrated in Equation 2.4, with nitrite being one of the intermediate products during denitrification [51]. Due to a higher conversion rate of nitrate over nitrite, nitrite is accumulated during nitrate reduction [52, 53]. Nitrite is toxic and imposes an inhibitory effect on the growth of *P. fluorescens* [54]. Although ammonia gas is not an intermediate during respiratory denitrification, nitrate metabolism in *Pseudomonas sp.* can still produce ammonia via the nirB gene [10, 55, 56]. The accumulation of ammonia gas is toxic to microorganisms, resulting in increasing pH of the environment and subsequent reductions in PHC bioremediation performance [19].

$$NO_3^- \rightarrow NO_2^- \rightarrow N_2O \rightarrow N_2 \qquad (2.4)$$

2.4.3.2 Effect of sulfate ions

The ANOVA results suggest sulfate ions alone do not have a significant effect on the maximum specific catechol degradation rate. Figure 2.1 shows that catechol was still fully degraded in the runs without sulfate ions dosed but with phosphate ions present (Runs 2 and 6).

Sulfur is primarily used as a component of cysteine and methionine as well as cellular cofactors for biomass constitution (e.g., biotin and coenzyme A) [57]. The use of sulfate as the electron acceptor for PHC biodegradation has been reported [58, 59].

Scott et al. suggest *Pseudomonas sp.* can grow under sulfur-limited conditions by an approximate five-fold reduction in the total soluble thiol content of the cell [57]. The isolated *P. fluorescens* are speculated to be able to survive under sulfur-limited conditions. Furthermore, sulfate ions do not affect phenol degradation by *Pseudomonas putida* [60]. No experimental evidence to date indicates *P. fluorescens* can use sulfate as the terminal electron acceptor. It has been reported that no gene in *P. fluorescens* SBW 25 is involved in sulfate reduction [61].

2.4.3.3 Effect of phosphate ions

Dosing with phosphate ions led to a higher specific catechol degradation rate and the absence of phosphate ions in the medium resulted in incomplete catechol bioremediation. For the runs without phosphate ions present, only 40 to 60% of the initial catechol was degraded.

Phosphorus is a key element in the biomass of microorganisms [62]. The source of phosphorus for microorganisms is limited, which results in the availability of phosphorus for microorganisms usually controlling the progress of PHC biodegradation [22]. Therefore, phosphate salts can be dosed into the PHC-impacted site to enhance the phosphorus availability for microorganisms to build up biomass. Moreover, dosing with phosphate salts can also lead to better bioremediation performance. Ponsin et al. highlight the importance of phosphate in petroleum hydrocarbon degradation [63].

The enhancement of PHC bioremediation performance may be explained by the secretion of organic acid by *P. fluorescens* when phosphate is involved [64]. An acidic environment can accelerate proton transfer and provide a better environment for ATP synthesis [29]. However, introducing phosphate salts to enhance bioremediation is not always feasible. Supplementing with inorganic phosphate salts may lead to precipitation or immobilization of phosphorus with calcium, aluminum, and ferric ions, resulting in a low phosphorus availability for microorganisms [65]. Xiong et al. suggest organic phosphate salts (e.g., triethyl phosphate) must be mineralized before they can be utilized by microorganisms [22]. However, *P. fluorescens* strains appear to have the ability to solubilize insoluble phosphate salts [66]. Therefore, it is postulated that supplementing with inorganic phosphate salts may be suitable for applications of *P. fluorescence* to treat PHC-contaminated soil.

2.4.3.4 Interactive effect of nitrate and sulfate ions

As shown in Equation 2.3, there was an interactive effect between sulfate and nitrate ions that is positively correlated with the maximum specific catechol degradation rate. The coexistence of nitrate and sulfate ions in the medium results in an increase in the maximum specific catechol degradation rate. This observation may be explained by the presence of sulfate ions that inhibit the nitrate reductase [67]. The presence of sulfate ions is postulated to slow down the conversion of nitrate to nitrite. As mentioned in Section 2.4.3.1, the accumulation of nitrite is due to the imbalance of a higher rate of conversion of nitrate to nitrite than rate of nitrite consumption (i.e., the conversion of nitrite to nitrous oxide). Therefore, the presence of sulfate ions can reduce the amount of accumulating nitrite as the presence of sulfate ions would reduce the nitrite production rate.

2.5 Conclusions

A catechol-degrading *P. fluoresence* strain was isolated from a local PHC-impacted site. A 2^3 factorial design was used to investigate the effect of various combinations of nitrate, sulfate, and phopshate ions on catechol bioremediation performance by the isolated strain. ANOVA results suggest dosing with nitrate ions alone leads to poorer catechol bioremediation performance. However, catechol bioremediation performance is enhanced when both nitrate and sulfate ions are introduced. Dosing with phosphate ions also enhances catechol bioremediation performance.

Chapter 3 Reconstruction and analysis of a three-compartment genome-scale metabolic model for *Pseudomonas fluorescens*

X. Huang and Y. Lin, "Reconstruction and analysis of a three-compartment genome-scale metabolic model for *Pseudomonas fluorescens*," *Biotechnology and applied biochemistry*, doi 10.1002/bab.1852, 2020.

3.1 Abstract

With the versatile metabolic diversity, *Pseudomonas fluorescens* is a potential candidate in petroleum aromatic hydrocarbon (PAH) bioremediation. Genome-scale metabolic model (GSMM) can provide systematic information to guide the development of metabolic engineering strategy to improve microbial activity.

In this study, the first GSMM for *P. fluorescens* SBW25 was reconstructed, termed lCW1057. The reconstruction was based on automatic reannotation and manual curation. The periplasmic compartment was constructed to better represent the proton gradient profile. The reconstructed proton transport chain has a P/O ratio at 11/8. Flux balance analysis (FBA) was performed to explore the whole-cell metabolic flow. The model suggested that instead of EMP pathway, ED pathway was used in glycolytic metabolism of *P. fluorescens*, indicating that the growth of *P. fluorescens* is more energy dependent. Furthermore, *P. fluorescens* can use nitrate as the terminal electron acceptor for the glucose metabolism. The β-ketoadipate pathway was involved in catechol metabolism. The uptake of oxygen is mandatory for the aromatic ring cleavage. The *in silico* and *in vitro* maximum specific growth rate was compared, resulting in 10% difference when catechol was used as the sole carbon source.

3.2 Introduction

Pseudomonas fluorescens can be found throughout terrestrial habitats, and it is abundant on the surfaces of plant roots and leaves [68]. It is a gram-negative, motile rods bacterium, and prefer to grow in aerobic and acidic condition [69]. With the versatile metabolic diversity and high environmental stress resistance, *P. fluorescens* is a candidate in petroleum aromatic hydrocarbon (PAH) bioremediation [70]. Bioremediation performance can be stimulated by enhancing the local nutrients condition [21]. However, overdosing nutrient would also cause environmental problems [71]. An extensive and systematic knowledge of *P. fluorescens* PAH metabolism is important as it can help to optimize the nutrients usage and provide background information for further genetic engineering of microorganisms [72].

Genome-scale metabolic model (GSMM) is such an example that the genomic and metabolic information are integrated in order to explore whole-cell metabolic flow. The GSMM was reconstructed based on stoichiometric relationship between reactants and products of a biochemical reaction catalyzed by a dominant enzyme [73]. The GSMM can be used to predict growth phenotype, analyze network properties, and interpret experimental data [72]. It also provides background information for metabolic engineering strategies and metabolic environment modification [74].

There have been no reports to date of GSMM for *P. fluorescens*. As the whole genome sequence of *P. fluorescens* SBW25 has been published, it is feasible to reconstruct its GSMM [68]. Such model can elucidate intracellular flux within *P. fluorescens* global metabolism. It would also be used to guide the design of metabolic regulation strategies, *in vitro* or *in vivo* [72].

Here, we describe the reconstruction of first GSMM of *P. fluorescens* SBW25, named lCW1057. It was fundamentally based on its gene annotation in conjunction with available physiological data. Its application on aromatic hydrocarbon biodegradation was highlighted. The metabolic pathway for catechol, an important metabolite during BTEX degradation, was elucidated.

3.3 Methods

3.3.1 Model reconstruction

Figure 3.1 illustrates the bottom-up reconstruction strategy for *P. fluorescens.* The genome of this strain was downloaded from *pseudomonas* database (psedumonas.com). It was blasted by using Rapid Annotation using Subsystem Technology (RAST) tool. The reaction list was converted into SBML by ModelSeed, and Optflux was used to carry out FBA.

During the reconstruction of GSMM, there are some metabolites can only be produced or consumed under steady-state condition owing to mis-annotation and/or un-annotation. These "gaps" block the network of reactions, leading to a failed simulation. To overcome these situations, gapfilling algorism was used to detect and modify these deadend nodes. In this study, a bottom-up gapfilling strategy was implemented [75]. Firstly, the model structure was checked by using FBA to simulate biomass formation. When all the biomass precursors' transferring equations were activated, the formation of biomass indicated a functional model structure. Then, the transferring equation was deactivated one at a time. A failed biomass growth after deactivation of the biomass precursor transferring equation indicated that there were gaps which block the generation of the biomass precursor. These gaps were manually examined based on physiological evidence and comparative study with *P. putida* Kt2440. This process was repeated until biomass can grow *in silico*. Moreover, there were only two compartments, that is extracellular (e0) and cytosolic (c0) compartments that were built in RAST tool. To better represent the electron transport chain (ETC), a periplasmic compartment (p0) was incorporated to create a 3-compartment GSMM for *P. fluorescens*. By doing so, a proton gradient profile between c0 an e0 compartments could be created and used to drive ATP synthase.

During the course of model reconstruction, GSMM for *P. putida* Kt2440 was chosen as the basis as both *P. putida* Kt2440 and *P. fluorescens* use ED pathway for glycolysis [74, 76]. When catechol was selected as the substrate, both strains take β-ketoadipate route for catechol degradation [77].

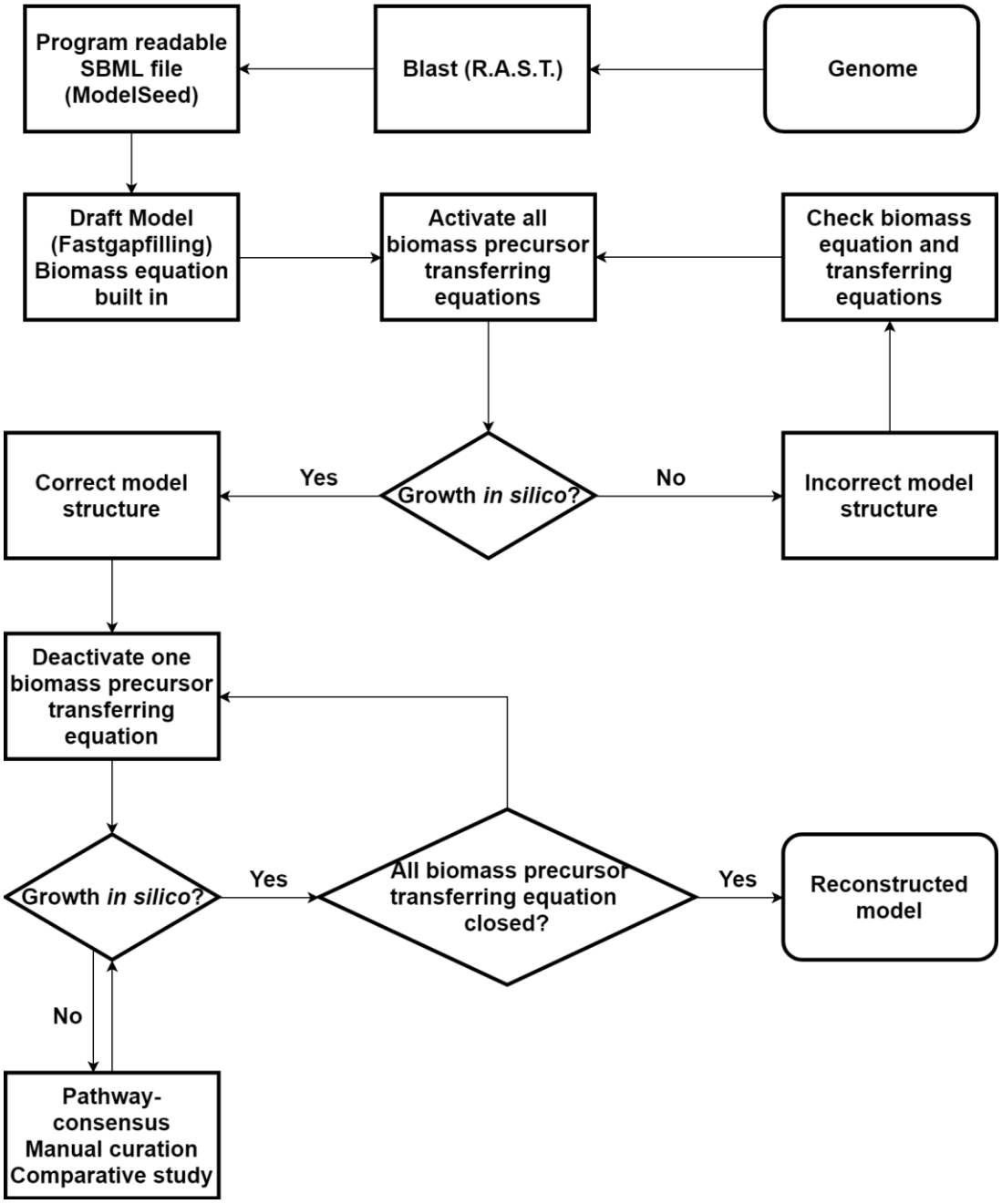

Figure 3.1 Bottom up GSMM reconstruction strategy

3.3.2 Overview of biomass constituting equation

The biomass equation was constituted based on major macromolecules present in microorganisms. They may include DNA, RNA, protein, lipid, and peptidoglycan. DNA composition can be estimated based on the nucleotide content and additional plasmids, while RNA composition is based on ORFs including tRNA sequence [75]. As there is no experimental information available for protein and lipids, it was estimated by using published *P. putida* Kt2440 information. Peptidoglycan's composition is estimated by using peptidoglycan subunit of *Escherichia coli*.

3.3.3 *In vitro* and *in silico* growth

Catechol, a crucial metabolic intermediate in BTEX biodegradation, was used as sole carbon source to investigate *P. fluorescens*' PAHs bioremediation performance. The data from batch fermentation was used to validate this model. A constrain based linear programming approach was applied to perform *in silico* growth simulation.

The samples collected during cultivation were centrifuged at 4 ^{o}C and 5000 rpm for 25 minutes. The supernatant was collected and filtered through 0.2 µm nylon membrane. High performance liquid chromatography (HPLC) equipped with UV detector with 254 nm wavelength was used to analyze these samples. The HPLC column used was C_{18} column (Agilent Eclipse XD8-C_{18} 4.6x150 mm) at 35 ^{o}C. Chromatography was isocratic in a mobile phase consisting of water/acetonitrile (50%/50% v/v). The flow rate was set at 1.2 mL/min. To determine the biomass dry weight, samples was centrifuged at 8000 rpm for 15 mins and dried in oven for 12 hours.

3.4 Results and discussion

3.4.1 Characteristics of model lCW1057

The GSMM was reconstructed by automatic annotation and manual curation. This reconstructed model, termed lCW1057, was the first GSMM for *P. fluorescens*. It consists of 1734 metabolites (including 1450 intracellular metabolites) involved in 1721 reactions (including 288 membrane transport reactions). There are 1057 enzyme-coded genes (17% of total 6162 total sequenced genes) assigned into 25 subsystems or specific pathways. Within these enzyme-coded genes, 291 genes are associated with carbohydrates metabolism, 114 are responsible for stress response, 103 genes are corresponding to the metabolism of aromatic compounds, and 50 genes are involved in phosphorus metabolism. The reconstructed biomass equation can be represented as $C_{31.28}H_{147.89}O_{19.41}N_{8.18}S_{0.22}P_{1.44}$ (mmol/gDW). The complete biomass equation is available in Appendix 1.

P/O ratio, a fundamental parameter for understanding ATP synthesis, indicates the number of ATP molecules synthesized by oxidative phosphorylation for each pair of electrons [78]. The compartmentation of electron transport chain (ETC) is listed in Table 3.1, and the overall ETC equation can be obtained by eliminating the common intermediates (see Equation 3.1 below). It suggests that a P/O ratio of 11/8 for this model (i.e., to generate 11 moles of ATP, it requires the consumption of 8 moles of oxygen atoms). This ratio is lower than the average P/O ratio, indicating relatively more electron acceptors are required during ATP generation [79]. Consequently, it impairs the growth of *P. fluorescens* under anaerobic conditions.

The overall ETC can be shown as follows:

$$11\ ADP + 11\ Phosphate + 8\ NADH + 19\ H^+ + 4\ O_2 <=> 19\ H_2O + 11\ ATP + 8\ NAD^+ \quad (3.1)$$

Table 3.1 Compartmentation of electron transport chain in *P. fluorescens*

Complex	Reaction
Complex I	$2\ NADH_{[c0]} + 9\ H^{+}_{[c0]} + 2\ Ubiquinone\text{-}8_{[c0]} <=> 2\ NAD^{+}_{[c0]} + 7\ H^{+}_{[p0]} + 2\ Ubiquinol\text{-}8_{[c0]}$
Complex III	$Ubiquinol\text{-}8_{[c0]} + 2\ Cytochrome\ c3^{+}_{[c0]} <=> 2\ H^{+}_{[p0]} + 2\ Cytochrome\ c2^{+}_{[c0]} + Ubiquinone\text{-}8_{[c0]}$
Complex IV	$O_{2[c0]} + 4\ H^{+}_{[c0]} + 4\ Cytochrome\ c2^{+}_{[c0]} <=> 2\ H_2O_{[c0]} + 4\ Cytochrome\ c3^{+}_{[c0]}$
Complex V	$ADP_{[c0]} + Phosphate_{[c0]} + 4\ H^{+}_{[p0]} <=> H_2O_{[c0]} + ATP_{[c0]} + 3\ H^{+}_{[c0]}$

e0, extracellular compartment; p0, periplasmic compartment; c0, cytosolic compartment.

3.4.2 Central metabolism

Central metabolic pathway of *P. fluorescens* has been analyzed *in silico* with glucose as the sole carbon source under both aerobic and anaerobic conditions. A complete list of reactions involved can be found in Appendix 2. Briefly, there are 231 enzyme-coded genes involved in glucose metabolism distributed into 10 subsystems, including amino acids and derivatives (34.72%), fatty acid metabolism (18.06%), and nucleosides metabolism (14.81%). The simulation result suggested that, under aerobic condition, when glucose uptake rates at 10 $\frac{mmol}{gDW \cdot h}$, the biomass growth rate was 0.744 $\frac{mmol}{gDW \cdot h}$. The biomass yield coefficient was 0.413 $\frac{g\ Biomass}{g\ Glucose}$. The glycolytic pathway for *P. fluorescens* is illustrated in Figure 3.2. Because of lack of the 6-phosphofructo-1-kinase, *P. fluorescens* SBW25 does not have the Embden-Meyerhof-Parnas (EMP) pathway while it has an additional Entner-Doudoroff (ED) pathway in glycolysis. There is only one ATP produced in ED pathway, which is half as much as the EMP pathway [80]. In ED pathway, KDPG is the only phosphorylated product from glucose and further cleavage into glyceraldehyde 3-phosphate (G3P) and pyruvate. As pyruvate did not support the formation of ATP, ATP can only be produced from G3P. In contrast to ED pathway, there are two triose-phosphates, G3P and dihydroxyacetone phosphate, can produce ATP in EMP pathway [81]. This indicates that *P. fluorescens* SBW25 is relatively more energy dependent [80]. Moreover, the gluconeogenesis pathway was found. β-D-glucose 6-phosphate was formed in glycolysis from 6-phospho-D-glucono-1,5-lactone with 12.58% efflux. This kind of carbon cycle may enhance *P. fluorescens* to counteract environmental stress [82].

The anaerobic growth of *P. fluorescens* by using the nitrate as the terminal electron acceptor has been studied [83]. It was validated by the presence of nitrate reductase in the model. Either glucose or fructose can be used as the sole carbon source for *P. fluorescens* growth. *In silico* anaerobic growth with glucose as the sole carbon source was performed. As can be seen in Table 3.2, the biomass growth rate under anaerobic condition was 0.590 $\frac{mmol}{gDW \cdot h}$ which was 79.3% of the biomass growth rate under aerobic condition when glucose uptake rate kept at 10 $\frac{mmol}{gDW \cdot h}$. The phosphate, hydrogen and sulfate uptake rates under anaerobic growth condition were also 79.3% of the ones under aerobic growth condition. However, the nitrate uptake rate increased from 4.780 $\frac{mmol}{gDW \cdot h}$ under aerobic growth condition to 64.121 $\frac{mmol}{gDW \cdot h}$ under anaerobic condition while nitrite was produced with 60.330 $\frac{mmol}{gDW \cdot h}$ as the reduced product. This significant increase of the nitrate uptake rate under the anaerobic growth conditions was owing to that the nitrate was used as the electron acceptor instead of oxygen. The reduction of 1 mole of nitrate to nitrite can only utilize 1 mole of electron while 1 mole of oxygen can consume 4 moles of electrons. The H_2O and CO_2 production rates are all increased under anaerobic condition than those under aerobic condition. It can be explained by, according to the simulation result, under the anaerobic growth conditions more carbon flux went to TCA cycle (10.419 $\frac{mmol}{gDW \cdot h}$) in comparison to the one under the aerobic growth condition (8.105 $\frac{mmol}{gDW \cdot h}$) while CO_2 was one of the metabolites from TCA cycle. As the glucose was the sole carbon source, with limited glucose, a higher CO_2 production rate would lead to a lower biomass growth rate and higher H_2O production rate.

Table 3.2 Glucose metabolism under aerobic growth and anaerobic growth conditions

	Reactant ($\frac{mmol}{gDW \cdot h}$)						**Product ($\frac{mmol}{gDW \cdot h}$)**			
Objective functions	Glucose	O_2	Phosphate	H^+	Nitrate	Sulfate	H_2O	CO_2	Biomass	Nitrite
Aerobic	10	22.538	0.762	5.094	4.780	0.157	39.811	35.684	0.744	-
Anaerobic	10	-	0.604	4.041	64.121	0.124	43.749	40.711	0.590	60.330

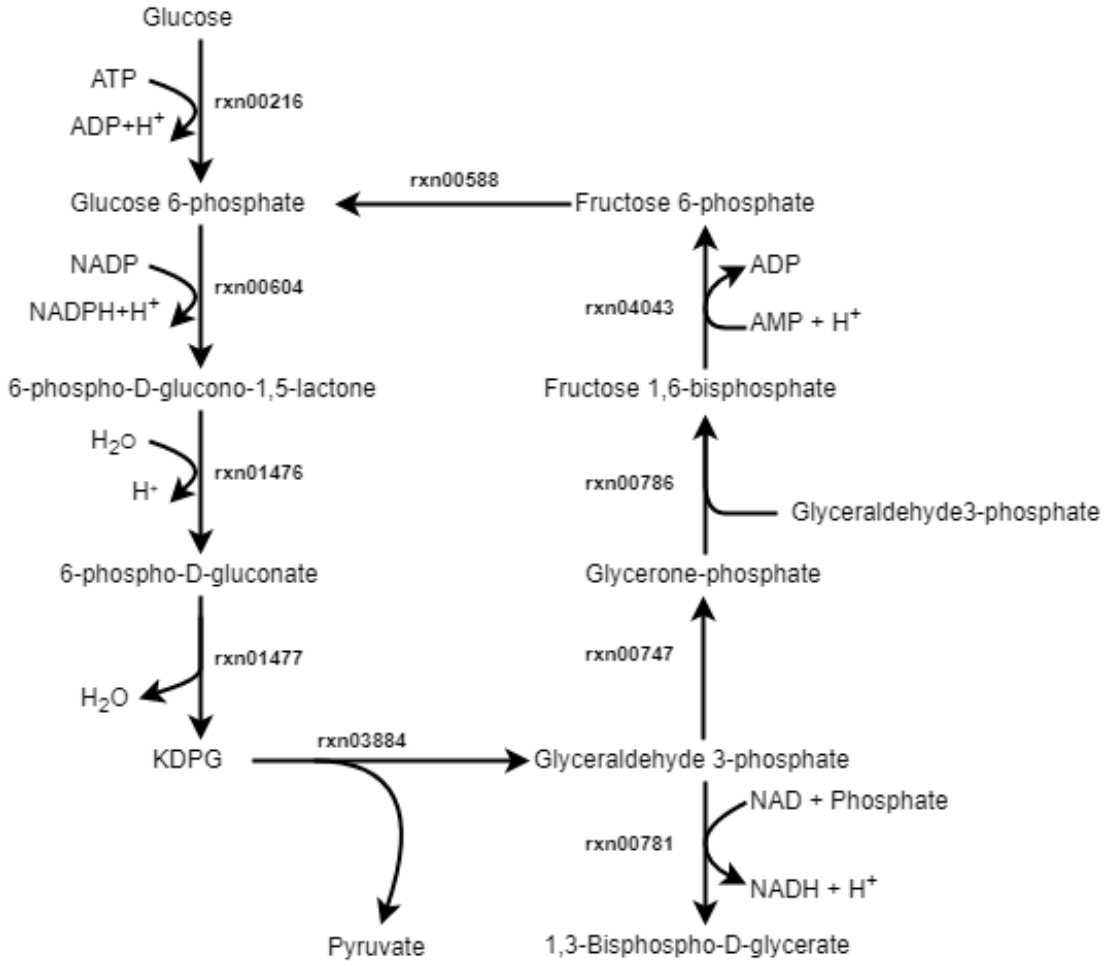

Figure 3.2 ED pathway in glycolysis for *P. fluorescens*

3.4.3 β-ketoadipate pathway

The carbon bonds on aromatic ring of PAH recalcitrant for bacteria [84]. Ring cleavage and ring fission are generally two step processes during aromatic biodegradation [85]. In ring cleavage, a dehydroxylate benzene ring is usually formed by mono-deoxygenation step while the tricarboxylic acid cycle intermediate was produced in ring fission step [85]. The ketoadipate pathway is such a pathway within which the aromatic hydrocarbon rings are being cleaved. In this pathway, catechol plays a crucial role in the ring cleavage phase of the process.

The metabolism of *P. fluorescens* using catechol as the sole carbon source was investigated under oxygen sufficient condition. The simulation condition and results are listed in Table 3.3. The detailed information can be seen in Appendix 3. There are 230 reactions involved in catechol metabolism under aerobic growth condition includes amino acids and derivatives (36.7%), carbohydrates (15.9%), and protein metabolism (15.5%). Figure 3.3 illustrates the metabolic pathway of catechol by *P. fluorescence*. Aromatic ring in catechol was oxidized by catechol 1,2-dioxygenase to cis,cis-muconate. Even though catechol 1,2-dioxygenase contains 1.3 g atoms of iron per mole of protein, its activity is inhibited by $FeSO_4$ and $FeCl_3$ [86]. Acetyl-CoA and succinyl-CoA are formed in the ring fission step. Citrate and malonyl-CoA are two major derivatives from acetyl-CoA. 105% efflux entered TCA cycle through citrate while 32.7% efflux from malonyl-CoA which is the precursor for phospholipid. The biomass yield coefficient was 0.708 $\frac{g\ biomass}{g\ catechol}$.

Table 3.3 *In silico* catechol metabolism with the objective to maximize biomass growth rate

	Reactant ($\frac{\mathbf{mmol}}{\mathbf{gDW \cdot h}}$)						**Product ($\frac{\mathbf{mmol}}{\mathbf{gDW \cdot h}}$)**		
Objective functions	O_2	Phosphate	H^+	Nitrate	Sulfate	Catechol	H_2O	CO_2	Biomass
Maximization of biomass growth rate	2.103	0.065	0.439	0.412	0.013	0.823	0.695	2.842	0.064

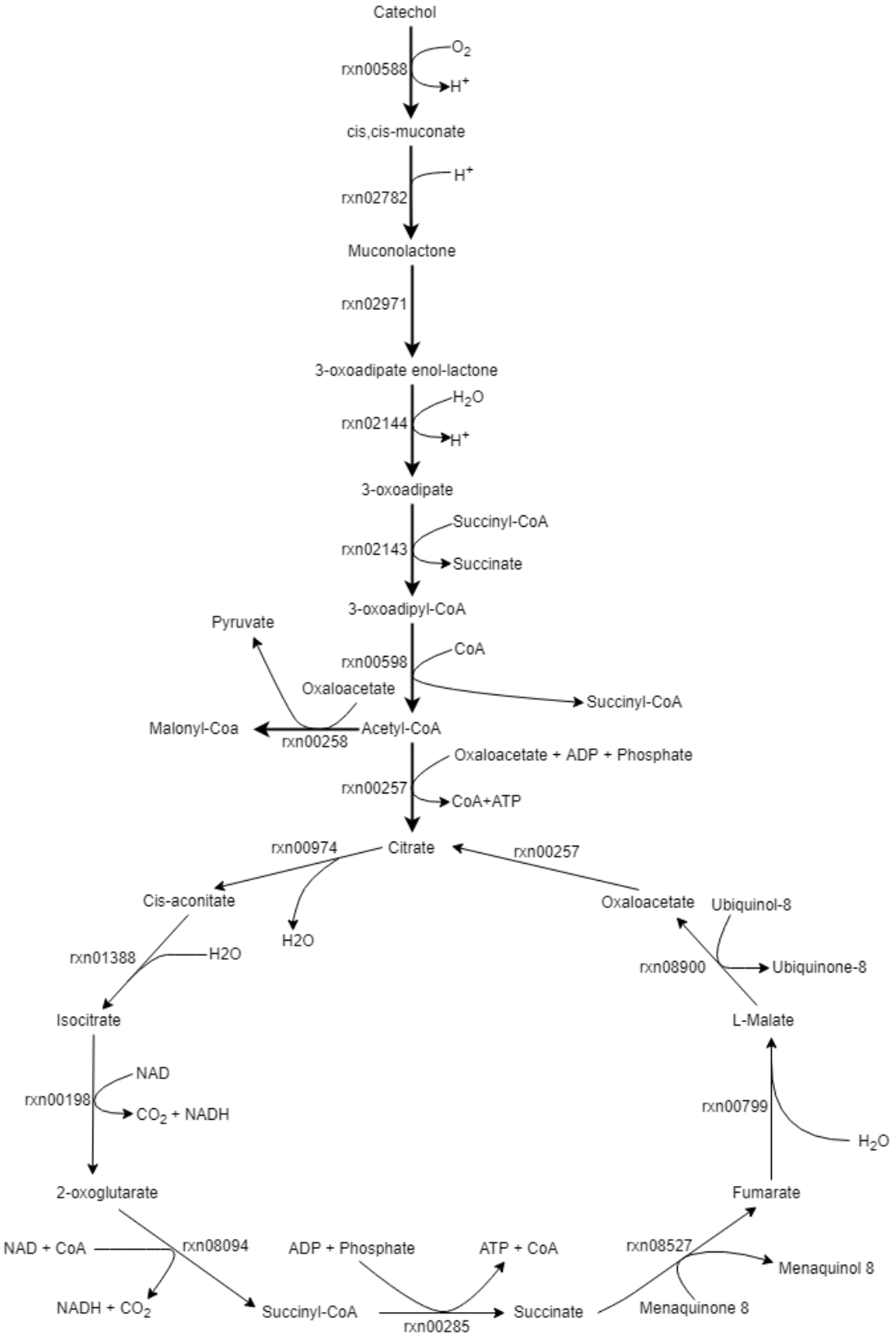

Figure 3.3 Catechol biodegradation pathway for *P. fluorescens*

3.4.4 Phenotype analysis

During BTEX degradation, it has been reported that nitrate, sulfate and phosphate were important ingredients to accelerate the degradation process [22]. To correlate their relationship to the growth rate in terms of biomass of *P. fluorescens* during catechol degradation, phenotype analysis was performed. Some microorganisms may use nitrate and sulfate as the terminal electron acceptor [16]. However, during the anaerobic simulation, sulfate cannot be used as terminal electron acceptor for *P. fluorescens*. The biomass growth rate has a linear relationship with sulfate and phosphate uptakes rates with coefficient 0.218 $\frac{mmol\ sulfate}{gDW\ biomass}$ and 1.068 $\frac{mmol\ phosphate}{gDW\ biomass}$, respectively. The effect of oxygen and nitrate uptake rates on specific biomass growth rate is illustrated in Figure 3.4. Under a specified biomass growth rate, an inverse correlation between oxygen uptake rate and nitrate uptake rate is observed. For example, to have a biomass growth rate of 0.23 h^{-1}, the oxygen uptake rate should be greater than 3 $\frac{mmol}{gDW \cdot h}$ while the nitrate uptake rate should keep at 5 $\frac{mmol}{gDW \cdot h}$ or greater. Furthermore, there is no biomass synthesized without oxygen uptake. This indicates that oxygen is essential for biomass growth by using catechol as the sole carbon source. In the other word, catechol can not be used the sole carbon source for *P. fluorescens* under strict anaerobic condition.

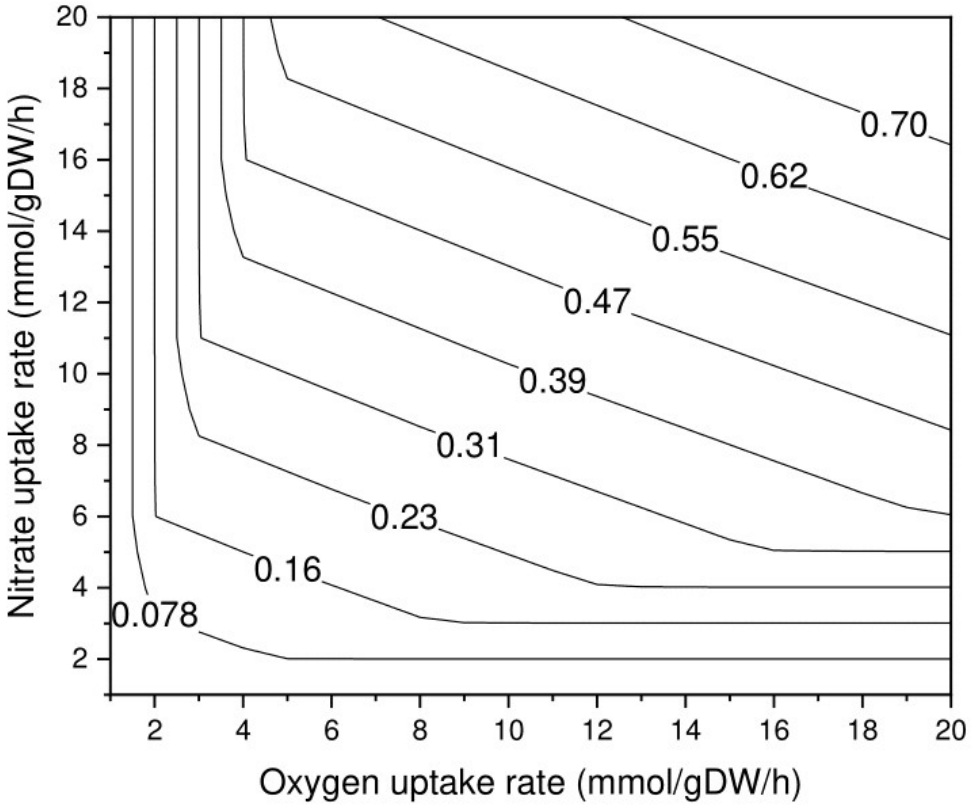

Figure 3.4 Phenotype analysis for oxygen and nitrate uptake rates in specific biomass growth rate for *P. fluorescens*

3.4.5 Model validation

The biomass growth profile and catechol degradation profile are illustrated in Figure 3.5. Based on this figure, the maximum specific growth rate and the catechol uptake rate were estimated as 0.072 h^{-1} and 0.823 $\frac{mmol}{gDW \cdot h}$, respectively. The *in silico* growth of *P. fluorescens* was performed with the objective of maximizing biomass growth rate under a constant catechol uptake rate at 0.823 $\frac{mmol}{gDW \cdot h}$. The reconstructed model predicts that the maximum specific growth rate is 0.064 h^{-1}. The 90% consistency between the *in vitro* and *in silico* maximum specific growth rate indicates that the reported GSMM can be implemented to estimate the intracellular metabolic flux distribution within *P. fluorescens* when catechol is used as the sole carbon source.

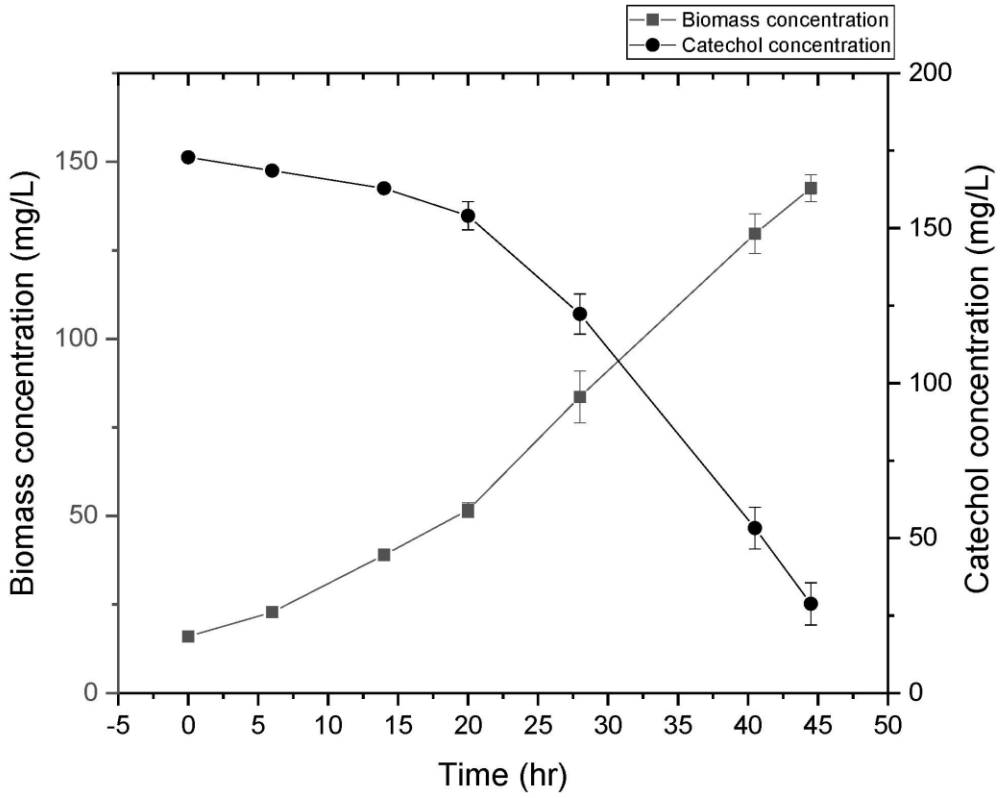

Figure 3.5 Growth profile by using catechol as sole carbon source for *P. fluorescens*

3.5 Conclusions

The first GSMM for *P. fluorescens* SBW25 termed lCW1057 was reconstructed. This model elucidates that the ED pathway is the pathway used by *P. fluorescens* during glycolysis. The built-in β-ketoadipate pathway can portray catechol degradation. Catechol, being an essential metabolic intermediate during BTEX degradation, was used to experimentally demonstrate the validity of the model. There is 10% difference in term of maximum specific growth rate between *in silico* and *in vitro* data when catechol was used as the sole carbon source. This GSMM can be applied to guide future bacterial manipulation and medium optimization during PAH bioremediation by *P. fluorescens*.

4 Concluding remarks

This thesis was prepared in manuscript-based format. The first manuscript reports the characterization of isolated *P. fluorescens* on the degradation of catechol. The second manuscript reports the reconstruction of a genome-scale metabolic model of the *P. fluorescens*.

The objective of the first manuscript (Chapter 2) was to investigate effects of nitrate, sulfate and phosphate ions on catechol biodegradation by the isolated *P. fluorescens* strain. The experiment was planned based on a 2^3 factorial design. The experimental results suggest that dosing nitrate ions alone would impose catechol bioremediation performance by *P. fluorescens*. The interactive effects between nitrate and sulfate ions can enhance catechol bioremediation performance. Introducing phosphate ions can lead to a better catechol bioremediation performance. These observations may help to optimizing medium to accelerate catechol degradation by *P. fluorescens*.

The reconstruction and analysis of the first GSMM for *P. fluorescens* was presented in the second manuscript (Chapter 3). The model was reconstructed by using bottom-up reconstruction strategy and validated by *in vitro* fermentation data. From the reconstructed model, glucose and catechol metabolism pathways were elucidated.

5 Recommendations and future works

5.1 Recommendation for Chapter 2

The effects of nutrients from seed medium on the bioremediation performance should be quantified and analyzed. It is speculated that the accumulation of byproducts during the denitrication process impaired the catechol bioremediation performance by *P. fluorescens*. Therefore, the concentrations of nitrate, nitrite, and ammonia need to be monitored during the course of biodegradation in order to identify the key inhibitory factors, lowering bioremediation performance. Furthermore, it is also postulated that organic acids were secreted when phosphate was involved. To validate this postulation, the pH value should be monitored during the catechol degradation process. To further understand bioremediation performance *P. fluorescens*, *in situ* or pilot plan size remediation investigation should be performed.

5.2 Recommendation for Chapter 3

There is no experimental data available about the biomass constitution of *P. fluorescens*. Therefore, during the reconstruction of GSMM, the biomass was constructed based on the biomass information of *P. putida*. To reconstruct a more accurate GSMM of *P. fluorescens*, its biomass constitution is suggested to be determined experimentally.

References

[1] S. Adipah, "Introduction of petroleum hydrocarbons contaminants and its human effects," *Journal of Environmental Science and Public Health,* vol. 3, no. 1, pp. 1-9, 2018.

[2] U.S. national repsonse team, "On Scene Coordinator Report Deepwater Horizon Oil Spill," 2011.

[3] National Oceanic and Atmospheric Administration, "Deepwater horizon incident," National Oceanic and Atmospheric Administration, [Online]. Available: https://oceanservice.noaa.gov/deepwaterhorizon/. [Accessed 01 09 2019].

[4] S. Kauppi, A. Sinkkonen and M. Romantschuk, "Enhancing bioremediation of diesel-fuel-contaminated soil in a boreal climate: Comparison of biostimulation and bioaugmentation," *International Biodeterioration & Biodegradation,* vol. 65, no. 2, pp. 359-368, 2011.

[5] X. Fu, X. Gu, S. Lu, V. Sharma, M. Brusseau, Y. Xue, M. Danish, G. Fu, Z. Qiu and Q. Sui, "Benzene depletion by Fe^{2+} catalyzed sodium percarbonate in aqueous solution," *Chemical Engineering Journal,* vol. 309, pp. 22-29, 2017.

[6] U.S. House of Representatives, ""Underground storage tanks: Hearing before the Subcommittee on Energy and Agriculture of the Committee on Small Business," U.S. Government Printing Office, Washington DC, 1988.

[7] Agency for toxic substances and disease registry, "Substance Priority List," 2017.

[8] A. Louis and F. Paolo, "Reassessing benzene cancer risks using internal doses," *Rish Analysis,* vol. 12, no. 3, pp. 401-410, 1992.

[9] B. Spycher, J. Lupatsch, A. Huss and J. Rischewski, "Parental occupational exposure to benzene and the risk of childhood cancer: A census-based cohort study," *Environment International,* vol. 07, no. 22, pp. 84-91, 2017.

[10] M. Kanehisa and S. Goto, "KEGG: Kyoto encyclopedia of genes and genomes," *Nucleic Acids Research,* vol. 28, pp. 27-30, 2000.

[11] N. Schweigert, J. Alexander, J. Zehnder and R. Eggen, "Chemical properties of catechols and their molecular modes of toxic action in cells from microoorganisms to mammals," *Environmenal Microbiology,* vol. 3, no. 81-91, 2001.

[12] B. Bukowska and S. Kowalska, "Phenol and catechol induce prehemolytic and hemolytic changes in human erythrocytes," *Toxicology Letters,* vol. 152, no. 1, pp. 73-84, 2004.

[13] S. Surendra, B. Mahalingam and M. Velan, "Degradation of monoaromatics by *Bacillus pumilus* MVSV3," *Brazilian Arichives of Biology and Technology*, vol. 60, p. 1678, 2017.

[14] G. Masciandaro, C. Macci, E. Peruzzi, B. Ceccanti and S. Doni, "Organic matter–microorganism–plant in soil bioremediation: a synergic approach," *Reviews in Environmental Science and Biotechnology*, vol. 12, pp. 399-419, 2013.

[15] D. Adriano, J. Bollag, W. Frankenberger and R. Sims, Biodegradation of contaminated soils, American Society of Agronomy, 1999.

[16] J. Cunningham, H. Rahme, G. Hopkins, C. Lebron and M. Reinhard, "Enhanced *in situ* bioremediation of BTEX-contaminated groundwater by combined injection of nitrate and sulfate," *Environmental Science & Technology*, vol. 35, pp. 1663-1670, 2001.

[17] M. Megaraj, B. Ramakrishnan, K. Venkateswarlu, N. Sethunathan and R. Naidu, "Bioremediation approaches for organic pollutants: a critical perspective.," *Environment International,* vol. 37, no. 8, pp. 1362-1375, 2011.

[18] K. Rockne and K. Reddy, Bioremediation of Contaminated Sites, Chicago: University of Illinois, 2003.

[19] F. Chaillan, C. Chaineau, V. Point, A. Saliot and J. Oudot, "Factors inhibiting bioremediation of soil contaminated with weathered oils and drill cuttings," *Environmental Pollution,* vol. 144, no. 1, pp. 255-265, 2006.

[20] R. Margesin and F. Schinner, "Biodegradation and bioremediation of hydrocarbons in extreme environments.," *Applied Microbiology and Biotechnology.,* vol. 56, pp. 650-663, 2001.

[21] G. Adams, P. Fufeyin, S. Okoro and I. Ehinomen, "Bioremediation, biostimulation and bioaugmention: A Review," *International Journal of Environmental Bioremediation & Biodegradation,* pp. 28-39, 2015.

[22] W. Xiong, C. Mathies, K. Bradshaw, T. Carlson, K. Tang and Y. Wang, "Benzene removal by a novel modification of enhanced anaerobic biostimulation," *Water Research,* vol. 46, pp. 4721-4731, 2012.

[23] C. Liang, C. Huang and Y. Chen, "Potential for activated persulfate degradation of BTEX contamination," *Water Research,* vol. 42, no. 15, pp. 4091-4100, 2008.

[24] P. Sturman, P. Stewart, A. Cunninghan, E. Bouwer and J. Wolfram, "Engineering scale-up of *in situ* bioremediation processes: a review," *Journal of Contaminant Hydrology,* vol. 19, no. 6, pp. 171-203, 1995.

[25] B. Brady, C. Kao, K. Dooley, F. Nkopf and R. Gambrell, "Supercritical extraction of toxic organics from soils," *Industrial & Engineering Chemistry Research,* vol. 26, no. 2, pp. 261-268, 1987.

[26] R. Zytner, Organic Compounds in Unsaturated Soil, Guelph: University of Guelph, 2002.

[27] C. Chen and R. Taylor, "Thermophilic biodegradation of BTEX by two *Thermus species*.," *Biotechnology and Bioengineering,* vol. 48, no. 6, pp. 614-624, 1995.

[28] M. Alexander, Biodegradation and bioremediation, Academic Press: London, 1999.

[29] K. Hara and A. Kondo, "ATP regulation in bioproduction," *Microbial Cell Factories,* vol. 14, 2015.

[30] K. Kurita, "Chitin and chitosan: functional biopolymers from matine crustaceans," *Marine Biotechnology,* vol. 8, pp. 203-226, 2006.

[31] E. Guibal, "Heterogeneous catalysis on chitosan-based materials: a review," *Progress in polymer science,* vol. 30, pp. 71-109, 2005.

[32] A. Angelim, S. Costa, C. Farias, L. Aquino and V. Melo, "An innovative bioremediaiton strategy using a bacterial consortium entrapped in chitosan beads," *Journal of Environmental Management,* no. 127, pp. 10-17, 2013.

[33] J. Monk, J. Nogales and B. Palsson, "Optimizing genome-scale network reconstructions," *Nature Biotechnology,* vol. 32, pp. 447-452, 2014.

[34] J. Orth, I. Thiele and B. Palsson, "What is flux balance analysis?," *Nature Biotechnology,* vol. 28, pp. 245-248, 2010.

[35] J. Teal and R. Howarth, "Oil spill studies: A review of ecological effects," *Environmental Management,* vol. 8, pp. 27-43, 1984.

[36] P. Alvarez and W. Illman, Bioremediation and natural attenuation: Process fundamentals and mathematical models, Hoboken: Wiley, 2006.

[37] D. Gibson, J. Koch and R. Kallio, "Oxidative degradation of aromatic hydrocarbons by microorganisms. I. Enzymic formation of catechol from benzene," *Biochemistry,* vol. 7, no. 7, pp. 2653-2662, 1968.

[38] D. Dobslaw and K. Engesser, "Degradation of toluene by ortho cleavage enzymes in *Burkholderia fungorum* FLU100," *Microbial Biotechnology,* vol. 8, no. 1, pp. 143-154, 2014.

[39] C. Aitken, D. Jones and S. Larter, "Anaerobic hydrocarbon biodegradation in deep subsurface oil reservoirs," *Nature,* vol. 431, pp. 291-294, 2004.

[40] L. Eriksson, L. Hallbeck, T. Ankner, K. Abrahamsson and A. Sjoling, "Indicators of petroleum hydrocarbon biodegradation in anaerobic granitic groundwater," *Geomicrobiology Journal,* vol. 23, pp. 45-48, 2008.

[41] A. Chauhan, Fazluirrahman, G. John and K. Rakesh, "Bacterial metabolism of polycyclic aromatic hydrocarbons: strategies for bioremediation," *Indian Journal of Microbiology,* vol. 48, pp. 95-113, 2008.

[42] B. Stallwood, J. Shears and K. Hughes, "Low temperature bioremediation of oil-contaminated soil using biostimulation and bioaugmentation with a *Pseudomonas sp*. from maritime Antarctica," *Journal of Applied Microbiology,* vol. 99, pp. 794-802, 2005.

[43] F. Suja, F. Rahim, M. Taha, N. Hambali, M. Razali, M. Khalid and A. Hamzad, "Effects of local microbial bioaugmentation and biostimulation on the bioremediation of total petroleum hydrocarbons (TPH) in crude oil contaminated soil based on laboratory and field observations," *International Biodeteroration & Biodegradation,* vol. 90, pp. 115-122, 2014.

[44] P. Raghavan and M. Vivekanandan, "Bioremediation of oil-spilled sites through seeding of naturally adapted *Pseudomonas putida*," *International Biodeterioration & Biodegradation,* vol. 44, pp. 29-32, 1999.

[45] P. Gkrezis, M. Daghio, A. Franzetti, J. Hamme, W. Sillen and J. Vangronsveld, "The interaction between plants and bacteria in the remediation of petroleum hydrocarbons: An environmental perspective," *Frotiers,* vol. 7, 2016.

[46] E. Silva, A. Fialho, I. Sa-Correia, R. Burns and L. Shaw, "Combined bioaugmentation and biostimulation to cleanup soil contaminated with high concentrations of atrazine," *Environmental Science & Technology,* vol. 38, no. 2, pp. 632-637, 2004.

[47] M. Fan, R. Xie and G. Qin, "Bioremediation of petroleum-contaminated soil by a combined system of biostimulation-bioaugmentation with yeast," *Environmental Technology*, vol. 35, no. 4, pp. 391-399, 2013.

[48] S. Hutchins, D. Miller and A. Thomas, "Combined laboratory/field study on the use of nitrate for *in situ* bioremediation of a fuel-contaminated aquifer," *Environmental Science and Technology,* vol. 32, pp. 1832-1840, 1998.

[49] H. Sweed, P. Bedient and S. Hutchins, "Surface appliacation system for in situ groundwater bioremediation: Site characterizetion and modeling," *Groundwater,* vol. 34, pp. 211-222, 1996.

[50] C. Scala, D. DeYong, H. Darlington, R. Sirabian, R. Aravena and R. Fisher, "Treatability comparison of biosparging and enhanced anaerobic oxidation as remediation alternatives for BTEX in groundwater," in *International Symposium on Bioremediation and Sustainable Environmental Technologies*, 2011.

[51] M. James, "Ecology of denitrification and dissimilatory nitrate reduction to ammonium," in *Environmental Microbiology of Anaerobes*, N.Y., John Wiley and Sons, 1988, pp. 179-244.

[52] J. Almeida, M. Reis and M. Carrondo, "Competition between nitrate and nitrite reduction in denitrification by *Pseudomonas fluorescens*," *Biotechnology and Bioengineering,* vol. 46, no. 5, 1995.

[53] M. Samuelsson, P. Cadez and L. Gustafsson, "Heat production by the denitrifying bacterium *Pseudomonas fluorescens* and the dissimilatory ammonium-producing bacterium *Pseudomonas putrefaciens* during anaerobic growth with nitrate as the

electron acceptor," *Applied and Environmental Microbiology,* vol. 54, no. 9, pp. 2220-2225, 1998.

[54] J. Bollag and N. Henninger, "Effects of nitrite toxicity on soil bacteria under aerobic and anaerobic conditions," *Soil Biology and Biochemistry,* vol. 10, no. 5, pp. 337-381, 1978.

[55] M. Kanehisa, "Toward understanding the origin and evolution of cellular organisms," *Protein Science,* 2019.

[56] M. Kanehisa, Y. Sato, M. Furumichi, K. Morishima and M. Tanabe, "New approach for understanding genome variations in KEGG," *Nucleic Acids Research,* vol. 47, pp. 590-595, 2019.

[57] C. Scott, M. Hilton, C. Coppin, R. Russell, J. Oakeshott and T. Sutherland, "A global response to sulfur starvation in *Pseudomonas putida* and its relationship to the expression of low-sulfur-content proteins.," *FEMS Microbiology Letters,* vol. 2, pp. 184-193, 2006.

[58] A. Roychoudhury and G. Merrett, "Redox pathways in a petroleum contaminated shallow sandy aquifer: Iron and sulfate reductions," *Science of The Toltal Environment,* vol. 366, pp. 262-274, 2006.

[59] J. Kleikemper, M. Schroth, W. Sigler, M. Schmucki, S. Bernascni and J. Zeyer, "Activity and diversity of sulfate-reducing bacteria in a petroleum hydrocarbon-contaminated aquifer," *Applied and Environmental Microbiology,* vol. 68, pp. 1516-1523, 2002.

[60] H. Muftah, A. Shaheen and M. Souzan, "Biodegradation of phenol by *Pseudomonas putida* immobilized in polyvinyl alcohol (PVA) gel," *Journal of Hazrdous Materials,* vol. 164, no. 2-3, pp. 720-725, 2009.

[61] X. Huang and Y. Lin, "Reconstruction and analysis of a three-compartment genome-scale metabolic model for *Pseudomonas fluorescens*," *Biotechnology and applied biochemistry*, doi 10.1002/bab.1852, 2020.

[62] C. Cleveland and D. Liptzin, "C:N:P stoichiometry in soil: is there a ‘‘Redfield ratio’’ for the microbial biomass?," *Biogeochemistry*, vol. 85, pp. 235-252, 2007.

[63] V. Ponsin, B. Coulomb, Y. Guelorget, J. Maier and P. Hohener, "*In situ* biostimulation of petroleum hydrocarbon degradation by nitrate and phosphate injection using a dipole well configuration," *Journal of Contaminant Hydrology*, vol. 171, pp. 22-31, 2014.

[64] E. Hoberg, P. Marschner and R. Lieberei, "Organic acid exudation and pH changes by *Gordonia sp.* and *Pseudomonas fluorescens* grown with P adsorbed to goethite," *Microbiological Research*, vol. 160, pp. 177-187, 2005.

[65] H. Rodriguez and R. Fraga, "Phosphate solubilizing bacteria and their role in plant growth promotion," *Biotechnology Advances*, vol. 17, pp. 319-339, 1999.

[66] K. Park, C. Lee and H. Son, "Mechanism of insoluble phosphate solubilization by *Pseudomonas fluorescens* RAF15 isolated from ginseng rhizosphere and its plant growth-promoting activities.," *Letters in Applied Microbiology*, vol. 49, 2009.

[67] V. Nguyen, Y. Park, H. Yang, J. Yu and T. Lee, "Effect of the cathode potential and sulfate ions on nitrate reduction in a microbial electrochemical denitrification system," *Journal of Industrial Microbiology & Biotechnology*, vol. 43, pp. 783-793, 2016.

[68] M. Silby, A. Tarrage, G. Vernikos, S. Giddens, R. Jackson, G. Preston, X. Zhang, C. Moon and S. Gehrig, "Genomic and genetic analyses of diversity and plant interactions of *Pseudomonas fluorescens*," *Genome Biology*, vol. 10, 2009.

[69] M. Schaechter, Encyclopedia of Microbiology, San Diego: Academic Press, 2009.

[70] H. Shim, B. Hwang, S. Lee and S. Kong, "Kinetics of BTEX biodegradation by a coculture of *Pseudomonas putida* and *Pseudomonas fluorescens* under hypoxic conditions," *Biodegradation,* vol. 16, 2005.

[71] N. Rao, "Nitrate pollution and its distribution in the groundwater of Srikakulam district, Andhra Pradesh, India," *Environmental Geology,* vol. 51, p. 631–645, 2006.

[72] Z. Ma, C. Ye, W. Deng, M. Xu, Q. Wang, G. Liu, F. Wang, L. Liu, Z. Xu, G. Shi and Z. Ding, "Reconstruction and analysis of a genome-scale metabolic model of *Ganoderma iucidum* for improved extracellular polysaccharide production," *Systems Microbiology,* vol. 26, pp. 354-364, 2018.

[73] F. Santos, J. Boele and B. Teusink, "A practical guide to genome-scale metabolic models and their analysis.," *Methods in Enzymology*, vol. 500, pp. 500-509, 2011.

[74] Q. Yuan, P. Li, T. Hao, F. Li, Z. Wang, X. Zhao, T. Chen and I. Goryanin, "Pathway-consensus approach to metabolic network reconstruction for *Pseudomonas putida* KT2440 by systematic comparison of published models," *Plos One,* vol. 12, 2017.

[75] R. Senger and E. Papoutsakis, "Genome-scale model for *Clostridium acetobutylicum*: Part I. metabolic network resolution and analysis," *Biotechnology and Bioengeering,* p. 1036–1052, 2008.

[76] S. Maleki, R. Hrudikova, B. Zotchev and H. Ertesvag, "Identification of a new phosphatase enzyme potentially involved in the sugar phosphate stress response in *Pseudomonas fluorescens*," *Applied and Environmental Microbiology,* vol. 83, 2017.

[77] J. Nogales, J. García and E. Díaz, "Degradation of aromatic compounds in *Pseudomonas*: A systems biology view," in *Handbook of Hydrocarbon and Lipid Microbiology*, Springer, 2017.

[78] S. Ferguson, "ATP synthase: From sequence to ring size to the P/O ratio," *National Academy of Sciences* , pp. 16755-16756, 2010.

[79] C. Kempes, P. Bodegom, D. Wolpert, E. Libby, J. Amend and T. Hoehler, "Drivers of bacterial maintenance and minimal energy requirements," *Frontiers in Microbiology,* p. 31, 2017.

[80] A. Flamholz, E. Noor, A. Even, W. Liebermeister and R. Milo, "Glycolytic strategy as a tradeoff between energy yield and protein cost," *PNAS,* pp. 10039-10044, 2013.

[81] A. Even, A. Flamholz, E. Noor and R. Milo, "On the biochemical logic of metabolic pathways," *Nature Chemical Biology,* vol. 8, no. 6, pp. 509-517, 2012.

[82] B. Vu, M. Chen, R. Crawford and E. Ivanova, "Bacterial extracellular polysaccharides involved in biofilm formation," *Molecules,* vol. 14, 2009.

[83] L. Bopp and H. Ehrlich, "Chromate resistance and reduction in *Pseudomonas fluorescens* strain LB300," *Archives of Microbiology,* pp. 426-431, 1988.

[84] A. Ragauskas and T. Well, "Biotechnological opportunities with the β-ketoadipate pathway," *Trends in Biotechnology,* vol. 30, no. 12, pp. 627-637, 2012.

[85] C. Harwood and R. Parales, "The β-ketoadipate pathway and the biology of self-identify," *Annual Review of Microbiology,* pp. 553-590, 1996.

[86] K. Aoki, T. Konohana, R. Shinke and H. Nishira, "Purification and characterization of catechol 1,2-dioxygenase from aniline-assimilating *Rhodococcus erythropolis* AN-13," *Agricultural and Biological Chemistry,* vol. 48, pp. 2087-2095, 1984.

Appendix

Appendix A Biomass information

The macromolecule composition of *P. fluorescens* was taken from reference or determined in this work. However, the sum of biomass composition is 1035 (mg/gDW). Therefore, the biomass composition was normalized with factor at 0.966.The biomass composition was simplified as equation shown below

Biomass = 0.966 Protein + 0.966 DNA + 0.966 RNA + 0.966 Phospholipid + 0.966 Peptidoglycan

Table A.1 Macromolecule composition for *P. fluorescens* SBW 25 biomass

Macromolecule	Composition (mg/gDW)	Comments
Protein	696.68	Taken from Yuan et al. (2017)*
DNA	36.05	Determined in this study
RNA	206.10	Determined in this study
Phospholipid	71.56	Taken from Sohn et al. (2010)**
Peptidoglycan	24.60	Taken from Yuan et al. (2017)*

*Q. Yuan, P. Li, T. Hao, F. Li, Z. Wang, X. Zhao, T. Chen and I. Goryanin, "Pathway-Consensus Approach to Metabolic Network Reconstruction for *Pseudomonas putida* KT2440 by Systematic Comparison of Published Models," *Plos One*, 2017

**S. Sohn, T. Kim, S. Lee and J. Park, "*In silico* genome-scale metabolic analysis of *Pseudomonas putida* KT2440 for polyhydroxyalkanoate synthesis, degradation of aromatics and anaerobic survival," *Biotechnology Journal*, vol. 5, pp. 739-750, 2010.

The macromolecules information can be found in following tables.

Table A.2 Composition for protein in *P. fluorescens* SBW 25 biomass

Table A.3 Composition for DNA in *P. fluorescens* SBW 25 biomass

Table A.4 Composition for RNA in *P. fluorescens* SBW 25 biomass

Table A.5 Composition for phospholipid in *P. fluorescens* SBW 25 biomass

Table A.6 Composition for peptidoglycan in *P. fluorescens* SBW 25 biomass

Table A.2 Composition for protein in *P. fluorescens* SBW 25 biomass *

Coded name	Component	Composition (mmol/gDW)	Molar mass (g/mol)	Composition (mg/gDW)
M_cpd00035_c0	Alanine	5.51×10^{-1}	89.09	49.04
M_cpd00051_c0	Arginine	2.34×10^{-1}	246.20	57.56
M_cpd00132_c0	Asparagine	2.24×10^{-1}	132.12	29.57
M_cpd00041_c0	Aspartate	2.24×10^{-1}	133.11	29.79
M_cpd00084_c0	Cysteine	0.81×10^{-1}	121.16	9.80
M_cpd00023_c0	Glutamate	2.58×10^{-1}	147.13	37.93
M_cpd00053_c0	Glutamine	2.58×10^{-1}	146.14	37.67
M_cpd00033_c0	Glycine	4.61×10^{-1}	75.07	34.58
M_cpd00119_c0	Histidine	0.09	155.15	13.95
M_cpd00322_c0	Isoleucine	1.88×10^{-1}	147.17	27.64
M_cpd00107_c0	Leucine	4.35×10^{-1}	131.17	56.99
M_cpd00039_c0	Lysine	2.41×10^{-1}	146.19	35.19
M_cpd00060_c0	Methionine	1.37×10^{-1}	149.21	20.41
M_cpd00066_c0	Phenylalanine	1.83×10^{-1}	165.19	30.20
M_cpd00129_c0	Proline	2.18×10^{-1}	115.13	25.07
M_cpd00054_c0	Serine	2.36×10^{-1}	105.09	24.78
M_cpd00161_c0	Threonine	2.32×10^{-1}	119.12	27.61
M_cpd00065_c0	Tryptophan	0.51×10^{-1}	204.23	10.40
M_cpd00069_c0	Tyrosine	1.32×10^{-1}	181.19	23.89
M_cpd00156_c0	Valine	2.96×10^{-1}	117.15	34.63
M_cpd00002_c0	ATP	40	507.16	20280.40
M_cpd00001_c0	H_2O	40	18.02	720.80
Product				
M_cpd00009_c0	phosphate	40	95.98	3839.20
M_cpd00008_c0	ADP	40	427.18	17080.20
M_Protein_c0	Protein	1000		696.68

*Q. Yuan, P. Li, T. Hao, F. Li, Z. Wang, X. Zhao, T. Chen and I. Goryanin, "Pathway-consensus approach to metabolic network reconstruction for *Pseudomonas putida* KT2440 by systematic comparison of published models," *Plos One,* 2017.

Table A.3 Composition for DNA in *P. fluorescens* SBW 25 biomass

Coded name	Component	Composition (mmol/gDW)	Molar mass (g/mol)	Composition (mg/gDW)
M_cpd00241_c0	dGTP	1.74×10^{-2}	504.16	8.62
M_cpd00356_c0	dCTP	1.74×10^{-2}	467.13	7.94
M_cpd00115_c0	dATP	1.13×10^{-2}	491.16	5.40
M_cpd00357_c0	dTTP	1.14×10^{-2}	482.14	5.30
M_cpd00002_co	ATP	4.39	507.16	2225.73
M_cpd00001_C0	H_2O	4.39	18.02	79.02
Product				
M_cpd00008_c0	ADP	4.39	427.18	1874.53
M_cpd00009_c0	phosphate	4.39	95.98	421.44
M_DNA_c0	DNA	1000		36.05

Table A.4 Composition for RNA in *P. fluorescens* SBW 25 biomass

Coded name	Component	Composition (mmol/gDW)	Molar mass (g/mol)	Composition (mg/gDW)
M_cpd00062_c0	UTP	8.13×10^{-2}	484.12	39.41
M_cpd00038_c0	GTP	1.24×10^{-1}	522.16	64.98
M_cpd00052_c0	CTP	1.00×10^{-1}	482.13	48.51
M_cpd00002_c0	ATP	1.35	507.16	684.45
M_cpd00001_c0	H_2O	1.25	18.02	22.53
Product				
M_cpd00008_c0	ADP	1.25	427.18	533.75
M_cpd00009_c0	phosphate	1.25	95.98	119.98
M_RNA_c0	RNA	1000		206.10

Table A.5 Composition for phospholipid in *P. fluorescens* SBW 25 biomass **

Coded name	Component	Composition (mmol/gDW)	Molar mass (g/mol)	Composition (mg/gDW)
M_Phosphatidylglycerol_c0	Phosphatidylglycerol	4.76×10^{-3}	3.91×10^{3}	18.60
M_Phosphatidylethanolamine_c0	Phosphatidylethanolamine	1.21×10^{-3}	3.47×10^{4}	41.87
M_Cardiolipin_c0	Cardiolipin	1.87×10^{-4}	5.95×10^{4}	11.10
Product				
M_Lipid_c0	Lipid	1000		71.56

**S. Sohn, T. Kim, S. Lee and J. Park, "*In silico* genome-scale metabolic analysis of *Pseudomonas putida* KT2440 for polyhydroxyalkanoate synthesis, degradation of aromatics and anaerobic survival," *Biotechnology Journal,* vol. 5, pp. 739-750, 2010.

Table A.6 Composition for peptidoglycan in *P. fluorescens* SBW 25 biomass*

Coded name	Component	Composition (mmol/gDW)	Molar mass (g/mol)	Composition (mg/gDW)
Ecoil_pep	Peptidoglycan subunit of Escherichia coli	2.48×10^{-2}	990.97	24.60
Product				
M_Peptidoglycan_c0	Peptidoglycan	1000.00		24.60

* Q. Yuan, P. Li, T. Hao, F. Li, Z. Wang, X. Zhao, T. Chen and I. Goryanin, "Pathway-consensus approach to metabolic network reconstruction for *Pseudomonas putida* KT2440 by systematic comparison of published models," *Plos One,* 2017.

Appendix B *P fluorescens* glucose metabolism

Table B.1 *P. fluorescens in silico* glucose metabolism Part 1

Coded reaction id	Reaction name	Flux (mmol/gDW/h)	Normalized flux (mmol/gDW/h)
R_rxn10042_c0	F1_ATPase_c0	48.6931	486.9307
R_rxn10113_c0	cytochrome_oxidase_bo3_ubiquinol_8__25_protons_c0	37.8481	378.4805
R_rxn10122_c0	NADH_dehydrogenase_ubiquinone_8__35_protons_c0	22.0936	220.9357
R_rxn08900_c0	FAD_dependent_malate_dehydrogenase_c0	15.7545	157.5448
R_rxn00154_c0	pyruvate:NAD+ 2-oxidoreductase CoA-acetylating	12.3336	123.3362
R_rxn08094_c0	2_Oxoglutarate_dehydrogenase_complex_c0	11.6032	116.0317
R_rxn01476_c0	6_Phospho_D_glucono_1_5_lactone_lactonohydrolase_c0	11.2587	112.5875
R_rxn03884_c0	2_dehydro_3_deoxy_D_gluconate_6_phosphate_D_glyceraldehyde_3_phosphate_lyase_c0	11.2149	112.1494
R_rxn01477_c0	6_Phospho_D_gluconate_hydro_lyase2_dehydro_3_deoxy_6_phospho_D_gluconate_forming_c0	11.2149	112.1494
R_rxn00216_c0	ATP_D_glucose_6_phosphotransferase_c0	10.0000	100.0000
R_rxn00604_c0	D_glucose_6_phosphate_NADP_plus__1_oxidoreductase_c0	10.0000	100.0000
R_rxn00001_c0	diphosphate_phosphohydrolase_c0	9.8026	98.0258
R_rxn00257_c0	acetyl_CoA_oxaloacetate_C_acetyltransferase_pro_S_carboxymethyl_forming__ADP_phosphorylating_c0	8.1054	81.0541
R_rxn00974_c0	citrate_hydro_lyase_cis_aconitate_forming_c0	8.1054	81.0541
R_rxn01388_c0	isocitrate_hydro_lyase_cis_aconitate_forming_c0	8.1054	81.0541
R_rxn00198_c0	isocitrate_transfer	8.1054	81.0541
R_rxn00182_c0	L_glutamate_NAD_plus__oxidoreductase_deaminating_c0	7.9061	79.0612
R_rxn10806_c0	cytochrome_oxidase_bd_menaquinol_8__2_protons_periplasm_c0	6.6325	66.3249
R_rxn00097_c0	ATP_AMP_phosphotransferase_c0	5.1771	51.7711
R_rxn00187_c0	L_Glutamate_ammonia_ligase_ADP_forming_c0	4.9410	49.4105

R_rxn10121_c0	Nitrate_reductase_Menaquinol_8_periplasm_c0	4.7798	47.7983
R_rxn05627_c0	nitrate_transport_in_via_proton_symport_c0	4.7798	47.7983
R_rxn00770_c0	ATP_D_ribose_5_phosphate_diphosphotransferase_c0	4.5438	45.4377
R_rxn03137_c0	10_Formyltetrahydrofolate_5_phosphoribosyl_5_amino_4_imidazolecarboxamide_formyltransferase_c0	4.2758	42.7577
R_rxn02473_c0	D_erythro_1_Imidazol_4_ylglycerol_3_phosphate_hydro_lyase_c0	4.2758	42.7577
R_rxn03175_c0	N_5_Phospho_D_ribosylformimino_5_amino_1__5_phospho_D_ribosyl_4_imidazolecarboxamide_ketol_isomerase_c0	4.2758	42.7577
R_rxn00859_c0	L_Histidinol_NAD_plus__oxidoreductase_c0	4.2758	42.7577
R_rxn01211_c0	5_10_Methenyltetrahydrofolate_5_hydrolase_decyclizing_c0	4.2758	42.7577
R_rxn02160_c0	L_Histidinol_phosphate_phosphohydrolase_c0	4.2758	42.7577
R_rxn02835_c0	1_5_phospho_D_ribosyl_AMP_1_6_hydrolase_c0	4.2758	42.7577
R_rxn02834_c0	Phosphoribosyl_ATP_pyrophosphohydrolase_c0	4.2758	42.7577
R_rxn03135_c0	R04558_c0	4.2758	42.7577
R_rxn00789_c0	1_5_phospho_D_ribosyl_ATP_diphosphate_phospho_alpha_D_ribosyl_transferase_c0	4.2758	42.7577
R_rxn00237_c0	ATP_GDP_phosphotransferase_c0	4.2633	42.6327
R_rxn01642_c0	4_imidazolone_5_propanoate_amidohydrolase_c0	4.2111	42.1109
R_rxn01640_c0	N_Formimino_L_glutamate_iminohydrolase_c0	4.2111	42.1109
R_rxn00867_c0	L_histidine_ammonia_lyase_urocanate_forming_c0	4.2111	42.1109
R_rxn00800_c0	N6_1_2_dicarboxyethylAMP_AMP_lyase_fumarate_forming_c0	4.1740	41.7397
R_rxn00838_c0	IMP_L_aspartate_ligase_GDP_forming_c0	4.1740	41.7397
R_rxn05465_c0	Malonyl_CoA_acyl_carrier_protein_S_malonyltransferase_c0	2.7351	27.3513
R_rxn00568_c0	NIRBD_RXNc_c0	2.6785	26.7846
R_rxn00569_c0	Nitrite_reductase_NADPH_c0	2.1014	21.0138
R_rxn00785_c0	D_Fructose_6_phosphate_D_glyceraldehyde_3_phosphate_glycolaldehyde_transferase_c0	1.6148	16.1475
R_rxn01200_c0	Sedoheptulose_7_phosphate_D_glyceraldehyde_3_phosphate_glycolaldehyde_transferase_c0	1.3517	13.5171
R_rxn01975_c0	beta_D_Glucose_6_phosphate_NADP_plus__1_oxoreductase_c0	1.2587	12.5875
P_Acid_8	P_Acid8	0.7187	7.1870
R_rxn01102_c0	ATP_R_glycerate_3_phosphotransferase_c0	0.7102	7.1022
R_rxn00420_c0	O_phospho_L_serine_phosphohydrolase_c0	0.7102	7.1022
R_rxn01101_c0	3_Phospho_D_glycerate_NAD_plus__2_oxidoreductase_c0	0.7102	7.1022
R_rxn00781_c0	D_glyceraldehyde_3_phosphate_NAD_plus__oxidoreductase_phosphorylating_c0	0.7102	7.1022
R_rxn00148_c0	ATP_pyruvate_2_O_phosphotransferase_c0	0.5437	5.4372
Malate_buildin	pyruvate_to_oxobuanoate	0.5254	5.2537
R_rxn05329_c0	(3R)-3-Hydroxybutanoyl-[acyl-carrier-protein] hydro-lyase	0.4559	4.5586
R_rxn05334_c0	(3R)-3-Hydroxybutanoyl-[acyl-carrier-protein] hydro-lyase	0.4559	4.5586
R_rxn05330_c0	(3R)-3-Hydroxybutanoyl-[acyl-carrier-protein] hydro-lyase	0.4559	4.5586

R_rxn05322_c0	Butyryl-[acyl-carrier protein]:malonyl-CoA C-acyltransferase(decarboxylating oxoacyl- and enoyl-reducing)	0.4559	4.5586
R_rxn05326_c0	Hexanoyl-[acyl-carrier protein]:malonyl-CoA C-acyltransferase(decarboxylating oxoacyl- and enoyl-reducing)	0.4559	4.5586
R_rxn05325_c0	Octanoyl-[acyl-carrier protein]:malonyl-CoA C-acyltransferase(decarboxylating oxoacyl- and enoyl-reducing)	0.4559	4.5586
R_rxn05349_c0	acetyl_CoA_acyl_carrier_protein_S_acetyltransferase_c0	0.4559	4.5586
R_rxn05346_c0	butyryl_acyl_carrier_protein_malonyl_acyl_carrier_protein_C_acyltransferase_decarboxylating_c0	0.4559	4.5586
R_rxn05350_c0	hexanoyl_acyl_carrier_protein_malonyl_acyl_carrier_protein_C_acyltransferase_decarboxylating_c0	0.4559	4.5586
R_rxn05347_c0	Acyl_acyl_carrier_protein_malonyl_acyl_carrier_protein_C_acyltransferase_decarboxylating_c0	0.4559	4.5586
R_rxn05343_c0	Octanoyl_acyl_carrier_protein_malonyl_acyl_carrier_protein_C_acyltransferase_decarboxylating_c0	0.4559	4.5586
R_rxn00904_c0	L_Valine_pyruvate_aminotransferase_c0	0.4489	4.4890
R_rxn05333_c0	(3R)-3-Hydroxybutanoyl-[acyl-carrier-protein] hydro-lyase	0.4148	4.1483
R_rxn05327_c0	Decanoyl-[acyl-carrier protein]:malonyl-CoA C-acyltransferase(decarboxylating oxoacyl- and enoyl-reducing)	0.4148	4.1483
R_rxn05348_c0	Decanoyl_acyl_carrier_protein_malonyl_acyl_carrier_protein_C_acyltransferase_decarboxylating_c0	0.4148	4.1483
R_rxn00747_c0	D_glyceraldehyde_3_phosphate_aldose_ketose_isomerase_c0	0.4057	4.0568
R_rxn05324_c0	Dodecanoyl-[acyl-carrier protein]:malonyl-CoA C-acyltransferase(decarboxylating oxoacyl- and enoyl-reducing)	0.3875	3.8748
R_rxn03240_c0	S_3_Hydroxyhexadecanoyl_CoA_hydro_lyase_c0	0.3875	3.8748
R_rxn05351_c0	Tetradecanoyl-[acyl-carrier protein]:malonyl-CoA C-acyltransferase(decarboxylating oxoacyl- and enoyl-reducing and thioester-hydrolysing)	0.3875	3.8748
R_rxn02804_c0	myristoyl_CoA_acetylCoA_C_myristoyltransferase_c0	0.3875	3.8748
R_rxn05457_c0	Acyl_carrier_protein_acetyltransferase_c0	0.3875	3.8748

R_rxn05331_c0	(3R)-3-Hydroxybutanoyl-[acyl-carrier-protein] hydro-lyase	0.3875	3.8748
R_rxn05345_c0	dodecanoyl_acyl_carrier_protein_malonyl_acyl_carrier_protein_C_acyltransferase_decarboxylating_c0	0.3875	3.8748
R_rxn05335_c0	(3R)-3-Hydroxypalmitoyl-[acyl-carrier-protein] hydro-lyase	0.3875	3.8748
R_rxn05732_c0	acyl_CoA_dehydrogenase_hexadecanoyl_CoA_c0	0.3875	3.8748
R_rxn00114_c0	ATP_carbamate_phosphotransferase_c0	0.3195	3.1953
R_rxn01208_c0	R01652_c0	0.3126	3.1263
R_rxn02789_c0	2_Isopropylmalate_hydro_lyase_c0	0.3126	3.1263
R_rxn00902_c0	acetyl_CoA_3_methyl_2_oxobutanoate_C_acetyltransferase_thioester_hydrolysing__carboxymethyl_forming_c0	0.3126	3.1263
R_rxn03062_c0	3_Isopropylmalate_NAD_plus__oxidoreductase_c0	0.3126	3.1263
R_rxn02213_c0	3_Dehydroquinate_hydro_lyase_c0	0.2630	2.6304
R_rxn01255_c0	5_O_1_Carboxyvinyl_3_phosphoshikimate_phosphate_lyase_chorismate_forming_c0	0.2630	2.6304
R_rxn01739_c0	ATP_shikimate_3_phosphotransferase_c0	0.2630	2.6304
R_rxn02212_c0	2_Dehydro_3_deoxy_D_arabino_heptonate_7_phosphate_phosphate_lyase_cyclyzing_c0	0.2630	2.6304
R_rxn01332_c0	Phosphoenolpyruvate_D_erythrose_4_phosphate_C_1_carboxyvinyltransferase_phosphate_hydrolysing__2_carboxy_2_oxoethyl_forming_c0	0.2630	2.6304
R_rxn02476_c0	Phosphoenolpyruvate_3_phosphoshikimate_5_O_1_carboxyvinyl_transferase_c0	0.2630	2.6304
R_rxn00364_c0	ATP_CMP_phosphotransferase_c0	0.2279	2.2793
R_rxn01256_c0	Chorismate_pyruvatemutase_c0	0.2264	2.2639
R_rxn00409_c0	ATP_CDP_phosphotransferase_c0	0.2154	2.1542
R_rxn05289_c0	NADPH_oxidized_thioredoxin_oxidoreductase_c0	0.1980	1.9800
lysine_formation	lysine4	0.1908	1.9084
R_rxn00790_c0	5_phosphoribosylamine_diphosphate_phospho_alpha_D_ribosyltransferase_glutamate_amidating_c0	0.1818	1.8179
R_rxn00117_c0	ATP_UDP_phosphotransferase_c0	0.1784	1.7843
R_rxn00119_c0	ATP_UMP_phosphotransferase_c0	0.1690	1.6899
R_rxn01434_c0	L_Citrulline_L_aspartate_ligase_AMP_forming_c0	0.1682	1.6818
R_rxn01917_c0	ATP_N_acetyl_L_glutamate_5_phosphotransferase_c0	0.1682	1.6818
R_rxn00192_c0	acetyl_CoA_L_glutamate_N_acetyltransferase_c0	0.1682	1.6818
R_rxn00469_c0	N2_Acetyl_L_ornithine_amidohydrolase_c0	0.1682	1.6818
R_rxn00802_c0	2_Nomega_L_argininosuccinate_arginine_lyase_fumarate_forming_c0	0.1682	1.6818
R_rxn02465_c0	N_acetyl_L_glutamate_5_semialdehyde_NADP_plus__5_oxidoreductase_phosphrylating_c0	0.1682	1.6818

R_rxn01019_c0	Carbamoyl_phosphate_L_ornithine_carbamoyltransferase_c0	0.1682	1.6818
R_rxn00416_c0	L_aspartate_L_glutamine_amido_ligase_AMP_forming_c0	0.1610	1.6099
R_rxn05256_c0	AMP_sulfite_thioredoxin_disulfide_oxidoreductaseadenosine_5_phosphosulfate_forming_c0	0.1567	1.5668
R_rxn00379_c0	ATP_sulfate_adenylyltransferase_c0	0.1567	1.5668
R_rxn05651_c0	sulfate_transport_in_via_proton_symport_c0	0.1567	1.5668
R_rxn01360_c0	(S)-dihydroorotate:fumarate oxidoreductase	0.1514	1.5135
R_rxn00710_c0	orotidine_5_phosphate_carboxy_lyase_UMP_forming_c0	0.1514	1.5135
R_rxn00205_c0	glutathione_hydrogen_peroxide_oxidoreductase_c0	0.1514	1.5135
R_rxn01018_c0	carbamoyl_phosphate_L_aspartate_carbamoyltransferase_c0	0.1514	1.5135
R_rxn01362_c0	Orotidine_5_phosphate_diphosphate_phospho_alpha_D_ribosyl_transferase_c0	0.1514	1.5135
R_rxn12017_c0	R08161	0.1459	1.4587
R_rxn08043_c0	pyruvate:2-oxobutanoate acetaldehydetransferase (decarboxylating)	0.1351	1.3512
R_rxn03436_c0	(S)-2-Aceto-2-hydroxybutanoate:NADP+ oxidoreductase (isomerizing)	0.1351	1.3512
R_rxn03435_c0	(R)-2,3-Dihydroxy-3-methylpentanoate:NADP+ oxidoreductase (isomerizing)	0.1351	1.3512
R_rxn03437_c0	R_2_3_Dihydroxy_3_methylpentanoate_hydro_lyase_c0	0.1351	1.3512
R_rxn01575_c0	L_Isoleucine_2_oxoglutarate_aminotransferase_c0	0.1351	1.3512
R_rxn00737_c0	L_threonine_ammonia_lyase_2_oxobutanoate_forming_c0	0.1351	1.3512
R_rxn08016_c0	palmitate-[acyl-carrier-protein] ligase	0.1322	1.3220
R_rxn10202_c0	glycerol_3_phosphate__acyl_coa_acyltransferase_16_0_c0	0.1322	1.3220
R_rxn08799_c0	Lysophospholipase_L1_2_acylglycerophosphotidate__n_C16_0_periplasm_c0	0.1322	1.3220
R_rxn01000_c0	prephenate_hydro_lyase_decarboxylating_phenylpyruvate_forming_c0	0.1315	1.3152
R_rxn07576_c0	3-oxoacyl-[acyl-carrier-protein] synthase	0.1094	1.0941
R_rxn07577_c0	3-oxoacyl-[acyl-carrier-protein] reductase	0.1094	1.0941
R_rxn07578_c0	R07764_c0	0.1094	1.0941
R_rxn00239_c0	ATP_GMP_phosphotransferase_c0	0.1018	1.0180
R_rxn00834_c0	IMP_NAD_plus__oxidoreductase_c0	0.1018	1.0180
xanthosine_build	XMP	0.1018	1.0180
R_rxn01303_c0	Acetyl_CoA_L_homoserine_O_acetyltransferase_c0	0.0985	0.9846
R_rxn00337_c0	ATP_L_aspartate_4_phosphotransferase_c0	0.0985	0.9846
R_rxn00952_c0	O_acetyl_L_homoserine_hydrogen_sulfide_S_3_amino_3_carboxypropyltransferase_c0	0.0985	0.9846
R_rxn00693_c0	5_Methyltetrahydrofolate_L_homocysteine_S_methyltransferase_c0	0.0985	0.9846
R_rxn01643_c0	L_Aspartate_4_semialdehyde_NADP_plus__oxidoreductase_phosphorylating_c0	0.0985	0.9846
R_rxn01269_c0	Prephenate_NADP_plus__oxidoreductasedecarboxylating_c0	0.0949	0.9487
R_rxn00410_c0	UTP_ammonia_ligase_ADP_forming_c0	0.0847	0.8466

R_rxn00907_c0	5_10_methylenetetrahydrofolate_NADP_plus__oxidoreductase_c0	0.0647	0.6468
R_rxn01115_c0	6_phospho_D_gluconate_NADP_plus__2_oxidoreductase_decarboxylating_c0	0.0438	0.4381
R_rxn02507_c0	1_2_Carboxyphenylamino_1_deoxy_D_ribulose_5_phosphate_carboxy_lyasecyclizing_c0	0.0367	0.3665
R_rxn01964_c0	L_serine_hydro_lyase_adding_1_C_indol_3_ylglycerol_3_phosphate_L_tryptophan_and_glyceraldehyde_3_phosphate_forming_c0	0.0367	0.3665
R_rxn02508_c0	N_5_Phospho_beta_D_ribosylanthranilate_ketol_isomerase_c0	0.0367	0.3665
R_rxn00726_c0	chorismate_pyruvate_lyase_amino_accepting_anthranilate_forming_c0	0.0367	0.3665
R_rxn00791_c0	N_5_Phospho_D_ribosylanthranilate_pyrophosphate_phosphoribosyl_transferase_c0	0.0367	0.3665
R_rxn03638_c0	Acetyl_CoA_D_glucosamine_1_phosphate_N_acetyltransferase_c0	0.0353	0.3527
R_rxn00283_c0	alanine_racemase_c0	0.0353	0.3527
R_rxn00555_c0	L_glutamine_D_fructose_6_phosphate_isomerase_deaminating_c0	0.0353	0.3527
R_rxn00293_c0	UTP_N_acetyl_alpha_D_glucosamine_1_phosphate_uridylyltransferase_c0	0.0353	0.3527
R_rxn00423_c0	acetyl_CoA_L_serine_O_acetyltransferase_c0	0.0352	0.3522
R_rxn00649_c0	O3_acetyl_L_serine_hydrogen_sulfide_2_amino_2_carboxyethyltransferase_c0	0.0352	0.3522
R_rxn05909_c0	L_serine_hydro_lyase_adding_hydrogen_sulfide__L_cysteine_forming_c0	0.0230	0.2300
R_rxn00193_c0	glutamate_racemase_c0	0.0176	0.1763
R_rxn00851_c0	D_alanine_D_alanine_ligase_ADP_forming_c0	0.0176	0.1763
R_rxn02008_c0	UDP_N_acetylmuramoyl_L_alanine_D_glutamate_ligaseADP_forming_c0	0.0176	0.1763
R_rxn02286_c0	UDP_N_acetylmuramate_L_alanine_ligase_ADP_forming_c0	0.0176	0.1763
R_rxn02011_c0	UDP_N_acetylmuramoyl_L_alanyl_D_glutamate_L_meso_2_6_diaminoheptanedioate_gamma_ligase_ADP_forming_c0	0.0176	0.1763
R_rxn03901_c0	undecaprenyl_diphosphate_phosphohydrolase_c0	0.0176	0.1763
R_rxn00461_c0	Phosphoenolpyruvate_UDP_N_acetyl_D_glucosamine_1_carboxyvinyl_transferase_c0	0.0176	0.1763
R_rxn03408_c0	UDP_N_acetyl_D_glucosamine_undecaprenyl_diphospho_N_acetylmuramoyl_L_alanyl_gamma_D_glutamyl_meso_2_6_diaminopimeloyl_D_alanyl_D_alanine_4_beta_N_acetylglucosaminlytransferase_c0	0.0176	0.1763
R_rxn03164_c0	UDP_N_acetylmuramoyl_L_alanyl_D_glutamyl_meso_2_6_diaminoheptanedioate_D_alanyl_D_alanine_ligaseADP_forming_c0	0.0176	0.1763
R_rxn03904_c0	UDP_N_acetylmuramoyl_L_alanyl_gamma_D_glutamyl_meso_2_6_diaminopimeloyl_D_alanyl_D_alanine_undecaprenyl_phosphate_phospho_N_acetylmuramoyl_pentapeptide_transferase_c0	0.0176	0.1763
R_rxn01673_c0	ATP_dCDP_phosphotransferase_c0	0.0125	0.1251
R_rxn01353_c0	ATP_dGDP_phosphotransferase_c0	0.0125	0.1251
R_rxn05233_c0	2_Deoxyguanosine_5_diphosphate_oxidized_thioredoxin_2_oxidoreductase_c0	0.0125	0.1251
R_rxn06076_c0	2_Deoxycytidine_diphosphate_oxidized_thioredoxin_2_oxidoreductase_c0	0.0125	0.1251
R_rxn01520_c0	5_10_Methylenetetrahydrofolate_dUMP_C_methyltransferase_c0	0.0082	0.0819
R_rxn01512_c0	ATP_dTDP_phosphotransferase_c0	0.0082	0.0819
R_rxn01513_c0	ATP_dTMP_phosphotransferase_c0	0.0082	0.0819
R_rxn06075_c0	2_Deoxyuridine_5_diphosphate_oxidized_thioredoxin_2_oxidoreductase_c0	0.0082	0.0819
R_rxn05231_c0	2_Deoxyadenosine_5_diphosphate_oxidized_thioredoxin_2_oxidoreductase_c0	0.0081	0.0812

R_rxn00839_c0	ATP_dADP_phosphotransferase_c0	0.0081	0.0812
P_Acid_2	P_Acid2	0.0046	0.0456
P_Acid_1	P_Acid	0.0046	0.0456
P_Acid_3	P_Acid3	0.0036	0.0355
P_Acid_4	P_Acid4	0.0036	0.0355
P_Acid_5	P_Acid5	0.0009	0.0087
P_Acid_6	P_Acid6	0.0009	0.0087
P_Acid_7	P_Acid7	0.0001	0.0013
R_rxn01517_c0	ATP_dUMP_phosphotransferase_c0	-0.0082	-0.0819
R_rxn00686_c0	5_6_7_8_tetrahydrofolate_NADP_plus__oxidoreductase_c0	-0.0082	-0.0819
R_rxn00313_c0	meso_2_6_diaminoheptanedioate_carboxy_lyase_L_lysine_forming_c0	-0.0176	-0.1763
R_rxn02285_c0	UDP_N_acetylmuramate_NADP_plus__oxidoreductase_c0	-0.0176	-0.1763
R_rxn01485_c0	D_Glucosamine_1_phosphate_1_6_phosphomutase_c0	-0.0353	-0.3527
R_rxn00527_c0	L_tyrosine_2_oxoglutarate_aminotransferase_c0	-0.0949	-0.9487
R_rxn04954_c0	5_methyltetrahydrofolate_NAD_plus__oxidoreductase_c0	-0.0985	-0.9846
R_rxn01301_c0	L_Homoserine_NAD_plus__oxidoreductase_c0	-0.0985	-0.9846
R_rxn00493_c0	L_Phenylalanine_2_oxoglutarate_aminotransferase_c0	-0.1315	-1.3152
R_rxn05332_c0	(3R)-3-Hydroxypalmitoyl-[acyl-carrier-protein] hydro-lyase	-0.1459	-1.4587
R_rxn00086_c0	glutathione_NADP_plus__oxidoreductase_c0	-0.1514	-1.5135
R_rxn01465_c0	S_dihydroorotate_amidohydrolase_c0	-0.1514	-1.5135
R_rxn00503_c0	S_1_pyrroline_5_carboxylate_NAD_plus__oxidoreductase_c0	-0.1567	-1.5668
R_rxn00623_c0	hydrogen_sulfide_NADP_plus__oxidoreductase_c0	-0.1567	-1.5668
R_rxn00929_c0	L_Proline_NAD_plus__5_oxidoreductase_c0	-0.1567	-1.5668
R_rxn01637_c0	N2_Acetyl_L_ornithine_2_oxoglutarate_aminotransferase_c0	-0.1682	-1.6818
R_rxn15112_c0	Ribose-5-phosphate:ammonia ligase (ADP-forming)	-0.1818	-1.8179
R_rxn01973_c0	N_Succinyl_LL_2_6_diaminoheptanedioate_amidohydrolase_c0	-0.1908	-1.9084
R_rxn00908_c0	glycine_synthase_c0	-0.2309	-2.3092
R_rxn05458_c0	Acyl_carrier_protein_acetyltransferase_c0	-0.2553	-2.5528
R_rxn01740_c0	Shikimate_NADP_plus__3_oxidoreductase_c0	-0.2630	-2.6304
R_rxn00506_c0	Acetaldehyde_NAD_plus__oxidoreductase_c0	-0.3019	-3.0185
R_rxn00541_c0	L_threonine_acetaldehyde_lyase_glycine_forming_c0	-0.3019	-3.0185
R_rxn00806_c0	L_Leucine_2_oxoglutarate_aminotransferase_c0	-0.3126	-3.1263
R_rxn02811_c0	3_Isopropylmalate_hydro_lyase_c0	-0.3126	-3.1263
R_rxn03239_c0	S_3_Hydroxyhexadecanoyl_CoA_NAD_plus__oxidoreductase_c0	-0.3875	-3.8748
R_rxn05342_c0	3R_3_Hydroxytetradecanoyl_acyl_carrier_protein_NADP_plus__oxidoreductase_c0	-0.3875	-3.8748
R_rxn00692_c0	5_10_Methylenetetrahydrofolate_glycine_hydroxymethyltransferase_c0	-0.4023	-4.0225
R_rxn00611_c0	sn_Glycerol_3_phosphate_NAD_plus__2_oxidoreductase_c0	-0.4057	-4.0568
R_rxn05340_c0	3R_3_Hydroxydodecanoyl_acyl_carrier_protein_NADP_plus__oxidoreductase_c0	-0.4148	-4.1483
R_rxn05339_c0	3R_3_Hydroxybutanoyl_acyl_carrier_protein_NADP_plus__oxidoreductase_c0	-0.4559	-4.5586

R_rxn05338_c0	3R_3_Hydroxydecanoyl_acyl_carrier_protein_NADP_plus__oxidoreductase_c0	-0.4559	-4.5586
R_rxn05341_c0	3R_3_Hydroxyoctanoyl_acyl_carrier_protein_NADP_plus__oxidoreductase_c0	-0.4559	-4.5586
R_rxn05337_c0	3R_3_Hydroxyhexanoyl_acyl_carrier_protein_NADP_plus__oxidoreductase_c0	-0.4559	-4.5586
R_rxn00903_c0	L_Valine_2_oxoglutarate_aminotransferase_c0	-0.6616	-6.6163
oxaloacetate_buildin	2pdg to 13bdg	-0.7102	-7.1022
R_rxn08647_c0	ATP_R_glycerate_2_phosphotransferase_c0	-0.7102	-7.1022
R_rxn02914_c0	3_Phosphoserine_2_oxoglutarate_aminotransferase_c0	-0.7102	-7.1022
R_rxn02380_c0	beta_D_Glucose_6_phosphate_ketol_isomerase_c0	-1.2587	-12.5875
R_rxn01333_c0	sedoheptulose_7_phosphate_D_glyceraldehyde_3_phosphate_glyceronetransferase_c0	-1.3517	-13.5171
R_rxn00258_c0	Malonyl_CoA_pyruvate_carboxytransferase_c0	-2.7351	-27.3513
R_rxn01116_c0	D_Ribulose_5_phosphate_3_epimerase_c0	-2.9665	-29.6646
R_rxn00777_c0	D_ribose_5_phosphate_aldose_ketose_isomerase_c0	-3.0103	-30.1027
R_rxn02085_c0	4_5_Dihydro_4_oxo_5_imidazolepropanoate_hydro_lyase_c0	-4.2111	-42.1109
R_rxn01652_c0	S_Aminomethyldihydrolipoylprotein_6S_tetrahydrofolate_aminomethyltransferase_ammonia_forming_c0	-4.2111	-42.1109
R_rxn02283_c0	5_Formyltetrahydrofolate_L_glutamate_N_formiminotransferase_c0	-4.2111	-42.1109
R_rxn04043_c0	ADP_D_fructose_6_phosphate_1_phosphotransferase_c0	-4.2605	-42.6047
R_rxn00786_c0	D_fructose_1_6_bisphosphate_D_glyceraldehyde_3_phosphate_lyase_glycerone_phosphate_forming_c0	-4.2605	-42.6047
R_rxn02320_c0	5_Amino_2_oxopentanoate_2_oxoglutarate_aminotransferase_c0	-4.2758	-42.7577
R_rxn00832_c0	IMP_1_2_hydrolase_decyclizing_c0	-4.2758	-42.7577
R_rxn00260_c0	L_Aspartate_2_oxoglutarate_aminotransferase_c0	-4.9139	-49.1394
R_rxn08527_c0	fumarate_reductase_c0	-11.4123	-114.1233
R_rxn00285_c0	Succinate_CoA_ligase_ADP_forming_c0	-11.6032	-116.0317
R_rxn00799_c0	S_malate_hydro_lyase_fumarate_forming_c0	-15.7545	-157.5448

Table B.1 *P. fluorescens in silico* glucose metabolism Part 2

Coded reaction id	Reaction
R_rxn10042_c0	ADP[c0] + Phosphate[c0] + (4) H+[e0] <=> H2O[c0] + ATP[c0] + (3) H+[c0]
R_rxn10113_c0	(0.5) O2[c0] + (2.5) H+[c0] + Ubiquinol-8[c0] => H2O[c0] + (2.5) H+[e0] + Ubiquinone-8[c0]
R_rxn10122_c0	NADH[c0] + (4.5) H+[c0] + Ubiquinone-8[c0] <=> NAD[c0] + (3.5) H+[e0] + Ubiquinol-8[c0]
R_rxn08900_c0	L-Malate[c0] + Ubiquinone-8[c0] => Oxaloacetate[c0] + Ubiquinol-8[c0]
R_rxn00154_c0	NAD + CoA + Pyruvate => NADH + CO2 + Acetyl-CoA
R_rxn08094_c0	NAD[c0] + CoA[c0] + 2-Oxoglutarate[c0] <=> NADH[c0] + CO2[c0] + Succinyl-CoA[c0]
R_rxn01476_c0	H2O[c0] + 6-phospho-D-glucono-1-5-lactone[c0] => H+[c0] + 6-Phospho-D-gluconate[c0]
R_rxn03884_c0	2-Keto-3-deoxy-6-phosphogluconate[c0] <=> Pyruvate[c0] + Glyceraldehyde3-phosphate[c0]
R_rxn01477_c0	6-Phospho-D-gluconate[c0] => H2O[c0] + 2-Keto-3-deoxy-6-phosphogluconate[c0]
R_rxn00216_c0	ATP[c0] + D-Glucose[c0] <=> ADP[c0] + H+[c0] + D-glucose-6-phosphate[c0]
R_rxn00604_c0	NADP[c0] + D-glucose-6-phosphate[c0] <=> NADPH[c0] + H+[c0] + 6-phospho-D-glucono-1-5-lactone[c0]
R_rxn00001_c0	H2O[c0] + PPi[c0] => (2) Phosphate[c0] + H+[c0]
R_rxn00257_c0	ATP[c0] + CoA[c0] + Citrate[c0] <=> ADP[c0] + Phosphate[c0] + Acetyl-CoA[c0] + Oxaloacetate[c0]
R_rxn00974_c0	Citrate[c0] <=> H2O[c0] + cis-Aconitate[c0]
R_rxn01388_c0	Isocitrate[c0] <=> H2O[c0] + cis-Aconitate[c0]
R_rxn00198_c0	NAD + Isocitrate => NADH + CO2 + 2-oxoglutarate
R_rxn00182_c0	NADH[c0] + NH3[c0] + 2-Oxoglutarate[c0] + H+[c0] <=> H2O[c0] + NAD[c0] + L-Glutamate[c0]
R_rxn10806_c0	(0.5) O2[c0] + (2) H+[c0] + Menaquinol 8[c0] => H2O[c0] + (2) H+[e0] + Menaquinone 8[c0]
R_rxn00097_c0	ATP[c0] + AMP[c0] + H+[c0] <=> (2) ADP[c0]
R_rxn00187_c0	H2O[c0] + NADP[c0] + L-Glutamate[c0] <=> NADPH[c0] + NH3[c0] + 2-Oxoglutarate[c0] + H+[c0]
R_rxn10121_c0	(2) H+[c0] + Nitrate[c0] + Menaquinol 8[c0] <=> H2O[c0] + (2) H+[e0] + Nitrite[c0] + Menaquinone 8[c0]

R_rxn05627_c0	H+[e0] + Nitrate[e0] <=> H+[c0] + Nitrate[c0]
R_rxn00770_c0	ATP[c0] + ribose-5-phosphate[c0] <=> AMP[c0] + H+[c0] + PRPP[c0]
R_rxn03137_c0	10-Formyltetrahydrofolate[c0] + AICAR[c0] <=> Tetrahydrofolate[c0] + FAICAR[c0]
R_rxn02473_c0	D-erythro-imidazol-glycerol-phosphate[c0] => H2O[c0] + imidazole acetol-phosphate[c0]
R_rxn03175_c0	H+[c0] + phosphoribosylformiminoaicar-phosphate[c0] <=> phosphoribulosylformimino-AICAR-phosphate[c0]
R_rxn00859_c0	H2O[c0] + (2) NAD[c0] + L-Histidinol[c0] <=> (2) NADH[c0] + (3) H+[c0] + L-Histidine[c0]
R_rxn01211_c0	H2O[c0] + 5-10-Methenyltetrahydrofolate[c0] <=> H+[c0] + 10-Formyltetrahydrofolate[c0
R_rxn02160_c0	H2O[c0] + L-histidinol-phosphate[c0] => Phosphate[c0] + L-Histidinol[c0]
R_rxn02835_c0	H2O[c0] + Phosphoribosyl-AMP[c0] <=> phosphoribosylformiminoaicar-phosphate[c0]
R_rxn02834_c0	H2O[c0] + Phosphoribosyl-ATP[c0] => PPi[c0] + (2) H+[c0] + Phosphoribosyl-AMP[c0]
R_rxn03135_c0	L-Glutamate[c0] + (2) H+[c0] + D-erythro-imidazol-glycerol-phosphate[c0] + AICAR[c0] <= L-Glutamine[c0] + phosphoribulosylformimino-AICAR-phosphate[c0]
R_rxn00789_c0	PPi[c0] + H+[c0] + Phosphoribosyl-ATP[c0] <= ATP[c0] + PRPP[c0]
R_rxn00237_c0	ATP[c0] + GDP[c0] <=> ADP[c0] + GTP[c0]
R_rxn01642_c0	H2O[c0] + H+[c0] + 4-Imidazolone-5-propanoate[c0] => N-Formimino-L-glutamate[c0]
R_rxn01640_c0	H2O[c0] + N-Formimino-L-glutamate[c0] <=> NH3[c0] + N-Formyl-L-glutamate[c0]
R_rxn00867_c0	L-Histidine[c0] => NH3[c0] + Urocanate[c0]
R_rxn00800_c0	Adenylosuccinate[c0] <=> AMP[c0] + Fumarate[c0]
R_rxn00838_c0	GTP[c0] + L-Aspartate[c0] + IMP[c0] => Phosphate[c0] + GDP[c0] + (2) H+[c0] + Adenylosuccinate[c0]
R_rxn05465_c0	H+[c0] + Malonyl-CoA[c0] + ACP[c0] <=> CoA[c0] + Malonyl-acyl-carrierprotein-[c0]
R_rxn00568_c0	D-glucose-6-phosphate[c0] <=> D-fructose-6-phosphate[c0]
R_rxn00569_c0	(2) H2O[c0] + (3) NADP[c0] + NH3[c0] <= (3) NADPH[c0] + (5) H+[c0] + Nitrite[c0]
R_rxn00785_c0	D-fructose-6-phosphate[c0] + Glyceraldehyde3-phosphate[c0] <=> D-Xylulose5-phosphate[c0] + D-Erythrose4-phosphate[c0]
R_rxn01200_c0	Glyceraldehyde3-phosphate[c0] + Sedoheptulose7-phosphate[c0] <=> ribose-5-phosphate[c0] + D-Xylulose5-phosphate[c0]

R_rxn01975_c0	NADP[c0] + beta-D-Glucose 6-phosphate[c0] <=> NADPH[c0] + H+[c0] + 6-phospho-D-glucono-1-5-lactone[c0]
P_Acid_8	Phosphatidylglycerol + Phosphatidylethanolamine + Cardiolipin -> Lipid
R_rxn01102_c0	ATP[c0] + Glycerate[c0] <=> ADP[c0] + H+[c0] + 3-Phosphoglycerate[c0]
R_rxn00420_c0	H2O[c0] + phosphoserine[c0] => Phosphate[c0] + L-Serine[c0]
R_rxn01101_c0	NAD[c0] + 3-Phosphoglycerate[c0] <=> NADH[c0] + H+[c0] + 3-Phosphonooxypyruvate[c0]
R_rxn00781_c0	NAD[c0] + Phosphate[c0] + Glyceraldehyde3-phosphate[c0] <=> NADH[c0] + H+[c0] + 1,3-Bisphospho-D-glycerate[c0]
R_rxn00148_c0	ATP[c0] + Pyruvate[c0] <=> ADP[c0] + Phosphoenolpyruvate[c0] + H+[c0]
Malate_buildin	H+ + Pyruvate + NADPH -> NADP+ CO2 + H2O + 3-Methyl-2-oxobutanoate
R_rxn05329_c0	1 (R)-3-Hydroxybutanoyl-[acyl-carrier protein] [0] <-> 1 H2O [0] + 1 But-2-enoyl-[acyl-carrier protein] [0]
R_rxn05334_c0	1 (R)-3-Hydroxyoctanoyl-[acyl-carrier protein] [0] <-> 1 H2O [0] + 1 (2E)-Octenoyl-[acp] [0]
R_rxn05330_c0	1 D-3-Hydroxyhexanoyl-[acp] [0] <-> 1 H2O [0] + 1 (2E)-Hexenoyl-[acp] [0]
R_rxn05322_c0	1 NAD [0] + 1 Butyryl-ACP [0] -> 1 NADH [0] + 2 H+ [0] + 1 But-2-enoyl-[acyl-carrier protein] [0]
R_rxn05326_c0	1 NAD [0] + 1 Hexanoyl-ACP [0] <- 1 NADH [0] + 1 H+ [0] + 1 (2E)-Hexenoyl-[acp] [0
R_rxn05325_c0	1 NAD [0] + 1 Octanoyl-ACP [0]<- 1 NADH [0] + 1 H+ [0] + 1 (2E)-Octenoyl-[acp] [0]
R_rxn05349_c0	Acetyl-CoA[c0] + ACP[c0] <=> CoA[c0] + Acetyl-ACP[c0]
R_rxn05346_c0	Butyryl-ACP[c0] + Malonyl-acyl-carrierprotein-[c0] => CO2[c0] + 3-Oxohexanoyl-[acp][c0] + ACP[c0]
R_rxn05350_c0	H+[c0] + Hexanoyl-ACP[c0] + Malonyl-acyl-carrierprotein-[c0] => CO2[c0] + 3-oxooctanoyl-acp[c0] + ACP[c0]
R_rxn05347_c0	Malonyl-acyl-carrierprotein-[c0] + Acetyl-ACP[c0] => CO2[c0] + Acetoacetyl-ACP[c0] + ACP[c0]
R_rxn05343_c0	Octanoyl-ACP[c0] + Malonyl-acyl-carrierprotein-[c0] => CO2[c0] + 3-oxodecanoyl-acp[c0] + ACP[c0]
R_rxn00904_c0	Pyruvate[c0] + L-Valine[c0] <=> L-Alanine[c0] + 3-Methyl-2-oxobutanoate[c0]
R_rxn05333_c0	(R)-3-Hydroxydecanoyl-[acyl-carrier protein] [0] <-> 1 H2O [0] + 1 H+ [0] + 1 (2E)-Decenoyl-[acp] [0]
R_rxn05327_c0	1 NAD [0] + 1 Decanoyl-ACP [0] <- 1 NADH [0] + 2 H+ [0] + 1 (2E)-Decenoyl-[acp] [0]
R_rxn05348_c0	Decanoyl-ACP[c0] + Malonyl-acyl-carrierprotein-[c0] => CO2[c0] + 3-oxododecanoyl-acp[c0] + ACP[c0]

R_rxn00747_c0	Glyceraldehyde3-phosphate[c0] <=> Glycerone-phosphate[c0]
R_rxn05324_c0	NAD [0] + 1 Dodecanoyl-ACP [0] <- 1 NADH [0] + 2 H+ [0] + 1 (2E)-Dodecenoyl-[acp] [0
R_rxn03240_c0	(S)-3-Hydroxyhexadecanoyl-CoA[c0] <=> H2O[c0] + (2E)-Hexadecenoyl-CoA[c0]
R_rxn05351_c0	1 NADP [0] + 1 Myristoyl-ACP [0] <- 1 NADPH [0] + 2 H+ [0] + 1 (2E)-Tetradecenoyl-[acp] [0]
R_rxn02804_c0	Acetyl-CoA[c0] + Myristoyl-CoA[c0] <=> CoA[c0] + 3-Oxopalmitoyl-CoA[c0]
R_rxn05457_c0	CoA[c0] + Myristoyl-ACP[c0] <=> Myristoyl-CoA[c0] + ACP[c0]
R_rxn05331_c0	D-3-Hydroxydodecanoyl-[acp] [0] <-> 1 H2O [0] + 1 (2E)-Dodecenoyl-[acp] [0]
R_rxn05345_c0	Dodecanoyl-ACP[c0] + Malonyl-acyl-carrierprotein-[c0] => CO2[c0] + 3-oxotetradecanoyl-acp[c0] + ACP[c0]
R_rxn05335_c0	HMA [0] <-> 1 H2O [0] + 1 (2E)-Tetradecenoyl-[acp] [0]
R_rxn05732_c0	NAD[c0] + Palmitoyl-CoA[c0] <= NADH[c0] + H+[c0] + (2E)-Hexadecenoyl-CoA[c0]
R_rxn00114_c0	ATP[c0] + CO2[c0] + NH3[c0] <=> ADP[c0] + (2) H+[c0] + Carbamoylphosphate[c0]
R_rxn01208_c0	CO2[c0] + 4MOP[c0] <= H+[c0] + 2-isopropyl-3-oxosuccinate[c0]
R_rxn02789_c0	2-Isopropylmalate[c0] <=> H2O[c0] + 2-Isopropylmaleate[c0]
R_rxn00902_c0	CoA[c0] + H+[c0] + 2-Isopropylmalate[c0] <= H2O[c0] + Acetyl-CoA[c0] + 3-Methyl-2-oxobutanoate[c0]
R_rxn03062_c0	NAD[c0] + 3-Isopropylmalate[c0] <=> NADH[c0] + H+[c0] + 2-isopropyl-3-oxosuccinate[c0]
R_rxn02213_c0	5-Dehydroquinate[c0] => H2O[c0] + 3-Dehydroshikimate[c0]
R_rxn01255_c0	5-O--1-Carboxyvinyl-3-phosphoshikimate[c0] => Phosphate[c0] + Chorismate[c0]
R_rxn01739_c0	ATP[c0] + Shikimate[c0] <=> ADP[c0] + H+[c0] + 3-phosphoshikimate[c0]
R_rxn02212_c0	DAHP[c0] => Phosphate[c0] + 5-Dehydroquinate[c0]
R_rxn01332_c0	H2O[c0] + Phosphoenolpyruvate[c0] + D-Erythrose4-phosphate[c0] => Phosphate[c0] + DAHP[c0]
R_rxn02476_c0	Phosphoenolpyruvate[c0] + 3-phosphoshikimate[c0] => Phosphate[c0] + 5-O--1-Carboxyvinyl-3-phosphoshikimate[c0]
R_rxn00364_c0	ATP[c0] + CMP[c0] + H+[c0] <=> ADP[c0] + CDP[c0]
R_rxn01256_c0	Chorismate[c0] => Prephenate[c0]

R_rxn00409_c0	ATP[c0] + CDP[c0] <=> ADP[c0] + CTP[c0]
R_rxn05289_c0	NADPH[c0] + H+[c0] + trdox[c0] <=> NADP[c0] + trdrd[c0]
lysine_formation	N-Succinyl-L-2,6-diaminopimelate + H2O -> L-Lysine + LL-2,6-Diaminopimelate
R_rxn00790_c0	PPi[c0] + L-Glutamate[c0] + H+[c0] + 5-Phosphoribosylamine[c0] <= H2O[c0] + L-Glutamine[c0] + PRPP[c0]
R_rxn00117_c0	ATP[c0] + UDP[c0] <=> ADP[c0] + UTP[c0]
R_rxn00119_c0	ATP[c0] + H+[c0] + UMP[c0] <=> ADP[c0] + UDP[c0]
R_rxn01434_c0	ATP[c0] + L-Aspartate[c0] + Citrulline[c0] <=> PPi[c0] + AMP[c0] + (2) H+[c0] + L-Argininosuccinate[c0]
R_rxn01917_c0	ATP[c0] + N-Acetyl-L-glutamate[c0] <=> ADP[c0] + n-acetylglutamyl-phosphate[c0]
R_rxn00192_c0	ATP[c0] + NH3[c0] + L-Glutamate[c0] => ADP[c0] + Phosphate[c0] + L-Glutamine[c0] + H+[c0]
R_rxn00469_c0	H2O[c0] + N-Acetylornithine[c0] <=> Acetate[c0] + Ornithine[c0]
R_rxn00802_c0	L-Argininosuccinate[c0] <=> L-Arginine[c0] + Fumarate[c0]
R_rxn02465_c0	NADP[c0] + Phosphate[c0] + 2-Acetamido-5-oxopentanoate[c0] <= NADPH[c0] + H+[c0] + n-acetylglutamyl-phosphate[c0]
R_rxn01019_c0	Ornithine[c0] + Carbamoylphosphate[c0] => Phosphate[c0] + H+[c0] + Citrulline[c0]
R_rxn00416_c0	H2O[c0] + ATP[c0] + L-Aspartate[c0] + L-Glutamine[c0] => PPi[c0] + AMP[c0] + L-Glutamate[c0] + (2) H+[c0] + L-Asparagine[c0]
R_rxn05256_c0	APS[c0] + trdrd[c0] => AMP[c0] + H+[c0] + Sulfite[c0] + trdox[c0]
R_rxn00379_c0	ATP[c0] + Sulfate[c0] <=> PPi[c0] + APS[c0]
R_rxn05651_c0	Sulfate[e0] + H+[e0] <=> Sulfate[c0] + H+[c0]
R_rxn01360_c0	1 O2 [0] + 1 S-Dihydroorotate [0] -> 1 H2O2 [0] + 1 Orotate [0]
R_rxn00710_c0	H+[c0] + Orotidylic acid[c0] => CO2[c0] + UMP[c0]
R_rxn00205_c0	H2O2[c0] + (2) GSH[c0] => (2) H2O[c0] + Oxidized glutathione[c0]
R_rxn01018_c0	L-Aspartate[c0] + Carbamoylphosphate[c0] => Phosphate[c0] + H+[c0] + N-Carbamoyl-L-aspartate[c0]
R_rxn01362_c0	PPi[c0] + H+[c0] + Orotidylic acid[c0] <= PRPP[c0] + Orotate[c0]
R_rxn12017_c0	O2 + hexadecanoyl-acp + AH2 => 2 H2O + A + hexadecenoyl-[acyl-carrier protein]

R_rxn08043_c0	Pyruvate [0] + 1 H+ [0] + 1 2-Oxobutyrate [0]-> 1 CO2 [0] + 1 2-Aceto-2-hydroxybutanoate [0]
R_rxn03436_c0	1 2-Aceto-2-hydroxybutanoate [0] <-> 1 (R)-3-Hydroxy-3-methyl-2-oxopentanoate [0]
R_rxn03435_c0	1 NADP [0] + 1 2,3-Dihydroxy-3-methylvalerate [0] <-> 1 NADPH [0] + 1 H+ [0] + 1 (R)-3-Hydroxy-3-methyl-2-oxopentanoate [0]
R_rxn03437_c0	2,3-Dihydroxy-3-methylvalerate[c0] => H2O[c0] + 3MOP[c0]
R_rxn01575_c0	2-Oxoglutarate[c0] + L-Isoleucine[c0] <=> L-Glutamate[c0] + 3MOP[c0]
R_rxn00737_c0	L-Threonine[c0] => NH3[c0] + 2-Oxobutyrate[c0]
R_rxn08016_c0	ATP [0] + 1 Palmitate [0] + 1 ACP [0] <-> 1 PPi [0] + 1 AMP [0] + 2 H+ [0] + 1 Palmitoyl-ACP [0
R_rxn10202_c0	H+[c0] + Glycerol-3-phosphate[c0] + Palmitoyl-CoA[c0] => CoA[c0] + 1-hexadecanoyl-sn-glycerol 3-phosphate[c0]
R_rxn08799_c0	H2O[c0] + 1-hexadecanoyl-sn-glycerol 3-phosphate[c0] <=> (2) H+[c0] + Glycerol-3-phosphate[c0] + Palmitate[c0]
R_rxn01000_c0	H+[c0] + Prephenate[c0] => H2O[c0] + CO2[c0] + Phenylpyruvate[c0]
R_rxn07576_c0	1 H+ [0] + 1 hexadecanoyl-acp [0] + 1 Malonyl-acyl-carrierprotein- [0] -> 1 CO2 [0] + 1 ACP [0] + 1 3-Oxostearoyl-[acp] [0]
R_rxn07577_c0	1 NADPH [0] + 1 H+ [0] + 1 3-Oxostearoyl-[acp] [0] 1 NADP [0] + 1 3-Hydroxystearoyl-[acp] [0]
R_rxn07578_c0	3-Hydroxystearoyl-[acp][c0] <=> H2O[c0] + (2E)-Octadecenoyl-[acp][c0]
R_rxn00239_c0	ATP[c0] + H+[c0] + GMP[c0] <=> ADP[c0] + GDP[c0]
R_rxn00834_c0	H2O[c0] + NAD[c0] + IMP[c0] <=> NADH[c0] + H+[c0] + XMP[c0]
xanthosine_build	ATP[c0] + H2O[c0] + XMP[c0] + L-Glutamine[c0] => H+[c0] + AMP[c0] + L-Glutamate[c0] + PRPP[c0] + GMP[c0]
R_rxn01303_c0	Acetyl-CoA[c0] + L-Homoserine[c0] => CoA[c0] + O-Acetyl-L-homoserine[c0]
R_rxn00337_c0	ATP[c0] + L-Aspartate[c0] <=> ADP[c0] + 4-Phospho-L-aspartate[c0]
R_rxn00952_c0	H2S[c0] + O-Acetyl-L-homoserine[c0] => Acetate[c0] + Homocysteine[c0]
R_rxn00693_c0	Homocysteine[c0] + 5-Methyltetrahydrofolate[c0] <=> L-Methionine[c0] + Tetrahydrofolate[c0]
R_rxn01643_c0	NADP[c0] + Phosphate[c0] + L-Aspartate4-semialdehyde[c0] <= NADPH[c0] + H+[c0] + 4-Phospho-L-aspartate[c0]
R_rxn01269_c0	NADP[c0] + Prephenate[c0] => NADPH[c0] + CO2[c0] + p-hydroxyphenylpyruvate[c0]
R_rxn00410_c0	ATP[c0] + NH3[c0] + UTP[c0] <=> ADP[c0] + Phosphate[c0] + CTP[c0] + (2) H+[c0]

R_rxn00907_c0	NADP[c0] + 5-10-Methylenetetrahydrofolate[c0] <=> NADPH[c0] + 5-10-Methenyltetrahydrofolate[c0]
R_rxn01115_c0	NADP[c0] + 6-Phospho-D-gluconate[c0] => NADPH[c0] + CO2[c0] + D-Ribulose5-phosphate[c0]
R_rxn02507_c0	H+[c0] + 1-(2-carboxyphenylamino)-1-deoxyribulose 5-phosphate[c0] => H2O[c0] + CO2[c0] + Indoleglycerol phosphate[c0]
R_rxn01964_c0	L-Serine[c0] + Indoleglycerol phosphate[c0] => H2O[c0] + L-Tryptophan[c0] + Glyceraldehyde3-phosphate[c0]
R_rxn02508_c0	N-5-phosphoribosyl-anthranilate[c0] <=> 1-(2-carboxyphenylamino)-1-deoxyribulose 5-phosphate[c0]
R_rxn00726_c0	NH3[c0] + Chorismate[c0] => H2O[c0] + Pyruvate[c0] + H+[c0] + Anthranilate[c0]
R_rxn00791_c0	PPi[c0] + H+[c0] + N-5-phosphoribosyl-anthranilate[c0] <= Anthranilate[c0] + PRPP[c0]
R_rxn03638_c0	Acetyl-CoA[c0] + D-Glucosamine1-phosphate[c0] => CoA[c0] + H+[c0] + N-Acetyl-D-glucosamine1-phosphate[c0]
R_rxn00283_c0	L-Alanine[c0] <=> D-Alanine[c0]
R_rxn00555_c0	L-Glutamine[c0] + D-fructose-6-phosphate[c0] <=> L-Glutamate[c0] + D-Glucosamine phosphate[c0]
R_rxn00293_c0	UTP[c0] + N-Acetyl-D-glucosamine1-phosphate[c0] <=> PPi[c0] + UDP-N-acetylglucosamine[c0]
R_rxn00423_c0	Acetyl-CoA[c0] + L-Serine[c0] => CoA[c0] + O-Acetyl-L-serine[c0]
R_rxn00649_c0	H2S[c0] + O-Acetyl-L-serine[c0] => Acetate[c0] + L-Cysteine[c0]
R_rxn05909_c0	L-Serine[c0] + H+[c0] + H2S[c0] <=> H2O[c0] + L-Cysteine[c0]
R_rxn00193_c0	Acetyl-CoA[c0] + L-Glutamate[c0] => CoA[c0] + H+[c0] + N-Acetyl-L-glutamate[c0]
R_rxn00851_c0	ATP[c0] + (2) D-Alanine[c0] => ADP[c0] + Ala-Ala[c0] + Phosphate[c0] + H+[c0]
R_rxn02008_c0	ATP[c0] + D-Glutamate[c0] + UDP-N-acetylmuramoyl-L-alanine[c0] => ADP[c0] + Phosphate[c0] + H+[c0] + UDP-N-acetylmuramoyl-L-alanyl-D-glutamate[c0]
R_rxn02286_c0	ATP[c0] + L-Alanine[c0] + UDP-MurNAc[c0] => ADP[c0] + UDP-N-acetylmuramoyl-L-alanine[c0] + H+[c0] + Phosphate[c0]
R_rxn02011_c0	ATP[c0] + meso-2,6-Diaminopimelate[c0] + UDP-N-acetylmuramoyl-L-alanyl-D-glutamate[c0] => ADP[c0] + Phosphate[c0] + H+[c0] + UDP-N-acetylmuramoyl-L-alanyl-D-gamma-glutamyl-meso-2-6-diaminopimelate[c0]
R_rxn03901_c0	H2O[c0] + Bactoprenyl diphosphate[c0] => Phosphate[c0] + (2) H+[c0] + Undecaprenylphosphate[c0]
R_rxn00461_c0	UDP-N-acetylglucosamine[c0] + Phosphoenolpyruvate[c0] <=> Phosphate[c0] + UDP-N-acetylglucosamine enolpyruvate[c0]
R_rxn03408_c0	UDP-N-acetylglucosamine[c0] + Undecaprenyl-diphospho-N-acetylmuramoyl-L-alanyl-D-glutamyl-meso-2-6-diaminopimeloyl-D-alanyl-D-alanine[c0] <=> UDP[c0] + Undecaprenyl-diphospho-N-acetylmuramoyl--N-acetylglucosamine-L-ala-D-glu-meso-2-6-diaminopimeloyl-D-ala-D-ala[c0]
R_rxn03164_c0	UDP-N-acetylmuramoyl-L-alanyl-D-gamma-glutamyl-meso-2-6-diaminopimelate[c0] + Ala-Ala[c0] + ATP[c0] => H+[c0] + Phosphate[c0] + UDP-N-acetylmuramoyl-L-alanyl-D-glutamyl-6-carboxy-L-lysyl-D-alanyl- D-alanine[c0] + ADP[c0]

R_rxn03904_c0	Undecaprenylphosphate[c0] + UDP-N-acetylmuramoyl-L-alanyl-D-glutamyl-6-carboxy-L-lysyl-D-alanyl- D-alanine[c0] <=> UMP[c0] + Undecaprenyl-diphospho-N-acetylmuramoyl-L-alanyl-D-glutamyl-meso-2-6-diaminopimeloyl-D-alanyl-D-alanine[c0]
R_rxn01673_c0	ATP[c0] + dCDP[c0] <=> ADP[c0] + dCTP[c0]
R_rxn01353_c0	ATP[c0] + dGDP[c0] <=> ADP[c0] + dGTP[c0]
R_rxn05233_c0	GDP[c0] + trdrd[c0] => H2O[c0] + dGDP[c0] + trdox[c0]
R_rxn06076_c0	H2O[c0] + dCDP[c0] + trdox[c0] <= CDP[c0] + trdrd[c0]
R_rxn01520_c0	5-10-Methylenetetrahydrofolate[c0] + dUMP[c0] => dTMP[c0] + Dihydrofolate[c0]
R_rxn01512_c0	ATP[c0] + dTDP[c0] <=> ADP[c0] + TTP[c0]
R_rxn01513_c0	ATP[c0] + H+[c0] + dTMP[c0] <=> ADP[c0] + dTDP[c0]
R_rxn06075_c0	H2O[c0] + dUDP[c0] + trdox[c0] <= UDP[c0] + trdrd[c0]
R_rxn05231_c0	ADP[c0] + trdrd[c0] => H2O[c0] + dADP[c0] + trdox[c0]
R_rxn00839_c0	ATP[c0] + dADP[c0] <=> ADP[c0] + dATP[c0]
P_Acid_2	50 H+ +50 CTP + PhosphatidicAcid -> 50 ppi + CDPdiacylglycerol
P_Acid_1	6 D-3-Hydroxydodecanoyl-[acp] + 50 Glycerol-3-phosphate + 9 (R)-3-Hydroxydecanoyl-[acyl-carrier protein] + 24(2E)-Octadecenoyl-[acp] + 32R-3-hydroxypalmitoyl-acyl-carrierprotein- + 29Palmitoyl-ACP -> 100 ACP + PhosphatidicAcid
P_Acid_3	50 Glycerol-3-phosphate + CDPdiacylglycerol -> 50 H+ + 50 CMP + Phosphatidylglycerophosphate
P_Acid_4	50 H2O + Phosphatidylglycerophosphate -> 50 phosphate + Phosphatidylglycerol
P_Acid_5	50 L-serine + CDPdiacylglycerol -> 50H+ + 50CMP + Phosphatidylserine_
P_Acid_6	Phosphatidylserine + 50 H+ -> 50 CO2 + Phosphatidylethanolamine
P_Acid_7	Phosphatidylglycerol + CDPdiacylglycerol -> 50H+ + 50CMP + Cardiolipin
R_rxn01517_c0	ATP[c0] + H+[c0] + dUMP[c0] <=> ADP[c0] + dUDP[c0]
R_rxn00686_c0	NADP[c0] + Tetrahydrofolate[c0] <=> NADPH[c0] + H+[c0] + Dihydrofolate[c0
R_rxn00313_c0	H+[c0] + meso-2,6-Diaminopimelate[c0] <=> CO2[c0] + L-Lysine[c0]
R_rxn02285_c0	NADP[c0] + UDP-MurNAc[c0] <=> NADPH[c0] + H+[c0] + UDP-N-acetylglucosamine enolpyruvate[c0]
R_rxn01485_c0	D-Glucosamine1-phosphate[c0] <=> D-Glucosamine phosphate[c0]
R_rxn00527_c0	ribose-5-phosphate[c0] <=> D-Ribulose5-phosphate[c0]
R_rxn04954_c0	NAD[c0] + 5-Methyltetrahydrofolate[c0] <=> NADH[c0] + H+[c0] + 5-10-Methylenetetrahydrofolate[c0]

R_rxn01301_c0	NAD[c0] + L-Homoserine[c0] <=> NADH[c0] + H+[c0] + L-Aspartate4-semialdehyde[c0]
R_rxn00493_c0	2-Oxoglutarate[c0] + L-Phenylalanine[c0] <=> L-Glutamate[c0] + Phenylpyruvate[c0
R_rxn05332_c0	1 R-3-hydroxypalmitoyl-acyl-carrierprotein- [0] <-> 1 H2O [0] + 1 (2E)-Hexadecenoyl-[acp] [0]
R_rxn00086_c0	NADP[c0] + (2) GSH[c0] <=> NADPH[c0] + H+[c0] + Oxidized glutathione[c0]
R_rxn01465_c0	H2O[c0] + S-Dihydroorotate[c0] <=> H+[c0] + N-Carbamoyl-L-aspartate[c0]
R_rxn00503_c0	(2) H2O[c0] + NAD[c0] + 1-Pyrroline-5-carboxylate[c0] <=> NADH[c0] + L-Glutamate[c0] + H+[c0]
R_rxn00623_c0	(3) H2O[c0] + (3) NADP[c0] + H2S[c0] <=> (3) NADPH[c0] + (3) H+[c0] + Sulfite[c0]
R_rxn00929_c0	NAD[c0] + L-Proline[c0] <=> NADH[c0] + (2) H+[c0] + 1-Pyrroline-5-carboxylate[c0]
R_rxn01637_c0	2-Oxoglutarate[c0] + N-Acetylornithine[c0] <=> L-Glutamate[c0] + 2-Acetamido-5-oxopentanoate[c0]
R_rxn15112_c0	1 ATP [0] + 1 NH3 [0] + 1 alpha-D-Ribose 5-phosphate [0] <-> 1 ADP [0] + 1 Phosphate [0] + 1 H+ [0] + 1 5-Phosphoribosylamine [0]
R_rxn01973_c0	H2O[c0] + N-Succinyl-L-2,6-diaminopimelate[c0] <=> Succinate[c0] + LL-2,6-Diaminopimelate[c0]
R_rxn00908_c0	NAD[c0] + Glycine[c0] + Tetrahydrofolate[c0] <=> NADH[c0] + CO2[c0] + NH3[c0] + 5-10-Methylenetetrahydrofolate[c0
R_rxn05458_c0	CoA[c0] + H+[c0] + hexadecanoyl-acp[c0] <=> Palmitoyl-CoA[c0] + ACP[c0]
R_rxn01740_c0	NADP[c0] + Shikimate[c0] <=> NADPH[c0] + H+[c0] + 3-Dehydroshikimate[c0]
R_rxn00506_c0	H2O[c0] + NAD[c0] + Acetaldehyde[c0] => NADH[c0] + Acetate[c0] + (2) H+[c0]
R_rxn00541_c0	L-Threonine[c0] <=> Glycine[c0] + Acetaldehyde[c0]
R_rxn00806_c0	2-Oxoglutarate[c0] + L-Leucine[c0] <=> L-Glutamate[c0] + 4MOP[c0]
R_rxn02811_c0	3-Isopropylmalate[c0] <=> H2O[c0] + 2-Isopropylmaleate[c0]
R_rxn03239_c0	NAD[c0] + (S)-3-Hydroxyhexadecanoyl-CoA[c0] <=> NADH[c0] + H+[c0] + 3-Oxopalmitoyl-CoA[c0]
R_rxn05342_c0	NADP[c0] + HMA[c0] <=> NADPH[c0] + 3-oxotetradecanoyl-acp[c0]
R_rxn00692_c0	H2O[c0] + Glycine[c0] + 5-10-Methylenetetrahydrofolate[c0] <=> L-Serine[c0] + Tetrahydrofolate[c0]
R_rxn00611_c0	NAD[c0] + Glycerol-3-phosphate[c0] <=> NADH[c0] + H+[c0] + Glycerone-phosphate[c0]
R_rxn05340_c0	NADP[c0] + D-3-Hydroxydodecanoyl-[acp][c0] <=> NADPH[c0] + 3-oxododecanoyl-acp[c0]

R_rxn05339_c0	NADP[c0] + (R)-3-Hydroxybutanoyl-[acyl-carrier protein][c0] <=> NADPH[c0] + Acetoacetyl-ACP[c0]
R_rxn05338_c0	NADP[c0] + (R)-3-Hydroxydecanoyl-[acyl-carrier protein][c0] <=> NADPH[c0] + H+[c0] + 3-oxodecanoyl-acp[c0]
R_rxn05341_c0	NADP[c0] + (R)-3-Hydroxyoctanoyl-[acyl-carrier protein][c0] <=> NADPH[c0] + H+[c0] + 3-oxooctanoyl-acp[c0]
R_rxn05337_c0	NADP[c0] + D-3-Hydroxyhexanoyl-[acp][c0] <=> NADPH[c0] + 3-Oxohexanoyl-[acp][c0]
R_rxn00903_c0	2-Oxoglutarate[c0] + L-Valine[c0] <=> L-Glutamate[c0] + 3-Methyl-2-oxobutanoate[c0]
oxaloacetate_buildin	2-Phospho-D-glycerate + ATP -> 1,3-Bisphospho-D-glycerate + ADP
R_rxn08647_c0	ATP[c0] + Glycerate[c0] <=> ADP[c0] + H+[c0] + 2-Phospho-D-glycerate[c0]
R_rxn02914_c0	2-Oxoglutarate[c0] + phosphoserine[c0] <=> L-Glutamate[c0] + 3-Phosphonooxypyruvate[c0]
R_rxn02380_c0	beta-D-Glucose 6-phosphate[c0] <=> D-fructose-6-phosphate[c0]
R_rxn01333_c0	Glyceraldehyde3-phosphate[c0] + Sedoheptulose7-phosphate[c0] <=> D-fructose-6-phosphate[c0] + D-Erythrose4-phosphate[c0]
R_rxn00258_c0	Pyruvate[c0] + Malonyl-CoA[c0] <=> Acetyl-CoA[c0] + Oxaloacetate[c0]
R_rxn01116_c0	D-Ribulose5-phosphate[c0] <=> D-Xylulose5-phosphate[c0]
R_rxn00777_c0	ribose-5-phosphate[c0] <=> D-Ribulose5-phosphate[c0]
R_rxn02085_c0	H+[c0] + 4-Imidazolone-5-propanoate[c0] <=> H2O[c0] + Urocanate[c0]
R_rxn01652_c0	H2O[c0] + 5-10-Methenyltetrahydrofolate[c0] <=> H+[c0] + 5-Formyltetrahydrofolate[c0]
R_rxn02283_c0	L-Glutamate[c0] + 5-Formyltetrahydrofolate[c0] <=> H+[c0] + Tetrahydrofolate[c0] + N-Formyl-L-glutamate[c0]
R_rxn04043_c0	ADP[c0] + D-fructose-6-phosphate[c0] <=> AMP[c0] + (2) H+[c0] + D-fructose-1,6-bisphosphate[c0]
R_rxn00786_c0	D-fructose-1,6-bisphosphate[c0] <=> Glycerone-phosphate[c0] + Glyceraldehyde3-phosphate[c0]
R_rxn02320_c0	2-Oxoglutarate[c0] + L-histidinol-phosphate[c0] <=> L-Glutamate[c0] + imidazole acetol-phosphate[c0]
R_rxn00832_c0	H2O[c0] + IMP[c0] <=> FAICAR[c0]
R_rxn00260_c0	2-Oxoglutarate[c0] + L-Aspartate[c0] <=> L-Glutamate[c0] + Oxaloacetate[c0]
R_rxn08527_c0	Fumarate[c0] + Menaquinol 8[c0] <=> Succinate[c0] + Menaquinone 8[c0]
R_rxn00285_c0	ATP[c0] + CoA[c0] + Succinate[c0] <=> ADP[c0] + Phosphate[c0] + Succinyl-CoA[c0]

R_rxn00799_c0	L-Malate[c0] <=> H2O[c0] + Fumarate[c0]

Table B.1 *P. fluorescens in silico* glucose metabolism Part 3

Coded reaction id	Genes	Subsystem
R_rxn10042_c0	fig|9606.20.peg.6146 fig|9606.20.peg.6143 fig|9606.20.peg.6144 fig|9606.20.peg.6151 fig|9606.20.peg.6147 fig|9606.20.peg.6145	
R_rxn10113_c0	fig|9606.20.peg.5156 fig|9606.20.peg.5154 fig|9606.20.peg.5153 fig|9606.20.peg.5155 fig|9606.20.peg.5368 fig|9606.20.peg.1900 fig|9606.20.peg.5367 fig|9606.20.peg.1901 fig|9606.20.peg.1816 fig|9606.20.peg.843	
R_rxn10122_c0	fig|9606.20.peg.3832 fig|9606.20.peg.3826 fig|9606.20.peg.3834 fig|9606.20.peg.3825 fig|9606.20.peg.3833 fig|9606.20.peg.3824 fig|9606.20.peg.3830 fig|9606.20.peg.3835 fig|9606.20.peg.3829 fig|9606.20.peg.3831 fig|9606.20.peg.3827 fig|9606.20.peg.3823 fig|9606.20.peg.3828	
R_rxn08900_c0	fig|9606.20.peg.1609 fig|9606.20.peg.906	
R_rxn00154_c0		Carbohydrates
R_rxn08094_c0	fig|9606.20.peg.1820 fig|9606.20.peg.1822 fig|9606.20.peg.1821 fig|9606.20.peg.2655	Carbohydrates
R_rxn01476_c0	fig|9606.20.peg.4851	Carbohydrates
R_rxn03884_c0	fig|9606.20.peg.4850	Carbohydrates
R_rxn01477_c0	fig|9606.20.peg.4977	Carbohydrates
R_rxn00216_c0	fig|9606.20.peg.4976	Carbohydrates
R_rxn00604_c0	fig|9606.20.peg.2695 fig|9606.20.peg.4852	Carbohydrates
R_rxn00001_c0	fig|9606.20.peg.1902	Phosphorus Metabolism
R_rxn00257_c0	fig|9606.20.peg.2297	Carbohydrates
R_rxn00974_c0	fig|9606.20.peg.3494 fig|9606.20.peg.1537	Carbohydrates
R_rxn01388_c0	fig|9606.20.peg.3494 fig|9606.20.peg.1537	Carbohydrates

R_rxn00198_c0	fig|9606.20.peg.743 fig|9606.20.peg.3562 fig|9606.20.peg.5972	Amino Acids and Derivatives
R_rxn00182_c0	fig|9606.20.peg.3510	Amino Acids and Derivatives
R_rxn10806_c0	fig|9606.20.peg.5156 fig|9606.20.peg.1900 fig|9606.20.peg.5368 fig|9606.20.peg.843 fig|9606.20.peg.5154 fig|9606.20.peg.1901 fig|9606.20.peg.5367 fig|9606.20.peg.1816 fig|9606.20.peg.5153 fig|9606.20.peg.5155	
R_rxn00097_c0	fig|9606.20.peg.2993	Stress Response
R_rxn00187_c0	fig|9606.20.peg.5347	Amino Acids and Derivatives
R_rxn10121_c0	fig|9606.20.peg.3430	
R_rxn05627_c0	fig|9606.20.peg.4619 fig|9606.20.peg.2309 fig|9606.20.peg.2201	Nitrogen Metabolism
R_rxn00770_c0	fig|9606.20.peg.735	Nucleosides and Nucleotides
R_rxn03137_c0	fig|9606.20.peg.614	Cofactors, Vitamins, Prosthetic Groups, Pigments
R_rxn02473_c0	fig|9606.20.peg.329 fig|9606.20.peg.3410	Amino Acids and Derivatives
R_rxn03175_c0	fig|9606.20.peg.332	Amino Acids and Derivatives
R_rxn00859_c0	fig|9606.20.peg.898	Amino Acids and Derivatives
R_rxn01211_c0	fig|9606.20.peg.3935 fig|9606.20.peg.2322 fig|9606.20.peg.2331	Cofactors, Vitamins, Prosthetic Groups, Pigments
R_rxn02160_c0	fig|9606.20.peg.9	Amino Acids and Derivatives
R_rxn02835_c0	fig|9606.20.peg.6118 fig|9606.20.peg.390 fig|9606.20.peg.389 fig|9606.20.peg.3328	Amino Acids and Derivatives
R_rxn02834_c0	fig|9606.20.peg.389 fig|9606.20.peg.390 fig|9606.20.peg.6118	Amino Acids and Derivatives
R_rxn03135_c0	fig|9606.20.peg.330	Amino Acids and Derivatives
R_rxn00789_c0	fig|9606.20.peg.529	Amino Acids and Derivatives
R_rxn00237_c0	fig|9606.20.peg.5074	Nucleosides and Nucleotides
R_rxn01642_c0	fig|9606.20.peg.373 fig|9606.20.peg.3263 fig|9606.20.peg.1122	Amino Acids and Derivatives
R_rxn01640_c0	fig|9606.20.peg.362	Amino Acids and Derivatives
R_rxn00867_c0	fig|9606.20.peg.370 fig|9606.20.peg.371	Amino Acids and Derivatives
R_rxn00800_c0	fig|9606.20.peg.3818	Nucleosides and Nucleotides
R_rxn00838_c0	fig|9606.20.peg.530	Nucleosides and Nucleotides
R_rxn05465_c0	fig|9606.20.peg.5764 fig|9606.20.peg.4717	Fatty Acids, Lipids, and Isoprenoids

R_rxn00568_c0	fig|9606.20.peg.5262	Carbohydrates
R_rxn00569_c0	fig|9606.20.peg.3430 fig|9606.20.peg.3429	Nitrogen Metabolism
R_rxn00785_c0	fig|9606.20.peg.3606 fig|9606.20.peg.5732 fig|9606.20.peg.3728 fig|9606.20.peg.3729	Carbohydrates
R_rxn01200_c0	fig|9606.20.peg.3606 fig|9606.20.peg.5732 fig|9606.20.peg.3728 fig|9606.20.peg.3729	Carbohydrates
R_rxn01975_c0	fig|9606.20.peg.4852 fig|9606.20.peg.2695	
P_Acid_8		Cell Wall and Capsule
R_rxn01102_c0	fig|9606.20.peg.1800 fig|9606.20.peg.3012 fig|9606.20.peg.6106	Fatty Acids, Lipids, and Isoprenoids
R_rxn00420_c0	fig|9606.20.peg.5846 fig|9606.20.peg.4651 fig|9606.20.peg.5826 fig|9606.20.peg.2034 fig|9606.20.peg.509	Amino Acids and Derivatives
R_rxn01101_c0	fig|9606.20.peg.855 fig|9606.20.peg.3367 fig|9606.20.peg.3696 fig|9606.20.peg.4304 fig|9606.20.peg.2310 fig|9606.20.peg.1513 fig|9606.20.peg.4042 fig|9606.20.peg.5855 fig|9606.20.peg.4305 fig|9606.20.peg.3498	Cofactors, Vitamins, Prosthetic Groups, Pigments
R_rxn00781_c0	fig|9606.20.peg.4978	Carbohydrates
R_rxn00148_c0	fig|9606.20.peg.1238	Nucleosides and Nucleotides
Malate_buildin		Carbohydrates
R_rxn05329_c0		Fatty Acids, Lipids, and Isoprenoids
R_rxn05334_c0		Fatty Acids, Lipids, and Isoprenoids
R_rxn05330_c0		Fatty Acids, Lipids, and Isoprenoids
R_rxn05322_c0		Cofactors, Vitamins, Prosthetic Groups, Pigments
R_rxn05326_c0		Fatty Acids, Lipids, and Isoprenoids
R_rxn05325_c0		Fatty Acids, Lipids, and Isoprenoids
R_rxn05349_c0	fig|9606.20.peg.3201 fig|9606.20.peg.2479 fig|9606.20.peg.4714 fig|9606.20.peg.3116 fig|9606.20.peg.1664 fig|9606.20.peg.3203 fig|9606.20.peg.1661 fig|9606.20.peg.4462	

R_rxn05346_c0	fig|9606.20.peg.3201 fig|9606.20.peg.2479 fig|9606.20.peg.4714 fig|9606.20.peg.3116 fig|9606.20.peg.1664 fig|9606.20.peg.3203 fig|9606.20.peg.4462 fig|9606.20.peg.1661 fig|9606.20.peg.1836	Fatty Acids, Lipids, and Isoprenoids
R_rxn05350_c0	fig|9606.20.peg.3201 fig|9606.20.peg.4714 fig|9606.20.peg.3116 fig|9606.20.peg.2479 fig|9606.20.peg.3203 fig|9606.20.peg.1664 fig|9606.20.peg.1661 fig|9606.20.peg.4462 fig|9606.20.peg.1836	Fatty Acids, Lipids, and Isoprenoids
R_rxn05347_c0	fig|9606.20.peg.1661 fig|9606.20.peg.4462 fig|9606.20.peg.3203 fig|9606.20.peg.1664 fig|9606.20.peg.3201 fig|9606.20.peg.2479 fig|9606.20.peg.4714 fig|9606.20.peg.3116 fig|9606.20.peg.1836	Fatty Acids, Lipids, and Isoprenoids
R_rxn05343_c0	fig|9606.20.peg.3203 fig|9606.20.peg.1664 fig|9606.20.peg.1661 fig|9606.20.peg.4462 fig|9606.20.peg.2479 fig|9606.20.peg.3116 fig|9606.20.peg.4714 fig|9606.20.peg.3201 fig|9606.20.peg.1836	Fatty Acids, Lipids, and Isoprenoids
R_rxn00904_c0	fig|9606.20.peg.5248	Amino Acids and Derivatives
R_rxn05333_c0		Fatty Acids, Lipids, and Isoprenoids
R_rxn05327_c0		Fatty Acids, Lipids, and Isoprenoids
R_rxn05348_c0	fig|9606.20.peg.3201 fig|9606.20.peg.3116 fig|9606.20.peg.4714 fig|9606.20.peg.2479 fig|9606.20.peg.4462 fig|9606.20.peg.1661 fig|9606.20.peg.1664 fig|9606.20.peg.3203 fig|9606.20.peg.1836	Fatty Acids, Lipids, and Isoprenoids
R_rxn00747_c0	fig|9606.20.peg.5275	Carbohydrates
R_rxn05324_c0		Fatty Acids, Lipids, and Isoprenoids
R_rxn03240_c0	fig|9606.20.peg.2455 fig|9606.20.peg.1548 fig|9606.20.peg.4671 fig|9606.20.peg.2203 fig|9606.20.peg.4962	Fatty Acids, Lipids, and Isoprenoids

R_rxn05351_c0		Fatty Acids, Lipids, and Isoprenoids
R_rxn02804_c0	fig|9606.20.peg.3038 fig|9606.20.peg.1549 fig|9606.20.peg.655 fig|9606.20.peg.4328 fig|9606.20.peg.4672 fig|9606.20.peg.3532 fig|9606.20.peg.3299	Amino Acids and Derivatives
R_rxn05457_c0	fig|9606.20.peg.4717 fig|9606.20.peg.5764	Fatty Acids, Lipids, and Isoprenoids
R_rxn05331_c0		Fatty Acids, Lipids, and Isoprenoids
R_rxn05345_c0	fig|9606.20.peg.3201 fig|9606.20.peg.4714 fig|9606.20.peg.3116 fig|9606.20.peg.2479 fig|9606.20.peg.4462 fig|9606.20.peg.1661 fig|9606.20.peg.1664 fig|9606.20.peg.3203 fig|9606.20.peg.1836	Fatty Acids, Lipids, and Isoprenoids
R_rxn05335_c0		Fatty Acids, Lipids, and Isoprenoids
R_rxn05732_c0	fig|9606.20.peg.3039	Cofactors, Vitamins, Prosthetic Groups, Pigments
R_rxn00114_c0	fig|9606.20.peg.1238	Nucleosides and Nucleotides
R_rxn01208_c0	fig|9606.20.peg.4204	Amino Acids and Derivatives
R_rxn02789_c0	fig|9606.20.peg.2051 fig|9606.20.peg.4206 fig|9606.20.peg.4207 fig|9606.20.peg.2050	Amino Acids and Derivatives
R_rxn00902_c0	fig|9606.20.peg.5063	Amino Acids and Derivatives
R_rxn03062_c0	fig|9606.20.peg.4204	Amino Acids and Derivatives
R_rxn02213_c0	fig|9606.20.peg.621 fig|9606.20.peg.4288 fig|9606.20.peg.5386	Amino Acids and Derivatives
R_rxn01255_c0	fig|9606.20.peg.4349	Amino Acids and Derivatives
R_rxn01739_c0	fig|9606.20.peg.416	Nucleosides and Nucleotides
R_rxn02212_c0	fig|9606.20.peg.417	Amino Acids and Derivatives
R_rxn01332_c0	fig|9606.20.peg.1704 fig|9606.20.peg.2184 fig|9606.20.peg.1723	Amino Acids and Derivatives
R_rxn02476_c0		Carbohydrates
R_rxn00364_c0	fig|9606.20.peg.1645	Nucleosides and Nucleotides
R_rxn01256_c0	fig|9606.20.peg.349	Amino Acids and Derivatives
R_rxn00409_c0	fig|9606.20.peg.5074	Nucleosides and Nucleotides
R_rxn05289_c0	fig|9606.20.peg.5178 fig|9606.20.peg.3644	Nucleosides and Nucleotides
lysine_formation		Carbohydrates
R_rxn00790_c0	fig|9606.20.peg.4194 fig|9606.20.peg.5583	Nucleosides and Nucleotides
R_rxn00117_c0	fig|9606.20.peg.4905	Amino Acids and Derivatives

R_rxn00119_c0	fig|9606.20.peg.5074	Nucleosides and Nucleotides
R_rxn01434_c0	fig|9606.20.peg.1155	Amino Acids and Derivatives
R_rxn01917_c0	fig|9606.20.peg.6013	Amino Acids and Derivatives
R_rxn00192_c0	fig|9606.20.peg.351	Amino Acids and Derivatives
R_rxn00469_c0	fig|9606.20.peg.4279 fig|9606.20.peg.5890 fig|9606.20.peg.4045 fig|9606.20.peg.3593	Amino Acids and Derivatives
R_rxn00802_c0	fig|9606.20.peg.5962	Amino Acids and Derivatives
R_rxn02465_c0	fig|9606.20.peg.5572	Amino Acids and Derivatives
R_rxn01019_c0	fig|9606.20.peg.1146 fig|9606.20.peg.4904	Amino Acids and Derivatives
R_rxn00416_c0	fig|9606.20.peg.2453 fig|9606.20.peg.4332	Amino Acids and Derivatives
R_rxn05256_c0	fig|9606.20.peg.4652	Sulfur Metabolism
R_rxn00379_c0	fig|9606.20.peg.762 fig|9606.20.peg.763	Amino Acids and Derivatives
R_rxn05651_c0	fig|9606.20.peg.25 fig|9606.20.peg.5198	Amino Acids and Derivatives
R_rxn01360_c0		Nucleosides and Nucleotides
R_rxn00710_c0	fig|9606.20.peg.1852	Nucleosides and Nucleotides
R_rxn00205_c0	fig|9606.20.peg.1734 fig|9606.20.peg.4492 fig|9606.20.peg.5182	Stress Response
R_rxn01018_c0	fig|9606.20.peg.5784	Nucleosides and Nucleotides
R_rxn01362_c0	fig|9606.20.peg.6014 fig|9606.20.peg.4194	Nucleosides and Nucleotides
R_rxn12017_c0		
R_rxn08043_c0		Carbohydrates
R_rxn03436_c0		
R_rxn03435_c0		
R_rxn03437_c0	fig|9606.20.peg.5822	Amino Acids and Derivatives
R_rxn01575_c0	fig|9606.20.peg.3971	Amino Acids and Derivatives
R_rxn00737_c0	fig|9606.20.peg.2739 fig|9606.20.peg.5848	Amino Acids and Derivatives
R_rxn08016_c0		Fatty Acids, Lipids, and Isoprenoids
R_rxn10202_c0	fig|9606.20.peg.1252	Fatty Acids, Lipids, and Isoprenoids
R_rxn08799_c0	fig|9606.20.peg.4845 fig|9606.20.peg.5862	Fatty Acids, Lipids, and Isoprenoids
R_rxn01000_c0	fig|9606.20.peg.1642 fig|9606.20.peg.1508	Amino Acids and Derivatives
R_rxn07576_c0		Fatty Acids, Lipids, and Isoprenoids
R_rxn07577_c0		Fatty Acids, Lipids, and Isoprenoids
R_rxn07578_c0	fig|9606.20.peg.3302	Fatty Acids, Lipids, and Isoprenoids
R_rxn00239_c0	fig|9606.20.peg.6019	Nucleosides and Nucleotides
R_rxn00834_c0	fig|9606.20.peg.5057	Nucleosides and Nucleotides
xanthosine_build		Nucleosides and Nucleotides

R_rxn01303_c0	fig|9606.20.peg.5792 fig|9606.20.peg.4944	Amino Acids and Derivatives
R_rxn00337_c0	fig|9606.20.peg.4756 fig|9606.20.peg.6013	Amino Acids and Derivatives
R_rxn00952_c0	fig|9606.20.peg.4193 fig|9606.20.peg.460	Amino Acids and Derivatives
R_rxn00693_c0	fig|9606.20.peg.2664	Amino Acids and Derivatives
R_rxn01643_c0	fig|9606.20.peg.4203	Amino Acids and Derivatives
R_rxn01269_c0	fig|9606.20.peg.1644	
R_rxn00410_c0	fig|9606.20.peg.1287 fig|9606.20.peg.1155	Nucleosides and Nucleotides
R_rxn00907_c0	fig|9606.20.peg.2331 fig|9606.20.peg.3935 fig|9606.20.peg.2322	Cofactors, Vitamins, Prosthetic Groups, Pigments
R_rxn01115_c0	fig|9606.20.peg.2694	
R_rxn02507_c0	fig|9606.20.peg.5582	Amino Acids and Derivatives
R_rxn01964_c0	fig|9606.20.peg.35 fig|9606.20.peg.36 fig|9606.20.peg.5939 fig|9606.20.peg.2148	Cofactors, Vitamins, Prosthetic Groups, Pigments
R_rxn02508_c0	fig|9606.20.peg.4199	Amino Acids and Derivatives
R_rxn00726_c0	fig|9606.20.peg.5584 fig|9606.20.peg.1383 fig|9606.20.peg.1382 fig|9606.20.peg.5585 fig|9606.20.peg.4642	Amino Acids and Derivatives
R_rxn00791_c0	fig|9606.20.peg.5583	Amino Acids and Derivatives
R_rxn03638_c0	fig|9606.20.peg.6142	Cell Wall and Capsule
R_rxn00283_c0	fig|9606.20.peg.5992 fig|9606.20.peg.3019	Amino Acids and Derivatives
R_rxn00555_c0	fig|9606.20.peg.1731	Amino Acids and Derivatives
R_rxn00293_c0	fig|9606.20.peg.6142	Cell Wall and Capsule
R_rxn00423_c0	fig|9606.20.peg.250 fig|9606.20.peg.4636 fig|9606.20.peg.5083	Amino Acids and Derivatives
R_rxn00649_c0	fig|9606.20.peg.1535 fig|9606.20.peg.4635 fig|9606.20.peg.4521	Amino Acids and Derivatives
R_rxn05909_c0	fig|9606.20.peg.3410	Amino Acids and Derivatives
R_rxn00193_c0	fig|9606.20.peg.5889 fig|9606.20.peg.4944	Amino Acids and Derivatives
R_rxn00851_c0		Carbohydrates
R_rxn02008_c0	fig|9606.20.peg.945	Cofactors, Vitamins, Prosthetic Groups, Pigments
R_rxn02286_c0		
R_rxn02011_c0	fig|9606.20.peg.942	Cofactors, Vitamins, Prosthetic Groups, Pigments
R_rxn03901_c0	fig|9606.20.peg.2397 fig|9606.20.peg.2811	Fatty Acids, Lipids, and Isoprenoids
R_rxn00461_c0	fig|9606.20.peg.896	Cell Wall and Capsule
R_rxn03408_c0	fig|9606.20.peg.947	

R_rxn03164_c0		
R_rxn03904_c0	fig|9606.20.peg.944	Fatty Acids, Lipids, and Isoprenoids
R_rxn01673_c0	fig|9606.20.peg.5074	Nucleosides and Nucleotides
R_rxn01353_c0	fig|9606.20.peg.5074	Nucleosides and Nucleotides
R_rxn05233_c0	fig|9606.20.peg.4776 fig|9606.20.peg.2786 fig|9606.20.peg.4737	Nucleosides and Nucleotides
R_rxn06076_c0	fig|9606.20.peg.2786 fig|9606.20.peg.4776 fig|9606.20.peg.4737	Nucleosides and Nucleotides
R_rxn01520_c0	fig|9606.20.peg.5840	Cofactors, Vitamins, Prosthetic Groups, Pigments
R_rxn01512_c0	fig|9606.20.peg.5074	Nucleosides and Nucleotides
R_rxn01513_c0	fig|9606.20.peg.4711	Nucleosides and Nucleotides
R_rxn06075_c0	fig|9606.20.peg.4776 fig|9606.20.peg.2786 fig|9606.20.peg.4737	Nucleosides and Nucleotides
R_rxn05231_c0	fig|9606.20.peg.2786 fig|9606.20.peg.4776 fig|9606.20.peg.4737	Nucleosides and Nucleotides
R_rxn00839_c0	fig|9606.20.peg.5074	Nucleosides and Nucleotides
P_Acid_2		Cell Wall and Capsule
P_Acid_1		Cell Wall and Capsule
P_Acid_3		Cell Wall and Capsule
P_Acid_4		Cell Wall and Capsule
P_Acid_5		Cell Wall and Capsule
P_Acid_6		Cell Wall and Capsule
P_Acid_7		Cell Wall and Capsule
R_rxn01517_c0	fig|9606.20.peg.6019	Nucleosides and Nucleotides
R_rxn00686_c0	fig|9606.20.peg.5173 fig|9606.20.peg.5828 fig|9606.20.peg.3875	Cofactors, Vitamins, Prosthetic Groups, Pigments
R_rxn00313_c0	fig|9606.20.peg.5971	Amino Acids and Derivatives
R_rxn02285_c0	fig|9606.20.peg.3772	Carbohydrates
R_rxn01485_c0	fig|9606.20.peg.5276	Cell Wall and Capsule
R_rxn00527_c0	fig|9606.20.peg.3179 fig|9606.20.peg.2127 fig|9606.20.peg.6089 fig|9606.20.peg.4473 fig|9606.20.peg.4632 fig|9606.20.peg.3502 fig|9606.20.peg.4308 fig|9606.20.peg.3658 fig|9606.20.peg.2233 fig|9606.20.peg.4031 fig|9606.20.peg.3464 fig|9606.20.peg.4219 fig|9606.20.peg.1643 fig|9606.20.peg.5151 fig|9606.20.peg.899	Amino Acids and Derivatives

R_rxn04954_c0	fig|9606.20.peg.5748	
R_rxn01301_c0	fig|9606.20.peg.2013 fig|9606.20.peg.5019	
R_rxn00493_c0	fig|9606.20.peg.4219 fig|9606.20.peg.1643 fig|9606.20.peg.899 fig|9606.20.peg.5151 fig|9606.20.peg.4473	Cofactors, Vitamins, Prosthetic Groups, Pigments
R_rxn05332_c0		Fatty Acids, Lipids, and Isoprenoids
R_rxn00086_c0	fig|9606.20.peg.5236	Amino Acids and Derivatives
R_rxn01465_c0	fig|9606.20.peg.5785 fig|9606.20.peg.6120 fig|9606.20.peg.1153 fig|9606.20.peg.373	Nucleosides and Nucleotides
R_rxn00503_c0	fig|9606.20.peg.456	Amino Acids and Derivatives
R_rxn00623_c0	fig|9606.20.peg.2659	Amino Acids and Derivatives
R_rxn00929_c0	fig|9606.20.peg.5790	Amino Acids and Derivatives
R_rxn01637_c0	fig|9606.20.peg.5628 fig|9606.20.peg.1621	Amino Acids and Derivatives
R_rxn15112_c0		Carbohydrates
R_rxn01973_c0	fig|9606.20.peg.1256	Amino Acids and Derivatives
R_rxn00908_c0	fig|9606.20.peg.4514	Cofactors, Vitamins, Prosthetic Groups, Pigments
R_rxn05458_c0	fig|9606.20.peg.4717 fig|9606.20.peg.5764	Fatty Acids, Lipids, and Isoprenoids
R_rxn01740_c0	fig|9606.20.peg.24 fig|9606.20.peg.5387 fig|9606.20.peg.2135	Amino Acids and Derivatives
R_rxn00506_c0	fig|9606.20.peg.3098 fig|9606.20.peg.2014 fig|9606.20.peg.6002 fig|9606.20.peg.2352 fig|9606.20.peg.3105 fig|9606.20.peg.5464 fig|9606.20.peg.3094 fig|9606.20.peg.5813	Fatty Acids, Lipids, and Isoprenoids
R_rxn00541_c0	fig|9606.20.peg.5678 fig|9606.20.peg.4758	Amino Acids and Derivatives
R_rxn00806_c0	fig|9606.20.peg.3971	Amino Acids and Derivatives
R_rxn02811_c0	fig|9606.20.peg.4206 fig|9606.20.peg.2051 fig|9606.20.peg.4207 fig|9606.20.peg.2050	Amino Acids and Derivatives
R_rxn03239_c0	fig|9606.20.peg.4671 fig|9606.20.peg.1548	Fatty Acids, Lipids, and Isoprenoids

R_rxn05342_c0	fig|9606.20.peg.3734 fig|9606.20.peg.1994 fig|9606.20.peg.1075 fig|9606.20.peg.2571 fig|9606.20.peg.3093 fig|9606.20.peg.300 fig|9606.20.peg.1957 fig|9606.20.peg.3196 fig|9606.20.peg.4716 fig|9606.20.peg.1953 fig|9606.20.peg.2379	Fatty Acids, Lipids, and Isoprenoids
R_rxn00692_c0	fig|9606.20.peg.5676 fig|9606.20.peg.5351 fig|9606.20.peg.3051	Cofactors, Vitamins, Prosthetic Groups, Pigments
R_rxn00611_c0	fig|9606.20.peg.1841	
R_rxn05340_c0	fig|9606.20.peg.2571 fig|9606.20.peg.3093 fig|9606.20.peg.3734 fig|9606.20.peg.1075 fig|9606.20.peg.1994 fig|9606.20.peg.1953 fig|9606.20.peg.4716 fig|9606.20.peg.2379 fig|9606.20.peg.300 fig|9606.20.peg.1957 fig|9606.20.peg.3196	Fatty Acids, Lipids, and Isoprenoids
R_rxn05339_c0	fig|9606.20.peg.3734 fig|9606.20.peg.1994 fig|9606.20.peg.1075 fig|9606.20.peg.2571 fig|9606.20.peg.3093 fig|9606.20.peg.300 fig|9606.20.peg.3196 fig|9606.20.peg.1957 fig|9606.20.peg.4716 fig|9606.20.peg.1953 fig|9606.20.peg.2379	Fatty Acids, Lipids, and Isoprenoids
R_rxn05338_c0	fig|9606.20.peg.3093 fig|9606.20.peg.2571 fig|9606.20.peg.1075 fig|9606.20.peg.1994 fig|9606.20.peg.3734 fig|9606.20.peg.2379 fig|9606.20.peg.1953 fig|9606.20.peg.4716 fig|9606.20.peg.1957 fig|9606.20.peg.3196 fig|9606.20.peg.300	Fatty Acids, Lipids, and Isoprenoids

R_rxn05341_c0	fig|9606.20.peg.1953 fig|9606.20.peg.4716 fig|9606.20.peg.2379 fig|9606.20.peg.300 fig|9606.20.peg.1957 fig|9606.20.peg.3196 fig|9606.20.peg.2571 fig|9606.20.peg.3093 fig|9606.20.peg.3734 fig|9606.20.peg.1075 fig|9606.20.peg.1994	Fatty Acids, Lipids, and Isoprenoids
R_rxn05337_c0	fig|9606.20.peg.300 fig|9606.20.peg.3196 fig|9606.20.peg.1957 fig|9606.20.peg.1953 fig|9606.20.peg.4716 fig|9606.20.peg.2379 fig|9606.20.peg.3734 fig|9606.20.peg.1075 fig|9606.20.peg.1994 fig|9606.20.peg.2571 fig|9606.20.peg.3093	Fatty Acids, Lipids, and Isoprenoids
R_rxn00903_c0	fig|9606.20.peg.3971	Amino Acids and Derivatives
oxaloacetate_buildin		Carbohydrates
R_rxn08647_c0	fig|9606.20.peg.6106	Cofactors, Vitamins, Prosthetic Groups, Pigments
R_rxn02914_c0	fig|9606.20.peg.1641	Cofactors, Vitamins, Prosthetic Groups, Pigments
R_rxn02380_c0	fig|9606.20.peg.5262	
R_rxn01333_c0	fig|9606.20.peg.3736 fig|9606.20.peg.1580	Carbohydrates
R_rxn00258_c0	fig|9606.20.peg.5784	Nucleosides and Nucleotides
R_rxn01116_c0	fig|9606.20.peg.5587 fig|9606.20.peg.292	Carbohydrates
R_rxn00777_c0	fig|9606.20.peg.5849	Carbohydrates
R_rxn02085_c0	fig|9606.20.peg.365	Amino Acids and Derivatives
R_rxn01652_c0	fig|9606.20.peg.4514	Cofactors, Vitamins, Prosthetic Groups, Pigments
R_rxn02283_c0	fig|9606.20.peg.17	
R_rxn04043_c0	fig|9606.20.peg.4167	Carbohydrates
R_rxn00786_c0	fig|9606.20.peg.5727	Carbohydrates
R_rxn02320_c0	fig|9606.20.peg.899 fig|9606.20.peg.5151 fig|9606.20.peg.1643	Amino Acids and Derivatives
R_rxn00832_c0	fig|9606.20.peg.614	Cofactors, Vitamins, Prosthetic Groups, Pigments

R_rxn00260_c0	fig|9606.20.peg.4031 fig|9606.20.peg.3464 fig|9606.20.peg.2233 fig|9606.20.peg.4308 fig|9606.20.peg.3658 fig|9606.20.peg.3179 fig|9606.20.peg.6089 fig|9606.20.peg.2127 fig|9606.20.peg.4632 fig|9606.20.peg.4473 fig|9606.20.peg.3502	Amino Acids and Derivatives
R_rxn08527_c0	fig|9606.20.peg.1818 fig|9606.20.peg.1816 fig|9606.20.peg.1817 fig|9606.20.peg.1819	Carbohydrates
R_rxn00285_c0	fig|9606.20.peg.1824 fig|9606.20.peg.1823	Carbohydrates
R_rxn00799_c0	fig|9606.20.peg.4964 fig|9606.20.peg.4326 fig|9606.20.peg.876	Carbohydrates

Appendix C *P fluorescens* catechol metabolism

Table C.1 *P. fluorescens in silico* catechol metabolism Part 1

Coded reaction id	Reaction name	Flux (mmol/gDW/h)	Normalized flux (mmol/gDW/h)
R_rxn00799_c0	S_malate_hydro_lyase_fumarate_forming_c0	-1.6235	-197.2663
R_rxn08527_c0	fumarate_reductase_c0	-1.6090	-195.5049
R_rxn00285_c0	Succinate_CoA_ligase_ADP_forming_c0	-0.8025	-97.5039
R_rxn00258_c0	Malonyl_CoA_pyruvate_carboxytransferase_c0	-0.2689	-32.6792
R_rxn04954_c0	5_methyltetrahydrofolate_NAD_plus__oxidoreductase_c0	-0.2285	-27.7624
R_rxn00781_c0	D_glyceraldehyde_3_phosphate_NAD_plus__oxidoreductase_phosphorylating_c0	-0.0898	-10.9112
R_rxn00260_c0	L_Aspartate_2_oxoglutarate_aminotransferase_c0	-0.0638	-7.7503
R_rxn02914_c0	3_Phosphoserine_2_oxoglutarate_aminotransferase_c0	-0.0612	-7.4387
R_rxn08647_c0	ATP_R_glycerate_2_phosphotransferase_c0	-0.0612	-7.4387
R_rxn00903_c0	L_Valine_2_oxoglutarate_aminotransferase_c0	-0.0570	-6.9298
R_rxn05339_c0	3R_3_Hydroxybutanoyl_acyl_carrier_protein_NADP_plus__oxidoreductase_c0	-0.0393	-4.7745
R_rxn05338_c0	3R_3_Hydroxydecanoyl_acyl_carrier_protein_NADP_plus__oxidoreductase_c0	-0.0393	-4.7745
R_rxn05341_c0	3R_3_Hydroxyoctanoyl_acyl_carrier_protein_NADP_plus__oxidoreductase_c0	-0.0393	-4.7745
R_rxn05337_c0	3R_3_Hydroxyhexanoyl_acyl_carrier_protein_NADP_plus__oxidoreductase_c0	-0.0393	-4.7745
R_rxn05340_c0	3R_3_Hydroxydodecanoyl_acyl_carrier_protein_NADP_plus__oxidoreductase_c0	-0.0358	-4.3448
R_rxn00611_c0	sn_Glycerol_3_phosphate_NAD_plus__2_oxidoreductase_c0	-0.0350	-4.2490
R_rxn00692_c0	5_10_Methylenetetrahydrofolate_glycine_hydroxymethyltransferase_c0	-0.0347	-4.2131
R_rxn05342_c0	3R_3_Hydroxytetradecanoyl_acyl_carrier_protein_NADP_plus__oxidoreductase_c0	-0.0334	-4.0584
R_rxn05336_c0	3R_3_Hydroxypalmitoyl_acyl_carrier_protein_NADP_plus__oxidoreductase_c0	-0.0332	-4.0320
R_rxn00806_c0	L_Leucine_2_oxoglutarate_aminotransferase_c0	-0.0269	-3.2745
R_rxn02811_c0	3_Isopropylmalate_hydro_lyase_c0	-0.0269	-3.2745
R_rxn00506_c0	Acetaldehyde_NAD_plus__oxidoreductase_c0	-0.0260	-3.1615
R_rxn00541_c0	L_threonine_acetaldehyde_lyase_glycine_forming_c0	-0.0260	-3.1615
R_rxn01740_c0	Shikimate_NADP_plus__3_oxidoreductase_c0	-0.0227	-2.7551
R_rxn12017_c0	R08161	-0.0206	-2.5041

R_rxn00908_c0	glycine_synthase_c0	-0.0199	-2.4186
R_rxn04043_c0	ADP_D_fructose_6_phosphate_1_phosphotransferase_c0	-0.0193	-2.3413
R_rxn00786_c0	D_fructose_1_6_bisphosphate_D_glyceraldehyde_3_phosphate_lyase_glycerone_phosphate_forming_c0	-0.0193	-2.3413
R_rxn01973_c0	N_Succinyl_LL_2_6_diaminoheptanedioate_amidohydrolase_c0	-0.0165	-1.9988
R_rxn01116_c0	D_Ribulose_5_phosphate_3_epimerase_c0	-0.0162	-1.9719
R_rxn00777_c0	D_ribose_5_phosphate_aldose_ketose_isomerase_c0	-0.0162	-1.9719
R_rxn15112_c0	Ribose-5-phosphate:ammonia ligase (ADP-forming)	-0.0157	-1.9041
R_rxn01637_c0	N2_Acetyl_L_ornithine_2_oxoglutarate_aminotransferase_c0	-0.0145	-1.7614
R_rxn00503_c0	S_1_pyrroline_5_carboxylate_NAD_plus__oxidoreductase_c0	-0.0135	-1.6410
R_rxn00623_c0	hydrogen_sulfide_NADP_plus__oxidoreductase_c0	-0.0135	-1.6410
R_rxn00929_c0	L_Proline_NAD_plus__5_oxidoreductase_c0	-0.0135	-1.6410
R_rxn01465_c0	S_dihydroorotate_amidohydrolase_c0	-0.0130	-1.5853
R_rxn00086_c0	glutathione_NADP_plus__oxidoreductase_c0	-0.0130	-1.5853
R_rxn00493_c0	L_Phenylalanine_2_oxoglutarate_aminotransferase_c0	-0.0113	-1.3775
R_rxn01301_c0	L_Homoserine_NAD_plus__oxidoreductase_c0	-0.0085	-1.0313
R_rxn00527_c0	L_tyrosine_2_oxoglutarate_aminotransferase_c0	-0.0082	-0.9936
R_rxn02320_c0	5_Amino_2_oxopentanoate_2_oxoglutarate_aminotransferase_c0	-0.0056	-0.6775
R_rxn00832_c0	IMP_1_2_hydrolase_decyclizing_c0	-0.0056	-0.6775
R_rxn01200_c0	Sedoheptulose_7_phosphate_D_glyceraldehyde_3_phosphate_glycolaldehyde_transferase_c0	-0.0032	-0.3916
R_rxn00134_c0	ATP_adenosine_5_phosphotransferase_c0	-0.0032	-0.3888
R_rxn01485_c0	D_Glucosamine_1_phosphate_1_6_phosphomutase_c0	-0.0030	-0.3694
R_rxn00313_c0	meso_2_6_diaminoheptanedioate_carboxy_lyase_L_lysine_forming_c0	-0.0015	-0.1847
R_rxn02285_c0	UDP_N_acetylmuramate_NADP_plus__oxidoreductase_c0	-0.0015	-0.1847
R_rxn01517_c0	ATP_dUMP_phosphotransferase_c0	-0.0007	-0.0858
R_rxn00686_c0	5_6_7_8_tetrahydrofolate_NADP_plus__oxidoreductase_c0	-0.0007	-0.0858
R_rxn03239_c0	S_3_Hydroxyhexadecanoyl_CoA_NAD_plus__oxidoreductase_c0	-0.0002	-0.0264
P_Acid_7	P_Acid7	0.0000	0.0014
P_Acid_5	P_Acid5	0.0001	0.0091
P_Acid_6	P_Acid6	0.0001	0.0091
R_rxn02804_c0	myristoyl_CoA_acetylCoA_C_myristoyltransferase_c0	0.0002	0.0264
R_rxn03240_c0	S_3_Hydroxyhexadecanoyl_CoA_hydro_lyase_c0	0.0002	0.0264
R_rxn05457_c0	Acyl_carrier_protein_acetyltransferase_c0	0.0002	0.0264
R_rxn05732_c0	acyl_CoA_dehydrogenase_hexadecanoyl_CoA_c0	0.0002	0.0264
P_Acid_3	P_Acid3	0.0003	0.0372

P_Acid_4	P_Acid4	0.0003	0.0372
P_Acid_2	P_Acid2	0.0004	0.0477
P_Acid_1	P_Acid	0.0004	0.0477
R_rxn05231_c0	2_Deoxyadenosine_5_diphosphate_oxidized_thioredoxin_2_oxidoreductase_c0	0.0007	0.0851
R_rxn00839_c0	ATP_dADP_phosphotransferase_c0	0.0007	0.0851
R_rxn01520_c0	5_10_Methylenetetrahydrofolate_dUMP_C_methyltransferase_c0	0.0007	0.0858
R_rxn01512_c0	ATP_dTDP_phosphotransferase_c0	0.0007	0.0858
R_rxn01513_c0	ATP_dTMP_phosphotransferase_c0	0.0007	0.0858
R_rxn06075_c0	2_Deoxyuridine_5_diphosphate_oxidized_thioredoxin_2_oxidoreductase_c0	0.0007	0.0858
R_rxn01673_c0	ATP_dCDP_phosphotransferase_c0	0.0011	0.1310
R_rxn01353_c0	ATP_dGDP_phosphotransferase_c0	0.0011	0.1310
R_rxn05233_c0	2_Deoxyguanosine_5_diphosphate_oxidized_thioredoxin_2_oxidoreductase_c0	0.0011	0.1310
R_rxn06076_c0	2_Deoxycytidine_diphosphate_oxidized_thioredoxin_2_oxidoreductase_c0	0.0011	0.1310
R_rxn00851_c0	D_alanine_D_alanine_ligase_ADP_forming_c0	0.0015	0.1847
R_rxn02008_c0	UDP_N_acetylmuramoyl_L_alanine_D_glutamate_ligaseADP_forming_c0	0.0015	0.1847
R_rxn02286_c0	UDP_N_acetylmuramate_L_alanine_ligase_ADP_forming_c0	0.0015	0.1847
R_rxn02011_c0	UDP_N_acetylmuramoyl_L_alanyl_D_glutamate_L_meso_2_6_diaminoheptanedioate_gamma_ligase_ADP_forming_c0	0.0015	0.1847
R_rxn03901_c0	undecaprenyl_diphosphate_phosphohydrolase_c0	0.0015	0.1847
R_rxn00193_c0	glutamate_racemase_c0	0.0015	0.1847
R_rxn00461_c0	Phosphoenolpyruvate_UDP_N_acetyl_D_glucosamine_1_carboxyvinyl_transferase_c0	0.0015	0.1847
R_rxn03408_c0	UDP_N_acetyl_D_glucosamine_undecaprenyl_diphospho_N_acetylmuramoyl_L_alanyl_gamma_D_glutamyl_meso_2_6_diaminopimeloyl_D_alanyl_D_alanine_4_beta_N_acetylglucosaminlytransferase_c0	0.0015	0.1847
R_rxn03164_c0	UDP_N_acetylmuramoyl_L_alanyl_D_glutamyl_meso_2_6_diaminoheptanedioate_D_alanyl_D_alanine_ligaseADP_forming_c0	0.0015	0.1847
R_rxn03904_c0	UDP_N_acetylmuramoyl_L_alanyl_gamma_D_glutamyl_meso_2_6_diaminopimeloyl_D_alanyl_D_alanine_undecaprenyl_phosphate_phospho_N_acetylmuramoyl_pentapeptide_transferase_c0	0.0015	0.1847
R_rxn05909_c0	L_serine_hydro_lyase_adding_hydrogen_sulfide__L_cysteine_forming_c0	0.0020	0.2409
R_rxn00423_c0	acetyl_CoA_L_serine_O_acetyltransferase_c0	0.0030	0.3688
R_rxn00649_c0	O3_acetyl_L_serine_hydrogen_sulfide_2_amino_2_carboxyethyltransferase_c0	0.0030	0.3688
R_rxn03638_c0	Acetyl_CoA_D_glucosamine_1_phosphate_N_acetyltransferase_c0	0.0030	0.3694
R_rxn00283_c0	alanine_racemase_c0	0.0030	0.3694
R_rxn00555_c0	L_glutamine_D_fructose_6_phosphate_isomerase_deaminating_c0	0.0030	0.3694
R_rxn00293_c0	UTP_N_acetyl_alpha_D_glucosamine_1_phosphate_uridylyltransferase_c0	0.0030	0.3694
R_rxn02507_c0	1_2_Carboxyphenylamino_1_deoxy_D_ribulose_5_phosphate_carboxy_lyasecyclizing_c0	0.0032	0.3839
R_rxn01964_c0	L_serine_hydro_lyase_adding_1_C_indol_3_ylglycerol_3_phosphate_L_tryptophan_and_glyceraldehyde_3_phosphate_forming_c0	0.0032	0.3839
R_rxn02508_c0	N_5_Phospho_beta_D_ribosylanthranilate_ketol_isomerase_c0	0.0032	0.3839

R_rxn00726_c0	chorismate_pyruvate_lyase_amino_accepting_anthranilate_forming_c0	0.0032	0.3839
R_rxn00791_c0	N_5_Phospho_D_ribosylanthranilate_pyrophosphate_phosphoribosyl_transferase_c0	0.0032	0.3839
R_rxn00772_c0	ATP_D_ribose_5_phosphotransferase_c0	0.0032	0.3888
R_rxn01137_c0	Adenosine_aminohydrolase_c0	0.0032	0.3888
R_rxn01299_c0	Inosine_ribohydrolase_c0	0.0032	0.3888
R_rxn00836_c0	IMP_diphosphate_phospho_D_ribosyltransferase_c0	0.0032	0.3888
R_rxn01333_c0	sedoheptulose_7_phosphate_D_glyceraldehyde_3_phosphate_glyceronetransferase_c0	0.0032	0.3916
R_rxn03135_c0	R04558_c0	0.0056	0.6775
R_rxn03137_c0	10_Formyltetrahydrofolate_5_phosphoribosyl_5_amino_4_imidazolecarboxamide_formyltransferase_c0	0.0056	0.6775
R_rxn02473_c0	D_erythro_1_Imidazol_4_ylglycerol_3_phosphate_hydro_lyase_c0	0.0056	0.6775
R_rxn03175_c0	N_5_Phospho_D_ribosylformimino_5_amino_1__5_phospho_D_ribosyl_4_imidazolecarboxamide_ketol_isomerase_c0	0.0056	0.6775
R_rxn00859_c0	L_Histidinol_NAD_plus__oxidoreductase_c0	0.0056	0.6775
R_rxn01211_c0	5_10_Methenyltetrahydrofolate_5_hydrolase_decyclizing_c0	0.0056	0.6775
R_rxn02160_c0	L_Histidinol_phosphate_phosphohydrolase_c0	0.0056	0.6775
R_rxn02835_c0	1_5_phospho_D_ribosyl_AMP_1_6_hydrolase_c0	0.0056	0.6775
R_rxn00907_c0	5_10_methylenetetrahydrofolate_NADP_plus__oxidoreductase_c0	0.0056	0.6775
R_rxn00789_c0	1_5_phospho_D_ribosyl_ATP_diphosphate_phospho_alpha_D_ribosyl_transferase_c0	0.0056	0.6775
R_rxn02834_c0	Phosphoribosyl_ATP_pyrophosphohydrolase_c0	0.0056	0.6775
R_rxn00410_c0	UTP_ammonia_ligase_ADP_forming_c0	0.0073	0.8867
R_rxn00237_c0	ATP_GDP_phosphotransferase_c0	0.0077	0.9353
R_rxn01269_c0	Prephenate_NADP_plus__oxidoreductasedecarboxylating_c0	0.0082	0.9936
R_rxn01303_c0	Acetyl_CoA_L_homoserine_O_acetyltransferase_c0	0.0085	1.0313
R_rxn00337_c0	ATP_L_aspartate_4_phosphotransferase_c0	0.0085	1.0313
R_rxn00952_c0	O_acetyl_L_homoserine_hydrogen_sulfide_S_3_amino_3_carboxypropyltransferase_c0	0.0085	1.0313
R_rxn00693_c0	5_Methyltetrahydrofolate_L_homocysteine_S_methyltransferase_c0	0.0085	1.0313
R_rxn01643_c0	L_Aspartate_4_semialdehyde_NADP_plus__oxidoreductase_phosphorylating_c0	0.0085	1.0313
R_rxn00239_c0	ATP_GMP_phosphotransferase_c0	0.0088	1.0663
xanthosine_build	XMP	0.0088	1.0663
R_rxn00834_c0	IMP_NAD_plus__oxidoreductase_c0	0.0088	1.0663
R_rxn07578_c0	R07764_c0	0.0094	1.1459
R_rxn07576_c0	3-oxoacyl-[acyl-carrier-protein] synthase	0.0094	1.1459
R_rxn07577_c0	3-oxoacyl-[acyl-carrier-protein] reductase	0.0094	1.1459
R_rxn05458_c0	Acyl_carrier_protein_acetyltransferase_c0	0.0112	1.3582
R_rxn01000_c0	prephenate_hydro_lyase_decarboxylating_phenylpyruvate_forming_c0	0.0113	1.3775

R_rxn08016_c0	palmitate-[acyl-carrier-protein] ligase	0.0114	1.3846
R_rxn10202_c0	glycerol_3_phosphate__acyl_coa_acyltransferase_16_0_c0	0.0114	1.3846
R_rxn08799_c0	Lysophospholipase_L1_2_acylglycerophosphotidate__n_C16_0_periplasm_c0	0.0114	1.3846
R_rxn03437_c0	R_2_3_Dihydroxy_3_methylpentanoate_hydro_lyase_c0	0.0116	1.4152
R_rxn03436_c0	(S)-2-Aceto-2-hydroxybutanoate:NADP+ oxidoreductase (isomerizing)	0.0116	1.4152
R_rxn01575_c0	L_Isoleucine_2_oxoglutarate_aminotransferase_c0	0.0116	1.4152
R_rxn00737_c0	L_threonine_ammonia_lyase_2_oxobutanoate_forming_c0	0.0116	1.4152
R_rxn03435_c0	(R)-2,3-Dihydroxy-3-methylpentanoate:NADP+ oxidoreductase (isomerizing)	0.0116	1.4152
R_rxn08043_c0	pyruvate:2-oxobutanoate acetaldehydetransferase (decarboxylating)	0.0116	1.4152
R_rxn00710_c0	orotidine_5_phosphate_carboxy_lyase_UMP_forming_c0	0.0130	1.5853
R_rxn00205_c0	glutathione_hydrogen_peroxide_oxidoreductase_c0	0.0130	1.5853
R_rxn01018_c0	carbamoyl_phosphate_L_aspartate_carbamoyltransferase_c0	0.0130	1.5853
R_rxn01360_c0	(S)-dihydroorotate:fumarate oxidoreductase	0.0130	1.5853
R_rxn01362_c0	Orotidine_5_phosphate_diphosphate_phospho_alpha_D_ribosyl_transferase_c0	0.0130	1.5853
R_rxn05256_c0	AMP_sulfite_thioredoxin_disulfide_oxidoreductaseadenosine_5_phosphosulfate_forming_c0	0.0135	1.6410
R_rxn00379_c0	ATP_sulfate_adenylyltransferase_c0	0.0135	1.6410
R_rxn05651_c0	sulfate_transport_in_via_proton_symport_c0	0.0135	1.6410
R_rxn00416_c0	L_aspartate_L_glutamine_amido_ligase_AMP_forming_c0	0.0139	1.6862
R_rxn00192_c0	acetyl_CoA_L_glutamate_N_acetyltransferase_c0	0.0145	1.7614
R_rxn01434_c0	L_Citrulline_L_aspartate_ligase_AMP_forming_c0	0.0145	1.7614
R_rxn01917_c0	ATP_N_acetyl_L_glutamate_5_phosphotransferase_c0	0.0145	1.7614
R_rxn00469_c0	N2_Acetyl_L_ornithine_amidohydrolase_c0	0.0145	1.7614
R_rxn00802_c0	2_Nomega_L_argininosuccinate_arginine_lyase_fumarate_forming_c0	0.0145	1.7614
R_rxn02465_c0	N_acetyl_L_glutamate_5_semialdehyde_NADP_plus__5_oxidoreductase_phosphrylating_c0	0.0145	1.7614
R_rxn01019_c0	Carbamoyl_phosphate_L_ornithine_carbamoyltransferase_c0	0.0145	1.7614
R_rxn00119_c0	ATP_UMP_phosphotransferase_c0	0.0146	1.7699
R_rxn00148_c0	ATP_pyruvate_2_O_phosphotransferase_c0	0.0151	1.8362
R_rxn00117_c0	ATP_UDP_phosphotransferase_c0	0.0154	1.8688
R_rxn00790_c0	5_phosphoribosylamine_diphosphate_phospho_alpha_D_ribosyltransferase_glutamate_amidating_c0	0.0157	1.9041
lysine_formation	lysine4	0.0165	1.9988
R_rxn05289_c0	NADPH_oxidized_thioredoxin_oxidoreductase_c0	0.0171	2.0738
R_rxn00409_c0	ATP_CDP_phosphotransferase_c0	0.0186	2.2563
R_rxn00785_c0	D_Fructose_6_phosphate_D_glyceraldehyde_3_phosphate_glycolaldehyde_transferase_c0	0.0195	2.3635
R_rxn01256_c0	Chorismate_pyruvatemutase_c0	0.0195	2.3712

R_rxn00364_c0	ATP_CMP_phosphotransferase_c0	0.0196	2.3873
R_rxn05332_c0	(3R)-3-Hydroxypalmitoyl-[acyl-carrier-protein] hydro-lyase	0.0206	2.5041
R_rxn02213_c0	3_Dehydroquinate_hydro_lyase_c0	0.0227	2.7551
R_rxn01255_c0	5_O_1_Carboxyvinyl_3_phosphoshikimate_phosphate_lyase_chorismate_forming_c0	0.0227	2.7551
R_rxn01739_c0	ATP_shikimate_3_phosphotransferase_c0	0.0227	2.7551
R_rxn02212_c0	2_Dehydro_3_deoxy_D_arabino_heptonate_7_phosphate_phosphate_lyase_cyclyzing_c0	0.0227	2.7551
R_rxn01332_c0	Phosphoenolpyruvate_D_erythrose_4_phosphate_C_1_carboxyvinyltransferase_phosphate_hydrolysing__2_carboxy_2_oxoethyl_forming_c0	0.0227	2.7551
R_rxn02476_c0	Phosphoenolpyruvate_3_phosphoshikimate_5_O_1_carboxyvinyl_transferase_c0	0.0227	2.7551
R_rxn02789_c0	2_Isopropylmalate_hydro_lyase_c0	0.0269	3.2745
R_rxn01208_c0	R01652_c0	0.0269	3.2745
R_rxn00902_c0	acetyl_CoA_3_methyl_2_oxobutanoate_C_acetyltransferase_thioester_hydrolysing__carboxymethyl_forming_c0	0.0269	3.2745
R_rxn03062_c0	3_Isopropylmalate_NAD_plus__oxidoreductase_c0	0.0269	3.2745
R_rxn00114_c0	ATP_carbamate_phosphotransferase_c0	0.0275	3.3467
R_rxn00770_c0	ATP_D_ribose_5_phosphate_diphosphotransferase_c0	0.0319	3.8732
R_rxn05344_c0	Tetradecanoyl_acyl_carrier_protein_malonyl_acyl_carrier_protein_C_acyltransferase_decarboxylating_c0	0.0332	4.0320
R_rxn05331_c0	(3R)-3-Hydroxybutanoyl-[acyl-carrier-protein] hydro-lyase	0.0334	4.0584
R_rxn05345_c0	dodecanoyl_acyl_carrier_protein_malonyl_acyl_carrier_protein_C_acyltransferase_decarboxylating_c0	0.0334	4.0584
R_rxn05335_c0	(3R)-3-Hydroxypalmitoyl-[acyl-carrier-protein] hydro-lyase	0.0334	4.0584
R_rxn05324_c0	Dodecanoyl-[acyl-carrier protein]:malonyl-CoA C-acyltransferase(decarboxylating oxoacyl- and enoyl-reducing)	0.0334	4.0584
R_rxn05351_c0	Tetradecanoyl-[acyl-carrier protein]:malonyl-CoA C-acyltransferase(decarboxylating oxoacyl- and enoyl-reducing and thioester-hydrolysing)	0.0334	4.0584
R_rxn00747_c0	D_glyceraldehyde_3_phosphate_aldose_ketose_isomerase_c0	0.0350	4.2490
R_rxn05333_c0	(3R)-3-Hydroxybutanoyl-[acyl-carrier-protein] hydro-lyase	0.0358	4.3448
R_rxn05348_c0	Decanoyl_acyl_carrier_protein_malonyl_acyl_carrier_protein_C_acyltransferase_decarboxylating_c0	0.0358	4.3448
R_rxn05327_c0	Decanoyl-[acyl-carrier protein]:malonyl-CoA C-acyltransferase(decarboxylating oxoacyl- and enoyl-reducing)	0.0358	4.3448
R_rxn00904_c0	L_Valine_pyruvate_aminotransferase_c0	0.0387	4.7017
R_rxn05329_c0	(3R)-3-Hydroxybutanoyl-[acyl-carrier-protein] hydro-lyase	0.0393	4.7745
R_rxn05334_c0	(3R)-3-Hydroxybutanoyl-[acyl-carrier-protein] hydro-lyase	0.0393	4.7745
R_rxn05349_c0	acetyl_CoA_acyl_carrier_protein_S_acetyltransferase_c0	0.0393	4.7745
R_rxn05346_c0	butyryl_acyl_carrier_protein_malonyl_acyl_carrier_protein_C_acyltransferase_decarboxylating_c0	0.0393	4.7745
R_rxn05330_c0	(3R)-3-Hydroxybutanoyl-[acyl-carrier-protein] hydro-lyase	0.0393	4.7745
R_rxn05350_c0	hexanoyl_acyl_carrier_protein_malonyl_acyl_carrier_protein_C_acyltransferase_decarboxylating_c0	0.0393	4.7745
R_rxn05347_c0	Acyl_acyl_carrier_protein_malonyl_acyl_carrier_protein_C_acyltransferase_decarboxylating_c0	0.0393	4.7745
R_rxn05325_c0	Octanoyl-[acyl-carrier protein]:malonyl-CoA C-acyltransferase(decarboxylating oxoacyl- and enoyl-reducing)	0.0393	4.7745
R_rxn05326_c0	Hexanoyl-[acyl-carrier protein]:malonyl-CoA C-acyltransferase(decarboxylating oxoacyl- and enoyl-reducing)	0.0393	4.7745

R_rxn05322_c0	Butyryl-[acyl-carrier protein]:malonyl-CoA C-acyltransferase(decarboxylating oxoacyl- and enoyl-reducing)	0.0393	4.7745
R_rxn05343_c0	Octanoyl_acyl_carrier_protein_malonyl_acyl_carrier_protein_C_acyltransferase_decarboxylating_c0	0.0393	4.7745
Malate_buildin	pyruvate_to_oxobuanoate	0.0453	5.5026
R_rxn01102_c0	ATP_R_glycerate_3_phosphotransferase_c0	0.0612	7.4387
R_rxn00420_c0	O_phospho_L_serine_phosphohydrolase_c0	0.0612	7.4387
R_rxn01101_c0	3_Phospho_D_glycerate_NAD_plus__2_oxidoreductase_c0	0.0612	7.4387
P_Acid_8	P_Acid8	0.0620	7.5275
R_rxn00187_c0	L_Glutamate_ammonia_ligase_ADP_forming_c0	0.0629	7.6454
R_rxn00097_c0	ATP_AMP_phosphotransferase_c0	0.0715	8.6826
oxaloacetate_buildin	2pdg to 13bdg	0.0898	10.9112
R_rxn00001_c0	diphosphate_phosphohydrolase_c0	0.1222	14.8468
R_rxn00459_c0	2_phospho_D_glycerate_hydro_lyase_phosphoenolpyruvate_forming_c0	0.1510	18.3498
R_rxn00251_c0	phosphate_oxaloacetate_carboxy_lyase_adding_phosphatephosphoenolpyruvate_forming_c0	0.1828	22.2084
R_rxn00910_c0	5_methyltetrahydrofolate_NADP_plus__oxidoreductase_c0	0.2200	26.7312
R_rxn00161_c0	S_Malate_NADP_plus__oxidoreductaseoxaloacetate_decarboxylating_c0	0.2440	29.6533
R_rxn05465_c0	Malonyl_CoA_acyl_carrier_protein_S_malonyltransferase_c0	0.2689	32.6792
R_rxn00182_c0	L_glutamate_NAD_plus__oxidoreductase_deaminating_c0	0.3217	39.0897
R_rxn00154_c0	pyruvate:NAD+ 2-oxidoreductase CoA-acetylating	0.4054	49.2608
R_rxn10121_c0	Nitrate_reductase_Menaquinol_8_periplasm_c0	0.4120	50.0630
R_rxn00568_c0	NIRBD_RXNc_c0	0.4120	50.0630
R_rxn05627_c0	nitrate_transport_in_via_proton_symport_c0	0.4120	50.0630
R_rxn08094_c0	2_Oxoglutarate_dehydrogenase_complex_c0	0.8025	97.5039
R_rxn00598_c0	Succinyl-CoA:acetyl-CoA C-acyltransferase [ADD]	0.8230	99.9998
R_rxn02144_c0	4-carboxymethylbut-3-en-4-olide enol-lactonohydrolase [ADD]	0.8230	99.9998
R_rxn02971_c0	5_oxo_2_5_dihydrofuran_2_acetate_delta3_delat2_isomerase_c0	0.8230	99.9998
R_rxn02782_c0	2_5_Dihydro_5_oxofuran_2_acetate_lyase_decyclizing_c0	0.8230	99.9998
R_rxn00588_c0	Catechol_oxygen_1_2_oxidoreductasedecyclizing_c0	0.8230	99.9998
R_rxn02143_c0	Succinyl-CoA:3-oxoadipate CoA-transferase [ADD reverse]	0.8230	99.9998
R_rxn00257_c0	acetyl_CoA_oxaloacetate_C_acetyltransferase_pro_S_carboxymethyl_forming__ADP_phosphorylating_c0	0.8639	104.9752
R_rxn00974_c0	citrate_hydro_lyase_cis_aconitate_forming_c0	0.8639	104.9752
R_rxn01388_c0	isocitrate_hydro_lyase_cis_aconitate_forming_c0	0.8639	104.9752
R_rxn00198_c0	isocitrate_transfer	0.8639	104.9752
R_rxn10806_c0	cytochrome_oxidase_bd_menaquinol_8__2_protons_periplasm_c0	1.1970	145.4419

R_rxn10113_c0	cytochrome_oxidase_bo3_ubiquinol_8__25_protons_c0	1.3795	167.6130
R_rxn08900_c0	FAD_dependent_malate_dehydrogenase_c0	1.3795	167.6130
R_rxn10042_c0	F1_ATPase_c0	1.6667	202.5106

Table C.1 *P. fluorescens in silico* catechol metabolism Part 2

Coded reaction id	Reaction
R_rxn00799_c0	L-Malate[c0] <=> H2O[c0] + Fumarate[c0]
R_rxn08527_c0	Fumarate[c0] + Menaquinol 8[c0] <=> Succinate[c0] + Menaquinone 8[c0]
R_rxn00285_c0	ATP[c0] + CoA[c0] + Succinate[c0] <=> ADP[c0] + Phosphate[c0] + Succinyl-CoA[c0]
R_rxn00258_c0	Pyruvate[c0] + Malonyl-CoA[c0] <=> Acetyl-CoA[c0] + Oxaloacetate[c0]
R_rxn04954_c0	NAD[c0] + 5-Methyltetrahydrofolate[c0] <=> NADH[c0] + H+[c0] + 5-10-Methylenetetrahydrofolate[c0]
R_rxn00781_c0	NAD[c0] + Phosphate[c0] + Glyceraldehyde3-phosphate[c0] <=> NADH[c0] + H+[c0] + 1,3-Bisphospho-D-glycerate[c0]
R_rxn00260_c0	2-Oxoglutarate[c0] + L-Aspartate[c0] <=> L-Glutamate[c0] + Oxaloacetate[c0]
R_rxn02914_c0	2-Oxoglutarate[c0] + phosphoserine[c0] <=> L-Glutamate[c0] + 3-Phosphonooxypyruvate[c0]
R_rxn08647_c0	ATP[c0] + Glycerate[c0] <=> ADP[c0] + H+[c0] + 2-Phospho-D-glycerate[c0]
R_rxn00903_c0	2-Oxoglutarate[c0] + L-Valine[c0] <=> L-Glutamate[c0] + 3-Methyl-2-oxobutanoate[c0]
R_rxn05339_c0	NADP[c0] + (R)-3-Hydroxybutanoyl-[acyl-carrier protein][c0] <=> NADPH[c0] + Acetoacetyl-ACP[c0]
R_rxn05338_c0	NADP[c0] + (R)-3-Hydroxydecanoyl-[acyl-carrier protein][c0] <=> NADPH[c0] + H+[c0] + 3-oxodecanoyl-acp[c0]
R_rxn05341_c0	NADP[c0] + (R)-3-Hydroxyoctanoyl-[acyl-carrier protein][c0] <=> NADPH[c0] + H+[c0] + 3-oxooctanoyl-acp[c0]
R_rxn05337_c0	NADP[c0] + D-3-Hydroxyhexanoyl-[acp][c0] <=> NADPH[c0] + 3-Oxohexanoyl-[acp][c0]
R_rxn05340_c0	NADP[c0] + D-3-Hydroxydodecanoyl-[acp][c0] <=> NADPH[c0] + 3-oxododecanoyl-acp[c0]
R_rxn00611_c0	NAD[c0] + Glycerol-3-phosphate[c0] <=> NADH[c0] + H+[c0] + Glycerone-phosphate[c0]
R_rxn00692_c0	H2O[c0] + Glycine[c0] + 5-10-Methylenetetrahydrofolate[c0] <=> L-Serine[c0] + Tetrahydrofolate[c0]
R_rxn05342_c0	NADP[c0] + HMA[c0] <=> NADPH[c0] + 3-oxotetradecanoyl-acp[c0]
R_rxn05336_c0	NADP[c0] + R-3-hydroxypalmitoyl-acyl-carrierprotein-[c0] <=> NADPH[c0] + 3-oxohexadecanoyl-acp[c0]
R_rxn00806_c0	2-Oxoglutarate[c0] + L-Leucine[c0] <=> L-Glutamate[c0] + 4MOP[c0]
R_rxn02811_c0	3-Isopropylmalate <=> H2O + 2-Isopropylmaleate
R_rxn00506_c0	H2O[c0] + NAD[c0] + Acetaldehyde[c0] => NADH[c0] + Acetate[c0] + (2) H+[c0]
R_rxn00541_c0	L-Threonine[c0] <=> Glycine[c0] + Acetaldehyde[c0]
R_rxn01740_c0	NADP[c0] + Shikimate[c0] <=> NADPH[c0] + H+[c0] + 3-Dehydroshikimate[c0]
R_rxn12017_c0	O2 + hexadecanoyl-acp + AH2 => 2 H2O + A + hexadecenoyl-[acyl-carrier protein]
R_rxn00908_c0	NAD[c0] + Glycine[c0] + Tetrahydrofolate[c0] <=> NADH[c0] + CO2[c0] + NH3[c0] + 5-10-Methylenetetrahydrofolate[c0]
R_rxn04043_c0	ADP[c0] + D-fructose-6-phosphate[c0] <=> AMP[c0] + (2) H+[c0] + D-fructose-1,6-bisphosphate[c0]
R_rxn00786_c0	D-fructose-1,6-bisphosphate[c0] <=> Glycerone-phosphate[c0] + Glyceraldehyde3-phosphate[c0]
R_rxn01973_c0	H2O[c0] + N-Succinyl-L-2,6-diaminopimelate[c0] <=> Succinate[c0] + LL-2,6-Diaminopimelate[c0]
R_rxn01116_c0	D-Ribulose5-phosphate[c0] <=> D-Xylulose5-phosphate[c0]
R_rxn00777_c0	ribose-5-phosphate[c0] <=> D-Ribulose5-phosphate[c0]
R_rxn15112_c0	ATP + NH3 + alpha-D-Ribose 5-phosphate => ADP + Phosphate + H+ + 5-Phosphoribosylamine
R_rxn01637_c0	2-Oxoglutarate[c0] + N-Acetylornithine[c0] <=> L-Glutamate[c0] + 2-Acetamido-5-oxopentanoate[c0]

R_rxn00503_c0	(2) H2O[c0] + NAD[c0] + 1-Pyrroline-5-carboxylate[c0] <=> NADH[c0] + L-Glutamate[c0] + H+[c0]
R_rxn00623_c0	(3) H2O[c0] + (3) NADP[c0] + H2S[c0] <=> (3) NADPH[c0] + (3) H+[c0] + Sulfite[c0]
R_rxn00929_c0	NAD[c0] + L-Proline[c0] <=> NADH[c0] + (2) H+[c0] + 1-Pyrroline-5-carboxylate[c0]
R_rxn01465_c0	H2O[c0] + S-Dihydroorotate[c0] <=> H+[c0] + N-Carbamoyl-L-aspartate[c0]
R_rxn00086_c0	NADP[c0] + (2) GSH[c0] <=> NADPH[c0] + H+[c0] + Oxidized glutathione[c0]
R_rxn00493_c0	2-Oxoglutarate[c0] + L-Phenylalanine[c0] <=> L-Glutamate[c0] + Phenylpyruvate[c0]
R_rxn01301_c0	NAD[c0] + L-Homoserine[c0] <=> NADH[c0] + H+[c0] + L-Aspartate4-semialdehyde[c0]
R_rxn00527_c0	2-Oxoglutarate[c0] + L-Tyrosine[c0] <=> L-Glutamate[c0] + p-hydroxyphenylpyruvate[c0]
R_rxn02320_c0	2-Oxoglutarate[c0] + L-histidinol-phosphate[c0] <=> L-Glutamate[c0] + imidazole acetol-phosphate[c0]
R_rxn00832_c0	H2O[c0] + IMP[c0] <=> FAICAR[c0]
R_rxn01200_c0	Glyceraldehyde3-phosphate[c0] + Sedoheptulose7-phosphate[c0] <=> ribose-5-phosphate[c0] + D-Xylulose5-phosphate[c0]
R_rxn00134_c0	ATP[c0] + Adenosine[c0] <=> ADP[c0] + AMP[c0] + H+[c0]
R_rxn01485_c0	D-Glucosamine1-phosphate[c0] <=> D-Glucosamine phosphate[c0]
R_rxn00313_c0	H+[c0] + meso-2,6-Diaminopimelate[c0] <=> CO2[c0] + L-Lysine[c0]
R_rxn02285_c0	NADP[c0] + UDP-MurNAc[c0] <=> NADPH[c0] + H+[c0] + UDP-N-acetylglucosamine enolpyruvate[c0]
R_rxn01517_c0	ATP[c0] + H+[c0] + dUMP[c0] <=> ADP[c0] + dUDP[c0]
R_rxn00686_c0	NADP[c0] + Tetrahydrofolate[c0] <=> NADPH[c0] + H+[c0] + Dihydrofolate[c0]
R_rxn03239_c0	NAD + (S)-3-Hydroxyhexadecanoyl-CoA <=> NADH + H+ + 3-Oxopalmitoyl-CoA
P_Acid_7	Phosphatidylglycerol [c0] + CDPdiacylglycerol[c0] => 50 H+[c0] + 50 CMP[c0] + Cardiolipin[c0]
P_Acid_5	50 L-serine[c0] + CDPdiacylglycerol[c0] => 50 H+[c0] + 50 CMP[c0] + Phosphatidylserine[c0]
P_Acid_6	Phosphatidylserine[c0] + 50 H+[c0] => 50 CO2[c0] + Phosphatidylethanolamine[c0]
R_rxn02804_c0	H2O[c0] + Phosphoribosyl-ATP[c0] => PPi[c0] + (2) H+[c0] + Phosphoribosyl-AMP[c0]
R_rxn03240_c0	(S)-3-Hydroxyhexadecanoyl-CoA <=> H2O + (2E)-Hexadecenoyl-CoA
R_rxn05457_c0	CoA + Myristoyl-ACP <=> Myristoyl-CoA + ACP
R_rxn05732_c0	NADH + H+ + (2E)-Hexadecenoyl-CoA => NAD + Palmitoyl-CoA
P_Acid_3	50 Glycerol-3-phosphate [c0] + CDPdiacylglycerol [c0]=> 50 H+ [c0]+ 50 CMP [c0]+ Phosphatidylglycerophosphate[c0]
P_Acid_4	50 H2O[c0] + Phosphatidylglycerophosphate[c0] => 50 Phosphate[c0] + Phosphatidylglycerol[c0]
P_Acid_2	50 H+[c0] + 50 CTP[c0] + PhosphatidicAcid[c0] => 50 PPi[c0] + CDPdiacylglycerol[c0]
P_Acid_1	6 D-3-Hydroxydodecanoyl-[acp][c0] + 50 Glycerol-3-phosphate[c0] + 9 (R)-3-Hydroxydecanoyl-[acyl-carrier protein] [c0]+ 24 (2E)-Octadecenoyl-[acp] [c0]+ 32 R-3-hydroxypalmitoyl-acyl-carrierprotein- [c0]+ 29 Palmitoyl-ACP[c0] => 100 ACP[c0] + PhosphatidicAcid[c0]
R_rxn05231_c0	ADP[c0] + trdrd[c0] => H2O[c0] + dADP[c0] + trdox[c0]
R_rxn00839_c0	ATP[c0] + dADP[c0] <=> ADP[c0] + dATP[c0]
R_rxn01520_c0	5-10-Methylenetetrahydrofolate[c0] + dUMP[c0] => dTMP[c0] + Dihydrofolate[c0]
R_rxn01512_c0	ATP[c0] + dTDP[c0] <=> ADP[c0] + TTP[c0]
R_rxn01513_c0	ATP[c0] + H+[c0] + dTMP[c0] <=> ADP[c0] + dTDP[c0]
R_rxn06075_c0	H2O[c0] + dUDP[c0] + trdox[c0] <= UDP[c0] + trdrd[c0]
R_rxn01673_c0	ATP[c0] + dCDP[c0] <=> ADP[c0] + dCTP[c0]
R_rxn01353_c0	ATP[c0] + dGDP[c0] <=> ADP[c0] + dGTP[c0]
R_rxn05233_c0	GDP[c0] + trdrd[c0] => H2O[c0] + dGDP[c0] + trdox[c0]
R_rxn06076_c0	H2O[c0] + dCDP[c0] + trdox[c0] <= CDP[c0] + trdrd[c0]
R_rxn00851_c0	ATP[c0] + (2) D-Alanine[c0] => ADP[c0] + Ala-Ala[c0] + Phosphate[c0] + H+[c0]

R_rxn02008_c0	ATP[c0] + D-Glutamate[c0] + UDP-N-acetylmuramoyl-L-alanine[c0] => ADP[c0] + Phosphate[c0] + H+[c0] + UDP-N-acetylmuramoyl-L-alanyl-D-glutamate[c0]
R_rxn02286_c0	ATP[c0] + L-Alanine[c0] + UDP-MurNAc[c0] => ADP[c0] + UDP-N-acetylmuramoyl-L-alanine[c0] + H+[c0] + Phosphate[c0]
R_rxn02011_c0	ATP[c0] + meso-2,6-Diaminopimelate[c0] + UDP-N-acetylmuramoyl-L-alanyl-D-glutamate[c0] => ADP[c0] + Phosphate[c0] + H+[c0] + UDP-N-acetylmuramoyl-L-alanyl-D-gamma-glutamyl-meso-2-6-diaminopimelate[c0]
R_rxn03901_c0	H2O[c0] + Bactoprenyl diphosphate[c0] => Phosphate[c0] + (2) H+[c0] + Undecaprenylphosphate[c0]
R_rxn00193_c0	L-Glutamate[c0] <=> D-Glutamate[c0]
R_rxn00461_c0	UDP-N-acetylglucosamine[c0] + Phosphoenolpyruvate[c0] <=> Phosphate[c0] + UDP-N-acetylglucosamine enolpyruvate[c0]
R_rxn03408_c0	UDP-N-acetylglucosamine[c0] + Undecaprenyl-diphospho-N-acetylmuramoyl-L-alanyl-D-glutamyl-meso-2-6-diaminopimeloyl-D-alanyl-D-alanine[c0] <=> UDP[c0] + Undecaprenyl-diphospho-N-acetylmuramoyl--N-acetylglucosamine-L-ala-D-glu-meso-2-6-diaminopimeloyl-D-ala-D-ala[c0]
R_rxn03164_c0	UDP-N-acetylmuramoyl-L-alanyl-D-gamma-glutamyl-meso-2-6-diaminopimelate[c0] + Ala-Ala[c0] + ATP[c0] => H+[c0] + Phosphate[c0] + UDP-N-acetylmuramoyl-L-alanyl-D-glutamyl-6-carboxy-L-lysyl-D-alanyl- D-alanine[c0] + ADP[c0]
R_rxn03904_c0	Undecaprenylphosphate[c0] + UDP-N-acetylmuramoyl-L-alanyl-D-glutamyl-6-carboxy-L-lysyl-D-alanyl-D-alanine[c0] <=> UMP[c0] + Undecaprenyl-diphospho-N-acetylmuramoyl-L-alanyl-D-glutamyl-meso-2-6-diaminopimeloyl-D-alanyl-D-alanine[c0]
R_rxn05909_c0	L-Serine[c0] + H+[c0] + H2S[c0] <=> H2O[c0] + L-Cysteine[c0]
R_rxn00423_c0	Acetyl-CoA[c0] + L-Serine[c0] => CoA[c0] + O-Acetyl-L-serine[c0]
R_rxn00649_c0	H2S[c0] + O-Acetyl-L-serine[c0] => Acetate[c0] + L-Cysteine[c0]
R_rxn03638_c0	Acetyl-CoA[c0] + D-Glucosamine1-phosphate[c0] => CoA[c0] + H+[c0] + N-Acetyl-D-glucosamine1-phosphate[c0]
R_rxn00283_c0	L-Alanine[c0] <=> D-Alanine[c0]
R_rxn00555_c0	L-Glutamine[c0] + D-fructose-6-phosphate[c0] <=> L-Glutamate[c0] + D-Glucosamine phosphate[c0]
R_rxn00293_c0	UTP[c0] + N-Acetyl-D-glucosamine1-phosphate[c0] <=> PPi[c0] + UDP-N-acetylglucosamine[c0]
R_rxn02507_c0	H+[c0] + 1-(2-carboxyphenylamino)-1-deoxyribulose 5-phosphate[c0] => H2O[c0] + CO2[c0] + Indoleglycerol phosphate[c0]
R_rxn01964_c0	L-Serine[c0] + Indoleglycerol phosphate[c0] => H2O[c0] + L-Tryptophan[c0] + Glyceraldehyde3-phosphate[c0]
R_rxn02508_c0	N-5-phosphoribosyl-anthranilate[c0] <=> 1-(2-carboxyphenylamino)-1-deoxyribulose 5-phosphate[c0]
R_rxn00726_c0	NH3[c0] + Chorismate[c0] => H2O[c0] + Pyruvate[c0] + H+[c0] + Anthranilate[c0]
R_rxn00791_c0	PPi[c0] + H+[c0] + N-5-phosphoribosyl-anthranilate[c0] <= Anthranilate[c0] + PRPP[c0]
R_rxn00772_c0	ATP[c0] + D-Ribose[c0] <=> ADP[c0] + H+[c0] + ribose-5-phosphate[c0]
R_rxn01137_c0	H2O[c0] + H+[c0] + Adenosine[c0] => NH3[c0] + Inosine[c0]
R_rxn01299_c0	H2O[c0] + Inosine[c0] <=> D-Ribose[c0] + HYXN[c0]
R_rxn00836_c0	PPi[c0] + H+[c0] + IMP[c0] <= PRPP[c0] + HYXN[c0]
R_rxn01333_c0	Glyceraldehyde3-phosphate[c0] + Sedoheptulose7-phosphate[c0] <=> D-fructose-6-phosphate[c0] + D-Erythrose4-phosphate[c0]
R_rxn03135_c0	L-Glutamate[c0] + (2) H+[c0] + D-erythro-imidazol-glycerol-phosphate[c0] + AICAR[c0] <= L-Glutamine[c0] + phosphoribulosylformimino-AICAR-phosphate[c0]
R_rxn03137_c0	10-Formyltetrahydrofolate[c0] + AICAR[c0] <=> Tetrahydrofolate[c0] + FAICAR[c0]
R_rxn02473_c0	D-erythro-imidazol-glycerol-phosphate[c0] => H2O[c0] + imidazole acetol-phosphate[c0]
R_rxn03175_c0	H+[c0] + phosphoribosylformiminoaicar-phosphate[c0] <=> phosphoribulosylformimino-AICAR-phosphate[c0]
R_rxn00859_c0	H2O[c0] + (2) NAD[c0] + L-Histidinol[c0] <=> (2) NADH[c0] + (3) H+[c0] + L-Histidine[c0]
R_rxn01211_c0	H2O[c0] + 5-10-Methenyltetrahydrofolate[c0] <=> H+[c0] + 10-Formyltetrahydrofolate[c0]
R_rxn02160_c0	H2O[c0] + L-histidinol-phosphate[c0] => Phosphate[c0] + L-Histidinol[c0]
R_rxn02835_c0	H2O[c0] + Phosphoribosyl-AMP[c0] <=> phosphoribosylformiminoaicar-phosphate[c0]
R_rxn00907_c0	NADP[c0] + 5-10-Methylenetetrahydrofolate[c0] <=> NADPH[c0] + 5-10-Methenyltetrahydrofolate[c0]
R_rxn00789_c0	PPi[c0] + H+[c0] + Phosphoribosyl-ATP[c0] <= ATP[c0] + PRPP[c0]

R_rxn02834_c0	H2O + Phosphoribosyl-ATP => PPi + 2 H+ + Phosphoribosyl-AMP
R_rxn00410_c0	ATP[c0] + NH3[c0] + UTP[c0] <=> ADP[c0] + Phosphate[c0] + CTP[c0] + (2) H+[c0]
R_rxn00237_c0	ATP[c0] + GDP[c0] <=> ADP[c0] + GTP[c0]
R_rxn01269_c0	NADP[c0] + Prephenate[c0] => NADPH[c0] + CO2[c0] + p-hydroxyphenylpyruvate[c0]
R_rxn01303_c0	Acetyl-CoA[c0] + L-Homoserine[c0] => CoA[c0] + O-Acetyl-L-homoserine[c0]
R_rxn00337_c0	ATP[c0] + L-Aspartate[c0] <=> ADP[c0] + 4-Phospho-L-aspartate[c0]
R_rxn00952_c0	H2S[c0] + O-Acetyl-L-homoserine[c0] => Acetate[c0] + Homocysteine[c0]
R_rxn00693_c0	Homocysteine[c0] + 5-Methyltetrahydrofolate[c0] <=> L-Methionine[c0] + Tetrahydrofolate[c0]
R_rxn01643_c0	NADP[c0] + Phosphate[c0] + L-Aspartate4-semialdehyde[c0] <= NADPH[c0] + H+[c0] + 4-Phospho-L-aspartate[c0]
R_rxn00239_c0	ATP[c0] + H+[c0] + GMP[c0] <=> ADP[c0] + GDP[c0]
xanthosine_build	ATP[c0] + H2O[c0] + XMP[c0] + L-Glutamine[c0] => H+[c0] + AMP[c0] + L-Glutamate[c0] + PRPP[c0] + GMP[c0]
R_rxn00834_c0	H2O[c0] + NAD[c0] + IMP[c0] <=> NADH[c0] + H+[c0] + XMP[c0]
R_rxn07578_c0	3-Hydroxystearoyl-[acp] <=> H2O + (2E)-Octadecenoyl-[acp]
R_rxn07576_c0	H+ + hexadecanoyl-acp + Malonyl-acyl-carrierprotein- => CO2 + ACP + 3-Oxostearoyl-[acp]
R_rxn07577_c0	NADPH + H+ + 3-Oxostearoyl-[acp] => NADP + 3-Hydroxystearoyl-[acp]
R_rxn05458_c0	CoA[c0] + H+[c0] + hexadecanoyl-acp[c0] <=> Palmitoyl-CoA[c0] + ACP[c0]
R_rxn01000_c0	H+[c0] + Prephenate[c0] => H2O[c0] + CO2[c0] + Phenylpyruvate[c0]
R_rxn08016_c0	ATP + Palmitate + ACP <=> PPi + AMP + 2 H+ + Palmitoyl-ACP
R_rxn10202_c0	H+[c0] + Glycerol-3-phosphate[c0] + Palmitoyl-CoA[c0] => CoA[c0] + 1-hexadecanoyl-sn-glycerol 3-phosphate[c0]
R_rxn08799_c0	H2O[c0] + 1-hexadecanoyl-sn-glycerol 3-phosphate[c0] <=> (2) H+[c0] + Glycerol-3-phosphate[c0] + Palmitate[c0]
R_rxn03437_c0	2,3-Dihydroxy-3-methylvalerate[c0] => H2O[c0] + 3MOP[c0]
R_rxn03436_c0	2-Aceto-2-hydroxybutanoate <=> (R)-3-Hydroxy-3-methyl-2-oxopentanoate
R_rxn01575_c0	2-Oxoglutarate[c0] + L-Isoleucine[c0] <=> L-Glutamate[c0] + 3MOP[c0]
R_rxn00737_c0	L-Threonine[c0] => NH3[c0] + 2-Oxobutyrate[c0]
R_rxn03435_c0	NADP + 2,3-Dihydroxy-3-methylvalerate <=> NADPH + H+ + (R)-3-Hydroxy-3-methyl-2-oxopentanoate
R_rxn08043_c0	Pyruvate[c0] + H+[c0] + 2-Oxobutyrate[c0] ->CO2[c0] + 2-Aceto-2-hydroxybutanoate[c0]
R_rxn00710_c0	H+[c0] + Orotidylic acid[c0] => CO2[c0] + UMP[c0]
R_rxn00205_c0	H2O2[c0] + (2) GSH[c0] => (2) H2O[c0] + Oxidized glutathione[c0]
R_rxn01018_c0	L-Aspartate[c0] + Carbamoylphosphate[c0] => Phosphate[c0] + H+[c0] + N-Carbamoyl-L-aspartate[c0]
R_rxn01360_c0	O2[c0] + S-Dihydroorotate[c0] => H2O2 [c0]+ Orotate[c0]
R_rxn01362_c0	PPi[c0] + H+[c0] + Orotidylic acid[c0] <= PRPP[c0] + Orotate[c0]
R_rxn05256_c0	APS[c0] + trdrd[c0] => AMP[c0] + H+[c0] + Sulfite[c0] + trdox[c0]
R_rxn00379_c0	ATP[c0] + Sulfate[c0] <=> PPi[c0] + APS[c0]
R_rxn05651_c0	Sulfate[e0] + H+[e0] <=> Sulfate[c0] + H+[c0]
R_rxn00416_c0	H2O[c0] + ATP[c0] + L-Aspartate[c0] + L-Glutamine[c0] => PPi[c0] + AMP[c0] + L-Glutamate[c0] + (2) H+[c0] + L-Asparagine[c0]
R_rxn00192_c0	Acetyl-CoA[c0] + L-Glutamate[c0] => CoA[c0] + H+[c0] + N-Acetyl-L-glutamate[c0]
R_rxn01434_c0	ATP[c0] + L-Aspartate[c0] + Citrulline[c0] <=> PPi[c0] + AMP[c0] + (2) H+[c0] + L-Argininosuccinate[c0]
R_rxn01917_c0	ATP[c0] + N-Acetyl-L-glutamate[c0] <=> ADP[c0] + n-acetylglutamyl-phosphate[c0]
R_rxn00469_c0	H2O[c0] + N-Acetylornithine[c0] <=> Acetate[c0] + Ornithine[c0]
R_rxn00802_c0	L-Argininosuccinate[c0] <=> L-Arginine[c0] + Fumarate[c0]

R_rxn02465_c0	NADP[c0] + Phosphate[c0] + 2-Acetamido-5-oxopentanoate[c0] <= NADPH[c0] + H+[c0] + n-acetylglutamyl-phosphate[c0]
R_rxn01019_c0	Ornithine[c0] + Carbamoylphosphate[c0] => Phosphate[c0] + H+[c0] + Citrulline[c0]
R_rxn00119_c0	ATP[c0] + H+[c0] + UMP[c0] <=> ADP[c0] + UDP[c0]
R_rxn00148_c0	ATP[c0] + Pyruvate[c0] <=> ADP[c0] + Phosphoenolpyruvate[c0] + H+[c0]
R_rxn00117_c0	ATP[c0] + UDP[c0] <=> ADP[c0] + UTP[c0]
R_rxn00790_c0	PPi[c0] + L-Glutamate[c0] + H+[c0] + 5-Phosphoribosylamine[c0] <= H2O[c0] + L-Glutamine[c0] + PRPP[c0]
lysine_formation	N-Succinyl-L-2,6-diaminopimelate[c0] + H2O[c0] <=> L-Lysine [c0]+ LL-2,6-Diaminopimelate[c0]
R_rxn05289_c0	NADPH[c0] + H+[c0] + trdox[c0] <=> NADP[c0] + trdrd[c0]
R_rxn00409_c0	ATP[c0] + CDP[c0] <=> ADP[c0] + CTP[c0]
R_rxn00785_c0	D-fructose-6-phosphate + Glyceraldehyde3-phosphate <=> D-Xylulose5-phosphate + D-Erythrose4-phosphate
R_rxn01256_c0	Chorismate[c0] => Prephenate[c0]
R_rxn00364_c0	ATP[c0] + CMP[c0] + H+[c0] <=> ADP[c0] + CDP[c0]
R_rxn05332_c0	R-3-hydroxypalmitoyl-acyl-carrierprotein[c0]- <=> H2O[c0] + (2E)-Hexadecenoyl-[acp][c0]
R_rxn02213_c0	5-Dehydroquinate[c0] => H2O[c0] + 3-Dehydroshikimate[c0]
R_rxn01255_c0	5-O--1-Carboxyvinyl-3-phosphoshikimate[c0] => Phosphate[c0] + Chorismate[c0]
R_rxn01739_c0	ATP[c0] + Shikimate[c0] <=> ADP[c0] + H+[c0] + 3-phosphoshikimate[c0]
R_rxn02212_c0	DAHP[c0] => Phosphate[c0] + 5-Dehydroquinate[c0]
R_rxn01332_c0	H2O[c0] + Phosphoenolpyruvate[c0] + D-Erythrose4-phosphate[c0] => Phosphate[c0] + DAHP[c0]
R_rxn02476_c0	Phosphoenolpyruvate[c0] + 3-phosphoshikimate[c0] => Phosphate[c0] + 5-O--1-Carboxyvinyl-3-phosphoshikimate[c0]
R_rxn02789_c0	2-Isopropylmalate[c0] <=> H2O[c0] + 2-Isopropylmaleate[c0]
R_rxn01208_c0	CO2[c0] + 4MOP[c0] <= H+[c0] + 2-isopropyl-3-oxosuccinate[c0]
R_rxn00902_c0	CoA[c0] + H+[c0] + 2-Isopropylmalate[c0] <= H2O[c0] + Acetyl-CoA[c0] + 3-Methyl-2-oxobutanoate[c0]
R_rxn03062_c0	NAD[c0] + 3-Isopropylmalate[c0] <=> NADH[c0] + H+[c0] + 2-isopropyl-3-oxosuccinate[c0]
R_rxn00114_c0	ATP[c0] + CO2[c0] + NH3[c0] <=> ADP[c0] + (2) H+[c0] + Carbamoylphosphate[c0]
R_rxn00770_c0	ATP[c0] + ribose-5-phosphate[c0] <=> AMP[c0] + H+[c0] + PRPP[c0]
R_rxn05344_c0	Myristoyl-ACP[c0] + Malonyl-acyl-carrierprotein-[c0] => CO2[c0] + 3-oxohexadecanoyl-acp[c0] + ACP[c0]
R_rxn05331_c0	D-3-Hydroxydodecanoyl-[acp] <=> H2O + (2E)-Dodecenoyl-[acp]
R_rxn05345_c0	Dodecanoyl-ACP[c0] + Malonyl-acyl-carrierprotein-[c0] => CO2[c0] + 3-oxotetradecanoyl-acp[c0] + ACP[c0]
R_rxn05335_c0	HMA[c0] <=> H2O[c0] + (2E)-Tetradecenoyl-[acp][c0]
R_rxn05324_c0	NADH[c0] + 2 H+[c0] + (2E)-Dodecenoyl-[acp][c0] => NAD[c0] + Dodecanoyl-ACP[c0]
R_rxn05351_c0	NADP + Myristoyl-ACP <=> NADPH + H+ + (2E)-Tetradecenoyl-[acp]
R_rxn00747_c0	Glyceraldehyde3-phosphate[c0] <=> Glycerone-phosphate[c0]
R_rxn05333_c0	(R)-3-Hydroxydecanoyl-[acyl-carrier protein] [c0]<=> H2O [c0]+ (2E)-Decenoyl-[acp][c0]
R_rxn05348_c0	Decanoyl-ACP[c0] + Malonyl-acyl-carrierprotein-[c0] => CO2[c0] + 3-oxododecanoyl-acp[c0] + ACP[c0]
R_rxn05327_c0	NADH[c0] + H+[c0] + (2E)-Decenoyl-[acp][c0] => NAD [c0]+ Decanoyl-ACP [c0]
R_rxn00904_c0	Pyruvate[c0] + L-Valine[c0] <=> L-Alanine[c0] + 3-Methyl-2-oxobutanoate[c0]
R_rxn05329_c0	(R)-3-Hydroxybutanoyl-[acyl-carrier protein][c0] <=> H2O [c0]+ But-2-enoyl-[acyl-carrier protein][c0]
R_rxn05334_c0	(R)-3-Hydroxyoctanoyl-[acyl-carrier protein] [c0]<=> H2O[c0] + (2E)-Octenoyl-[acp][c0]
R_rxn05349_c0	Acetyl-CoA[c0] + ACP[c0] <=> CoA[c0] + Acetyl-ACP[c0]
R_rxn05346_c0	Butyryl-ACP[c0] + Malonyl-acyl-carrierprotein-[c0] => CO2[c0] + 3-Oxohexanoyl-[acp][c0] + ACP[c0]

R_rxn05330_c0	D-3-Hydroxyhexanoyl-[acp][c0] <=> H2O[c0] + (2E)-Hexenoyl-[acp][c0]
R_rxn05350_c0	H+[c0] + Hexanoyl-ACP[c0] + Malonyl-acyl-carrierprotein-[c0] => CO2[c0] + 3-oxooctanoyl-acp[c0] + ACP[c0]
R_rxn05347_c0	Malonyl-acyl-carrierprotein-[c0] + Acetyl-ACP[c0] => CO2[c0] + Acetoacetyl-ACP[c0] + ACP[c0]
R_rxn05325_c0	NADH[c0] + H+ [c0]+ (2E)-Octenoyl-[acp][c0] => NAD[c0] + Octanoyl-ACP [c0]
R_rxn05326_c0	NADH[c0] + H+[c0] + (2E)-Hexenoyl-[acp][c0] => NAD[c0] + Hexanoyl-ACP[c0]
R_rxn05322_c0	NADH[c0] + H+[c0] + But-2-enoyl-[acyl-carrier protein] [c0]=> NAD [c0]+ Butyryl-ACP[c0]
R_rxn05343_c0	Octanoyl-ACP[c0] + Malonyl-acyl-carrierprotein-[c0] => CO2[c0] + 3-oxodecanoyl-acp[c0] + ACP[c0]
Malate_buildin	2H+[c0] + Pyruvate[c0] + NADPH[c0] => NADP[c0] + CO2[c0] + H2O[c0] + 3-Methyl-2-oxobutanoate[c0]
R_rxn01102_c0	ATP[c0] + Glycerate[c0] <=> ADP[c0] + H+[c0] + 3-Phosphoglycerate[c0]
R_rxn00420_c0	H2O[c0] + phosphoserine[c0] => Phosphate[c0] + L-Serine[c0]
R_rxn01101_c0	NAD[c0] + 3-Phosphoglycerate[c0] <=> NADH[c0] + H+[c0] + 3-Phosphonooxypyruvate[c0]
P_Acid_8	0.00476 Phosphatidylglycerol[c0] + 0.00121 Phosphatidylethanolamine[c0] + 0.0001864 Cardiolipin[c0] => Lipid[c0]
R_rxn00187_c0	ATP[c0] + NH3[c0] + L-Glutamate[c0] => ADP[c0] + Phosphate[c0] + L-Glutamine[c0] + H+[c0]
R_rxn00097_c0	ATP[c0] + AMP[c0] + H+[c0] <=> (2) ADP[c0]
oxaloacetate_buildin	2-Phospho-D-glycerate [c0] + ATP [c0] => 1,3-Bisphospho-D-glycerate[c0] + ADP [c0]
R_rxn00001_c0	H2O[c0] + PPi[c0] => (2) Phosphate[c0] + H+[c0]
R_rxn00459_c0	2-Phospho-D-glycerate[c0] <=> H2O[c0] + Phosphoenolpyruvate[c0]
R_rxn00251_c0	Phosphate + Oxaloacetate + H+ => H2O + CO2 + Phosphoenolpyruvate
R_rxn00910_c0	NADP + 5-Methyltetrahydrofolate <=> NADPH + H+ + 5-10-Methylenetetrahydrofolate
R_rxn00161_c0	NADP[c0] + L-Malate[c0] => NADPH[c0] + CO2[c0] + Pyruvate[c0]
R_rxn05465_c0	H+[c0] + Malonyl-CoA[c0] + ACP[c0] <=> CoA[c0] + Malonyl-acyl-carrierprotein-[c0]
R_rxn00182_c0	H2O[c0] + NAD[c0] + L-Glutamate[c0] <=> NADH[c0] + NH3[c0] + 2-Oxoglutarate[c0] + H+[c0]
R_rxn00154_c0	NAD + CoA + Pyruvate => NADH + CO2 + Acetyl-CoA
R_rxn10121_c0	(2) H+[c0] + Nitrate[c0] + Menaquinol 8[c0] <=> H2O[c0] + (2) H+[e0] + Nitrite[c0] + Menaquinone 8[c0]
R_rxn00568_c0	(2) H2O[c0] + (3) NAD[c0] + NH3[c0] <= (3) NADH[c0] + (5) H+[c0] + Nitrite[c0]
R_rxn05627_c0	H+[e0] + Nitrate[e0] <=> H+[c0] + Nitrate[c0]
R_rxn08094_c0	NAD[c0] + CoA[c0] + 2-Oxoglutarate[c0] <=> NADH[c0] + CO2[c0] + Succinyl-CoA[c0]
R_rxn00598_c0	CoA + 3-Oxoadipyl-CoA => Acetyl-CoA + Succinyl-CoA
R_rxn02144_c0	H2O[c0] + 3-oxoadipate-enol-lactone[c0] => H+[c0] + 3-Oxoadipate[c0]
R_rxn02971_c0	Muconolactone[c0] <=> 3-oxoadipate-enol-lactone[c0]
R_rxn02782_c0	Muconolactone[c0] <=> H+[c0] + cis,cis-Muconate[c0]
R_rxn00588_c0	O2[c0] + Catechol[c0] => (2) H+[c0] + cis,cis-Muconate[c0]
R_rxn02143_c0	Succinyl-CoA + 3-Oxoadipate => Succinate + 3-Oxoadipyl-CoA
R_rxn00257_c0	ATP[c0] + CoA[c0] + Citrate[c0] <=> ADP[c0] + Phosphate[c0] + Acetyl-CoA[c0] + Oxaloacetate[c0]
R_rxn00974_c0	Citrate[c0] <=> H2O[c0] + cis-Aconitate[c0]
R_rxn01388_c0	Isocitrate[c0] <=> H2O[c0] + cis-Aconitate[c0]
R_rxn00198_c0	NAD + Isocitrate => NADH + CO2 + 2-oxoglutarate
R_rxn10806_c0	(0.5) O2[c0] + (2) H+[c0] + Menaquinol 8[c0] => H2O[c0] + (2) H+[e0] + Menaquinone 8[c0]
R_rxn10113_c0	(0.5) O2[c0] + (2.5) H+[c0] + Ubiquinol-8[c0] => H2O[c0] + (2.5) H+[e0] + Ubiquinone-8[c0]
R_rxn08900_c0	L-Malate[c0] + Ubiquinone-8[c0] => Oxaloacetate[c0] + Ubiquinol-8[c0]
R_rxn10042_c0	ADP[c0] + Phosphate[c0] + (4) H+[e0] <=> H2O[c0] + ATP[c0] + (3) H+[c0]

Table C.1 *P. fluorescens in silico* catechol metabolism Part 3

Coded reaction id	genes	Subsystem
R_rxn00799_c0	fig|9606.20.peg.4964 fig|9606.20.peg.4326 fig|9606.20.peg.876	Protein Metabolism
R_rxn08527_c0	fig|9606.20.peg.1818 fig|9606.20.peg.1816 fig|9606.20.peg.1817 fig|9606.20.peg.1819	Carbohydrates
R_rxn00285_c0	fig|9606.20.peg.1824 fig|9606.20.peg.1823	Carbohydrates
R_rxn00258_c0	fig|9606.20.peg.5784	Nucleosides and Nucleotides
R_rxn04954_c0	fig|9606.20.peg.5748	Stress Response
R_rxn00781_c0	fig|9606.20.peg.4978	Stress Response
R_rxn00260_c0	fig|9606.20.peg.4031 fig|9606.20.peg.3464 fig|9606.20.peg.2233 fig|9606.20.peg.4308 fig|9606.20.peg.3658 fig|9606.20.peg.3179 fig|9606.20.peg.6089 fig|9606.20.peg.2127 fig|9606.20.peg.4632 fig|9606.20.peg.4473 fig|9606.20.peg.3502	Amino Acids and Derivatives
R_rxn02914_c0	fig|9606.20.peg.1641	Cofactors, Vitamins, Prosthetic Groups, Pigments
R_rxn08647_c0	fig|9606.20.peg.6106	Cofactors, Vitamins, Prosthetic Groups, Pigments
R_rxn00903_c0	fig|9606.20.peg.3971	Amino Acids and Derivatives
R_rxn05339_c0	fig|9606.20.peg.3734 fig|9606.20.peg.1994 fig|9606.20.peg.1075 fig|9606.20.peg.2571 fig|9606.20.peg.3093 fig|9606.20.peg.300 fig|9606.20.peg.3196 fig|9606.20.peg.1957 fig|9606.20.peg.4716 fig|9606.20.peg.1953 fig|9606.20.peg.2379	Fatty Acids, Lipids, and Isoprenoids

R_rxn05338_c0	fig|9606.20.peg.3093 fig|9606.20.peg.2571 fig|9606.20.peg.1075 fig|9606.20.peg.1994 fig|9606.20.peg.3734 fig|9606.20.peg.2379 fig|9606.20.peg.1953 fig|9606.20.peg.4716 fig|9606.20.peg.1957 fig|9606.20.peg.3196 fig|9606.20.peg.300	Fatty Acids, Lipids, and Isoprenoids
R_rxn05341_c0	fig|9606.20.peg.1953 fig|9606.20.peg.4716 fig|9606.20.peg.2379 fig|9606.20.peg.300 fig|9606.20.peg.1957 fig|9606.20.peg.3196 fig|9606.20.peg.2571 fig|9606.20.peg.3093 fig|9606.20.peg.3734 fig|9606.20.peg.1075 fig|9606.20.peg.1994	Fatty Acids, Lipids, and Isoprenoids
R_rxn05337_c0	fig|9606.20.peg.300 fig|9606.20.peg.3196 fig|9606.20.peg.1957 fig|9606.20.peg.1953 fig|9606.20.peg.4716 fig|9606.20.peg.2379 fig|9606.20.peg.3734 fig|9606.20.peg.1075 fig|9606.20.peg.1994 fig|9606.20.peg.2571 fig|9606.20.peg.3093	Fatty Acids, Lipids, and Isoprenoids

R_rxn05340_c0	fig|9606.20.peg.2571 fig|9606.20.peg.3093 fig|9606.20.peg.3734 fig|9606.20.peg.1075 fig|9606.20.peg.1994 fig|9606.20.peg.1953 fig|9606.20.peg.4716 fig|9606.20.peg.2379 fig|9606.20.peg.300 fig|9606.20.peg.1957 fig|9606.20.peg.3196	Fatty Acids, Lipids, and Isoprenoids
R_rxn00611_c0	fig|9606.20.peg.1841	Cofactors, Vitamins, Prosthetic Groups, Pigments
R_rxn00692_c0	fig|9606.20.peg.5676 fig|9606.20.peg.5351 fig|9606.20.peg.3051	Cofactors, Vitamins, Prosthetic Groups, Pigments
R_rxn05342_c0	fig|9606.20.peg.3734 fig|9606.20.peg.1994 fig|9606.20.peg.1075 fig|9606.20.peg.2571 fig|9606.20.peg.3093 fig|9606.20.peg.300 fig|9606.20.peg.1957 fig|9606.20.peg.3196 fig|9606.20.peg.4716 fig|9606.20.peg.1953 fig|9606.20.peg.2379	Fatty Acids, Lipids, and Isoprenoids
R_rxn05336_c0	fig|9606.20.peg.3734 fig|9606.20.peg.1075 fig|9606.20.peg.1994 fig|9606.20.peg.3093 fig|9606.20.peg.2571 fig|9606.20.peg.1957 fig|9606.20.peg.3196 fig|9606.20.peg.300 fig|9606.20.peg.2379 fig|9606.20.peg.1953 fig|9606.20.peg.4716	Fatty Acids, Lipids, and Isoprenoids
R_rxn00806_c0	fig|9606.20.peg.3971	Amino Acids and Derivatives
R_rxn02811_c0		Amino Acids and Derivatives

R_rxn00506_c0	fig|9606.20.peg.3098 fig|9606.20.peg.2014 fig|9606.20.peg.6002 fig|9606.20.peg.2352 fig|9606.20.peg.3105 fig|9606.20.peg.5464 fig|9606.20.peg.3094 fig|9606.20.peg.5813	Fatty Acids, Lipids, and Isoprenoids
R_rxn00541_c0	fig|9606.20.peg.5678 fig|9606.20.peg.4758	Amino Acids and Derivatives
R_rxn01740_c0	fig|9606.20.peg.24 fig|9606.20.peg.5387 fig|9606.20.peg.2135	Amino Acids and Derivatives
R_rxn12017_c0		
R_rxn00908_c0	fig|9606.20.peg.4514	Fatty Acids, Lipids, and Isoprenoids
R_rxn04043_c0	fig|9606.20.peg.4167	Carbohydrates
R_rxn00786_c0	fig|9606.20.peg.5727	Amino Acids and Derivatives
R_rxn01973_c0	fig|9606.20.peg.1256	Cofactors, Vitamins, Prosthetic Groups, Pigments
R_rxn01116_c0	fig|9606.20.peg.5587 fig|9606.20.peg.292	Carbohydrates
R_rxn00777_c0	fig|9606.20.peg.5849	Carbohydrates
R_rxn15112_c0		Amino Acids and Derivatives
R_rxn01637_c0	fig|9606.20.peg.5628 fig|9606.20.peg.1621	Amino Acids and Derivatives
R_rxn00503_c0	fig|9606.20.peg.456	Amino Acids and Derivatives
R_rxn00623_c0	fig|9606.20.peg.2659	Amino Acids and Derivatives
R_rxn00929_c0	fig|9606.20.peg.5790	Amino Acids and Derivatives
R_rxn01465_c0	fig|9606.20.peg.5785 fig|9606.20.peg.6120 fig|9606.20.peg.1153 fig|9606.20.peg.373	Nucleosides and Nucleotides
R_rxn00086_c0	fig|9606.20.peg.2993	Amino Acids and Derivatives
R_rxn00493_c0	fig|9606.20.peg.4219 fig|9606.20.peg.1643 fig|9606.20.peg.899 fig|9606.20.peg.5151 fig|9606.20.peg.4473	Cofactors, Vitamins, Prosthetic Groups, Pigments
R_rxn01301_c0	fig|9606.20.peg.2013 fig|9606.20.peg.5019	Amino Acids and Derivatives

R_rxn00527_c0	fig|9606.20.peg.3179 fig|9606.20.peg.2127 fig|9606.20.peg.6089 fig|9606.20.peg.4473 fig|9606.20.peg.4632 fig|9606.20.peg.3502 fig|9606.20.peg.4308 fig|9606.20.peg.3658 fig|9606.20.peg.2233 fig|9606.20.peg.4031 fig|9606.20.peg.3464 fig|9606.20.peg.4219 fig|9606.20.peg.1643 fig|9606.20.peg.5151 fig|9606.20.peg.899	Amino Acids and Derivatives
R_rxn02320_c0	fig|9606.20.peg.899 fig|9606.20.peg.5151 fig|9606.20.peg.1643	Amino Acids and Derivatives
R_rxn00832_c0	fig|9606.20.peg.614	Cofactors, Vitamins, Prosthetic Groups, Pigments
R_rxn01200_c0	fig|9606.20.peg.3606 fig|9606.20.peg.5732 fig|9606.20.peg.3728 fig|9606.20.peg.3729	Carbohydrates
R_rxn00134_c0	fig|9606.20.peg.793	Cofactors, Vitamins, Prosthetic Groups, Pigments
R_rxn01485_c0	fig|9606.20.peg.5276	Cell Wall and Capsule
R_rxn00313_c0	fig|9606.20.peg.5971	Amino Acids and Derivatives
R_rxn02285_c0	fig|9606.20.peg.3772	Amino Acids and Derivatives
R_rxn01517_c0	fig|9606.20.peg.6019	Nucleosides and Nucleotides
R_rxn00686_c0	fig|9606.20.peg.5173 fig|9606.20.peg.5828 fig|9606.20.peg.3875	Cofactors, Vitamins, Prosthetic Groups, Pigments
R_rxn03239_c0		Fatty Acids, Lipids, and Isoprenoids
P_Acid_7		Cell Wall and Capsule
P_Acid_5		Cell Wall and Capsule
P_Acid_6		Cell Wall and Capsule
R_rxn02804_c0	fig|9606.20.peg.389 fig|9606.20.peg.390 fig|9606.20.peg.6118	Amino Acids and Derivatives
R_rxn03240_c0		Fatty Acids, Lipids, and Isoprenoids
R_rxn05457_c0		Fatty Acids, Lipids, and Isoprenoids
R_rxn05732_c0		Cofactors, Vitamins, Prosthetic Groups, Pigments
P_Acid_3		Cell Wall and Capsule

P_Acid_4		Cell Wall and Capsule
P_Acid_2		Cell Wall and Capsule
P_Acid_1		Cell Wall and Capsule
R_rxn05231_c0	fig|9606.20.peg.2786 fig|9606.20.peg.4776 fig|9606.20.peg.4737	Nucleosides and Nucleotides
R_rxn00839_c0	fig|9606.20.peg.5074	Nucleosides and Nucleotides
R_rxn01520_c0	fig|9606.20.peg.5840	Nucleosides and Nucleotides
R_rxn01512_c0	fig|9606.20.peg.5074	Nucleosides and Nucleotides
R_rxn01513_c0	fig|9606.20.peg.4711	Nucleosides and Nucleotides
R_rxn06075_c0	fig|9606.20.peg.4776 fig|9606.20.peg.2786 fig|9606.20.peg.4737	Nucleosides and Nucleotides
R_rxn01673_c0	fig|9606.20.peg.5074	Nucleosides and Nucleotides
R_rxn01353_c0	fig|9606.20.peg.5074	Nucleosides and Nucleotides
R_rxn05233_c0	fig|9606.20.peg.4776 fig|9606.20.peg.2786 fig|9606.20.peg.4737	Nucleosides and Nucleotides
R_rxn06076_c0	fig|9606.20.peg.2786 fig|9606.20.peg.4776 fig|9606.20.peg.4737	Nucleosides and Nucleotides
R_rxn00851_c0		Carbohydrates
R_rxn02008_c0	fig|9606.20.peg.945	Amino Acids and Derivatives
R_rxn02286_c0		Amino Acids and Derivatives
R_rxn02011_c0	fig|9606.20.peg.942	Amino Acids and Derivatives
R_rxn03901_c0	fig|9606.20.peg.2397 fig|9606.20.peg.2811	Fatty Acids, Lipids, and Isoprenoids
R_rxn00193_c0	fig|9606.20.peg.743 fig|9606.20.peg.5972 fig|9606.20.peg.3562	Amino Acids and Derivatives
R_rxn00461_c0	fig|9606.20.peg.896	Cell Wall and Capsule
R_rxn03408_c0	fig|9606.20.peg.947	Transferases
R_rxn03164_c0		
R_rxn03904_c0	fig|9606.20.peg.944	Transferases
R_rxn05909_c0	fig|9606.20.peg.3410	Amino Acids and Derivatives
R_rxn00423_c0	fig|9606.20.peg.250 fig|9606.20.peg.4636 fig|9606.20.peg.5083	Amino Acids and Derivatives
R_rxn00649_c0	fig|9606.20.peg.1535 fig|9606.20.peg.4635 fig|9606.20.peg.4521	Amino Acids and Derivatives
R_rxn03638_c0	fig|9606.20.peg.6142	Cell Wall and Capsule

R_rxn00283_c0	fig|9606.20.peg.5992 fig|9606.20.peg.3019	Amino Acids and Derivatives
R_rxn00555_c0	fig|9606.20.peg.1731	Carbohydrates
R_rxn00293_c0	fig|9606.20.peg.6142	Cell Wall and Capsule
R_rxn02507_c0	fig|9606.20.peg.5582	Amino Acids and Derivatives
R_rxn01964_c0	fig|9606.20.peg.35 fig|9606.20.peg.36 fig|9606.20.peg.5939 fig|9606.20.peg.2148	Cofactors, Vitamins, Prosthetic Groups, Pigments
R_rxn02508_c0	fig|9606.20.peg.4199	Amino Acids and Derivatives
R_rxn00726_c0	fig|9606.20.peg.5584 fig|9606.20.peg.1383 fig|9606.20.peg.1382 fig|9606.20.peg.5585 fig|9606.20.peg.4642	Amino Acids and Derivatives
R_rxn00791_c0	fig|9606.20.peg.5583	Amino Acids and Derivatives
R_rxn00772_c0	fig|9606.20.peg.4167	Carbohydrates
R_rxn01137_c0	fig|9606.20.peg.667	Nucleosides and Nucleotides
R_rxn01299_c0	fig|9606.20.peg.4165	Nucleosides and Nucleotides
R_rxn00836_c0	fig|9606.20.peg.902	Nucleosides and Nucleotides
R_rxn01333_c0	fig|9606.20.peg.3736 fig|9606.20.peg.1580	Carbohydrates
R_rxn03135_c0	fig|9606.20.peg.330	Amino Acids and Derivatives
R_rxn03137_c0	fig|9606.20.peg.614	Cofactors, Vitamins, Prosthetic Groups, Pigments
R_rxn02473_c0	fig|9606.20.peg.329 fig|9606.20.peg.3410	Amino Acids and Derivatives
R_rxn03175_c0	fig|9606.20.peg.332	Amino Acids and Derivatives
R_rxn00859_c0	fig|9606.20.peg.898	Amino Acids and Derivatives
R_rxn01211_c0	fig|9606.20.peg.3935 fig|9606.20.peg.2322 fig|9606.20.peg.2331	Cofactors, Vitamins, Prosthetic Groups, Pigments
R_rxn02160_c0	fig|9606.20.peg.9	Amino Acids and Derivatives
R_rxn02835_c0	fig|9606.20.peg.6118 fig|9606.20.peg.390 fig|9606.20.peg.389 fig|9606.20.peg.3328	Amino Acids and Derivatives
R_rxn00907_c0	fig|9606.20.peg.2331 fig|9606.20.peg.3935 fig|9606.20.peg.2322	Cofactors, Vitamins, Prosthetic Groups, Pigments
R_rxn00789_c0	fig|9606.20.peg.529	Amino Acids and Derivatives
R_rxn02834_c0		Amino Acids and Derivatives

R_rxn00410_c0	fig|9606.20.peg.1287 fig|9606.20.peg.1155	Nucleosides and Nucleotides
R_rxn00237_c0	fig|9606.20.peg.5074	Nucleosides and Nucleotides
R_rxn01269_c0	fig|9606.20.peg.1644	Amino Acids and Derivatives
R_rxn01303_c0	fig|9606.20.peg.5792 fig|9606.20.peg.4944	Amino Acids and Derivatives
R_rxn00337_c0	fig|9606.20.peg.4756 fig|9606.20.peg.6013	Amino Acids and Derivatives
R_rxn00952_c0	fig|9606.20.peg.4193 fig|9606.20.peg.460	Amino Acids and Derivatives
R_rxn00693_c0	fig|9606.20.peg.2664	Amino Acids and Derivatives
R_rxn01643_c0	fig|9606.20.peg.4203	Amino Acids and Derivatives
R_rxn00239_c0	fig|9606.20.peg.6019	Nucleosides and Nucleotides
xanthosine_build		Nucleosides and Nucleotides
R_rxn00834_c0	fig|9606.20.peg.5057	Nucleosides and Nucleotides
R_rxn07578_c0		Fatty Acids, Lipids, and Isoprenoids
R_rxn07576_c0		Fatty Acids, Lipids, and Isoprenoids
R_rxn07577_c0		Fatty Acids, Lipids, and Isoprenoids
R_rxn05458_c0	fig|9606.20.peg.4717 fig|9606.20.peg.5764	Fatty Acids, Lipids, and Isoprenoids
R_rxn01000_c0	fig|9606.20.peg.1642 fig|9606.20.peg.1508	Amino Acids and Derivatives
R_rxn08016_c0		Fatty Acids, Lipids, and Isoprenoids
R_rxn10202_c0	fig|9606.20.peg.1252	Fatty Acids, Lipids, and Isoprenoids
R_rxn08799_c0	fig|9606.20.peg.4845 fig|9606.20.peg.5862	Fatty Acids, Lipids, and Isoprenoids
R_rxn03437_c0	fig|9606.20.peg.5822	Amino Acids and Derivatives
R_rxn03436_c0		Amino Acids and Derivatives
R_rxn01575_c0	fig|9606.20.peg.3971	Amino Acids and Derivatives
R_rxn00737_c0	fig|9606.20.peg.2739 fig|9606.20.peg.5848	Amino Acids and Derivatives
R_rxn03435_c0		Amino Acids and Derivatives
R_rxn08043_c0		Amino Acids and Derivatives
R_rxn00710_c0	fig|9606.20.peg.1852	Nucleosides and Nucleotides
R_rxn00205_c0	fig|9606.20.peg.1734 fig|9606.20.peg.4492 fig|9606.20.peg.5182	Amino Acids and Derivatives
R_rxn01018_c0	fig|9606.20.peg.5784	Nucleosides and Nucleotides
R_rxn01360_c0		Nucleosides and Nucleotides
R_rxn01362_c0	fig|9606.20.peg.6014 fig|9606.20.peg.4194	Nucleosides and Nucleotides
R_rxn05256_c0	fig|9606.20.peg.4652	Sulfur Metabolism

R_rxn00379_c0	fig|9606.20.peg.762 fig|9606.20.peg.763	Sulfur Metabolism
R_rxn05651_c0	fig|9606.20.peg.25 fig|9606.20.peg.5198	Sulfur Metabolism
R_rxn00416_c0	fig|9606.20.peg.2453 fig|9606.20.peg.4332	Amino Acids and Derivatives
R_rxn00192_c0	fig|9606.20.peg.5889 fig|9606.20.peg.4944	Amino Acids and Derivatives
R_rxn01434_c0	fig|9606.20.peg.1155	Amino Acids and Derivatives
R_rxn01917_c0	fig|9606.20.peg.6013	Amino Acids and Derivatives
R_rxn00469_c0	fig|9606.20.peg.4279 fig|9606.20.peg.5890 fig|9606.20.peg.4045 fig|9606.20.peg.3593	Amino Acids and Derivatives
R_rxn00802_c0	fig|9606.20.peg.5962	Amino Acids and Derivatives
R_rxn02465_c0	fig|9606.20.peg.5572	Amino Acids and Derivatives
R_rxn01019_c0	fig|9606.20.peg.1146 fig|9606.20.peg.4904	Amino Acids and Derivatives
R_rxn00119_c0	fig|9606.20.peg.1238 fig|9606.20.peg.6019	Nucleosides and Nucleotides
R_rxn00148_c0	fig|9606.20.peg.4961 fig|9606.20.peg.1799	Nucleosides and Nucleotides
R_rxn00117_c0	fig|9606.20.peg.5074	Amino Acids and Derivatives
R_rxn00790_c0	fig|9606.20.peg.4194 fig|9606.20.peg.5583	Amino Acids and Derivatives
lysine_formation		Carbohydrates
R_rxn05289_c0	fig|9606.20.peg.5178 fig|9606.20.peg.3644	Nucleosides and Nucleotides
R_rxn00409_c0	fig|9606.20.peg.5074	Nucleosides and Nucleotides
R_rxn00785_c0		
R_rxn01256_c0	fig|9606.20.peg.349	Amino Acids and Derivatives
R_rxn00364_c0	fig|9606.20.peg.1645	Nucleosides and Nucleotides
R_rxn05332_c0		Fatty Acids, Lipids, and Isoprenoids
R_rxn02213_c0	fig|9606.20.peg.621 fig|9606.20.peg.4288 fig|9606.20.peg.5386	Amino Acids and Derivatives
R_rxn01255_c0	fig|9606.20.peg.4349	Amino Acids and Derivatives
R_rxn01739_c0	fig|9606.20.peg.416	Amino Acids and Derivatives
R_rxn02212_c0	fig|9606.20.peg.417	Amino Acids and Derivatives
R_rxn01332_c0	fig|9606.20.peg.1704 fig|9606.20.peg.2184 fig|9606.20.peg.1723	Metabolism of Aromatic Compounds

R_rxn02476_c0		Carbohydrates
R_rxn02789_c0	fig|9606.20.peg.2051 fig|9606.20.peg.4206 fig|9606.20.peg.4207 fig|9606.20.peg.2050	Amino Acids and Derivatives
R_rxn01208_c0	fig|9606.20.peg.4204	Amino Acids and Derivatives
R_rxn00902_c0	fig|9606.20.peg.5063	Amino Acids and Derivatives
R_rxn03062_c0	fig|9606.20.peg.4204	Amino Acids and Derivatives
R_rxn00114_c0	fig|9606.20.peg.4905	Amino Acids and Derivatives
R_rxn00770_c0	fig|9606.20.peg.735	Nucleosides and Nucleotides
R_rxn05344_c0	fig|9606.20.peg.1661 fig|9606.20.peg.4462 fig|9606.20.peg.1664 fig|9606.20.peg.3203 fig|9606.20.peg.3201 fig|9606.20.peg.2479 fig|9606.20.peg.3116 fig|9606.20.peg.4714 fig|9606.20.peg.1836	Fatty Acids, Lipids, and Isoprenoids
R_rxn05331_c0		Fatty Acids, Lipids, and Isoprenoids
R_rxn05345_c0	fig|9606.20.peg.3201 fig|9606.20.peg.4714 fig|9606.20.peg.3116 fig|9606.20.peg.2479 fig|9606.20.peg.4462 fig|9606.20.peg.1661 fig|9606.20.peg.1664 fig|9606.20.peg.3203 fig|9606.20.peg.1836	Fatty Acids, Lipids, and Isoprenoids
R_rxn05335_c0		Fatty Acids, Lipids, and Isoprenoids
R_rxn05324_c0		
R_rxn05351_c0		
R_rxn00747_c0	fig|9606.20.peg.5275	Carbohydrates
R_rxn05333_c0		

R_rxn05348_c0	fig|9606.20.peg.3201 fig|9606.20.peg.3116 fig|9606.20.peg.4714 fig|9606.20.peg.2479 fig|9606.20.peg.4462 fig|9606.20.peg.1661 fig|9606.20.peg.1664 fig|9606.20.peg.3203 fig|9606.20.peg.1836	Fatty Acids, Lipids, and Isoprenoids
R_rxn05327_c0		
R_rxn00904_c0	fig|9606.20.peg.5248	Amino Acids and Derivatives
R_rxn05329_c0		
R_rxn05334_c0		
R_rxn05349_c0	fig|9606.20.peg.3201 fig|9606.20.peg.2479 fig|9606.20.peg.4714 fig|9606.20.peg.3116 fig|9606.20.peg.1664 fig|9606.20.peg.3203 fig|9606.20.peg.1661 fig|9606.20.peg.4462	Fatty Acids, Lipids, and Isoprenoids
R_rxn05346_c0	fig|9606.20.peg.3201 fig|9606.20.peg.2479 fig|9606.20.peg.4714 fig|9606.20.peg.3116 fig|9606.20.peg.1664 fig|9606.20.peg.3203 fig|9606.20.peg.4462 fig|9606.20.peg.1661 fig|9606.20.peg.1836	Fatty Acids, Lipids, and Isoprenoids
R_rxn05330_c0		Fatty Acids, Lipids, and Isoprenoids
R_rxn05350_c0	fig|9606.20.peg.3201 fig|9606.20.peg.4714 fig|9606.20.peg.3116 fig|9606.20.peg.2479 fig|9606.20.peg.3203 fig|9606.20.peg.1664 fig|9606.20.peg.1661 fig|9606.20.peg.4462 fig|9606.20.peg.1836	Fatty Acids, Lipids, and Isoprenoids

R_rxn05347_c0	fig|9606.20.peg.1661 fig|9606.20.peg.4462 fig|9606.20.peg.3203 fig|9606.20.peg.1664 fig|9606.20.peg.3201 fig|9606.20.peg.2479 fig|9606.20.peg.4714 fig|9606.20.peg.3116 fig|9606.20.peg.1836	Fatty Acids, Lipids, and Isoprenoids
R_rxn05325_c0		
R_rxn05326_c0		
R_rxn05322_c0		
R_rxn05343_c0	fig|9606.20.peg.3203 fig|9606.20.peg.1664 fig|9606.20.peg.1661 fig|9606.20.peg.4462 fig|9606.20.peg.2479 fig|9606.20.peg.3116 fig|9606.20.peg.4714 fig|9606.20.peg.3201 fig|9606.20.peg.1836	Fatty Acids, Lipids, and Isoprenoids
Malate_buildin		Carbohydrates
R_rxn01102_c0	fig|9606.20.peg.1800 fig|9606.20.peg.3012 fig|9606.20.peg.6106	Cofactors, Vitamins, Prosthetic Groups, Pigments
R_rxn00420_c0	fig|9606.20.peg.5846 fig|9606.20.peg.4651 fig|9606.20.peg.5826 fig|9606.20.peg.2034 fig|9606.20.peg.509	Amino Acids and Derivatives
R_rxn01101_c0	fig|9606.20.peg.855 fig|9606.20.peg.3367 fig|9606.20.peg.3696 fig|9606.20.peg.4304 fig|9606.20.peg.2310 fig|9606.20.peg.1513 fig|9606.20.peg.4042 fig|9606.20.peg.5855 fig|9606.20.peg.4305 fig|9606.20.peg.3498	Cofactors, Vitamins, Prosthetic Groups, Pigments
P_Acid_8		Cell Wall and Capsule

R_rxn00187_c0	fig|9606.20.peg.351 fig|9606.20.peg.2326	Carbohydrates
R_rxn00097_c0	fig|9606.20.peg.1238	Nucleosides and Nucleotides
oxaloacetate_buildin		Carbohydrates
R_rxn00001_c0	fig|9606.20.peg.1902 fig|9606.20.peg.5471	Phosphorus Metabolism
R_rxn00459_c0	fig|9606.20.peg.1289 fig|9606.20.peg.1903	Carbohydrates
R_rxn00251_c0		Carbohydrates
R_rxn00910_c0		Carbohydrates
R_rxn00161_c0	fig|9606.20.peg.410	Carbohydrates
R_rxn05465_c0	fig|9606.20.peg.5764 fig|9606.20.peg.4717	Fatty Acids, Lipids, and Isoprenoids
R_rxn00182_c0	fig|9606.20.peg.3510	Amino Acids and Derivatives
R_rxn00154_c0		Carbohydrates
R_rxn10121_c0	fig|9606.20.peg.3430	Nitrogen Metabolism
R_rxn00568_c0	fig|9606.20.peg.3429 fig|9606.20.peg.3430	Nitrogen Metabolism
R_rxn05627_c0	fig|9606.20.peg.4619 fig|9606.20.peg.2309 fig|9606.20.peg.2201	Nitrogen Metabolism
R_rxn08094_c0	fig|9606.20.peg.1820 fig|9606.20.peg.1822 fig|9606.20.peg.1821 fig|9606.20.peg.2655	Carbohydrates
R_rxn00598_c0		Carbohydrates
R_rxn02144_c0	fig|9606.20.peg.1368 fig|9606.20.peg.1857	Carbohydrates
R_rxn02971_c0	fig|9606.20.peg.5206	Metabolism of Aromatic Compounds
R_rxn02782_c0	fig|9606.20.peg.5207	Metabolism of Aromatic Compounds
R_rxn00588_c0	fig|9606.20.peg.5205	Metabolism of Aromatic Compounds
R_rxn02143_c0		Carbohydrates
R_rxn00257_c0	fig|9606.20.peg.2297	Carbohydrates
R_rxn00974_c0	fig|9606.20.peg.3494 fig|9606.20.peg.1537	Carbohydrates
R_rxn01388_c0	fig|9606.20.peg.3494 fig|9606.20.peg.1537	Carbohydrates
R_rxn00198_c0		Carbohydrates

R_rxn10806_c0	fig|9606.20.peg.5156 fig|9606.20.peg.1900 fig|9606.20.peg.5368 fig|9606.20.peg.843 fig|9606.20.peg.5154 fig|9606.20.peg.1901 fig|9606.20.peg.5367 fig|9606.20.peg.1816 fig|9606.20.peg.5153 fig|9606.20.peg.5155	
R_rxn10113_c0	fig|9606.20.peg.5156 fig|9606.20.peg.5154 fig|9606.20.peg.5153 fig|9606.20.peg.5155 fig|9606.20.peg.5368 fig|9606.20.peg.1900 fig|9606.20.peg.5367 fig|9606.20.peg.1901 fig|9606.20.peg.1816 fig|9606.20.peg.843	
R_rxn08900_c0	fig|9606.20.peg.1609 fig|9606.20.peg.906	
R_rxn10042_c0	fig|9606.20.peg.6146 fig|9606.20.peg.6143 fig|9606.20.peg.6144 fig|9606.20.peg.6151 fig|9606.20.peg.6147 fig|9606.20.peg.6145	